AD-A187 720 REDUCTION OF RESIDUAL STRESSES AND DISTORTION IN GIRTH WELDED PIPES(U) MASSACHUSETTS INST OF TECH CAMBRIDGE DEPT OF OCEAN ENGINEERING P K BARNES JUN 87 1/2

UNCLASSIFIED N00228-85-G-3262 F/G 11/6.2 NL

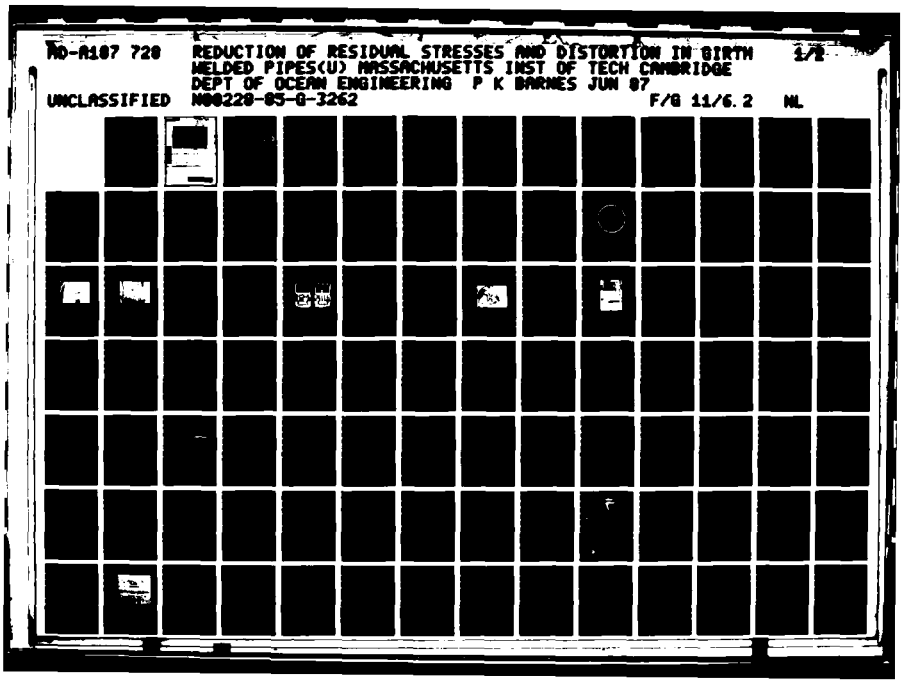

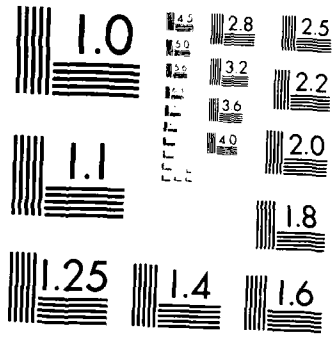

DEPARTMENT OF OCEAN ENGINEERING

MASSACHUSETTS INSTITUTE OF TECHNOLOGY

CAMBRIDGE, MASSACHUSETTS 02139

(1)

REDUCTION OF RESIDUAL STRESSES AND DISTORTION IN GIRTH WELDED PIPES

by

PAMELA KAY BARNES

Ocean Engineering - Course XIIIA

NAVAL ENG. & SM(ME)

June 1987

(1)

REDUCTION OF RESIDUAL STRESSES AND DISTORTION IN GIRTH WELDED PIPES

by

PAMELA KAY BARNES

B.S., South Dakota School of Mines and Technology
(1977)

Submitted to the Department of
Ocean Engineering
in Fulfillment of the
Requirements for the Degrees of

NAVAL ENGINEER

and

MASTER OF SCIENCE IN MECHANICAL ENGINEERING

at the

MASSACHUSETTS INSTITUTE OF TECHNOLOGY

June 1987

N00228-85-G-3262

Signature of Author: Pamela Kay Barnes
Department of Ocean Engineering, 8 May 1987

Certified by: Kanti Masubuchi
K. Masubuchi, Thesis Supervisor
Professor, Department of Ocean Engineering
Thesis Reader, Department of Mechanical Engineering

Accepted by: A. Douglas Carmichael
A. Douglas Carmichael, Chairman
Departmental Graduate Committee
Department of Ocean Engineering

REDUCTION OF RESIDUAL STRESSES

AND DISTORTION

IN GIRTH WELDED PIPES

by

PAMELA KAY BARNES

Submitted to the Department of Ocean Engineering
on May 8, 1987 in fulfillment of the
requirements for the Degrees of Naval Engineer
and Master of Science in Mechanical Engineering.

ABSTRACT

Conventionally, welding control has been used to assure that the quality of the weld itself is maintained. Residual stresses and distortion result from the non-uniform temperature distribution, form the weld process. In this thesis, an investigation into the reduction of residual stresses and distortion is performed. Potential benefits of reducing these include prevention of stress corrosion cracking, fatigue failure, brittle fracture and collapse strength, are discussed.

In an attempt to reduce residual stresses and distortion, a hydraulic restraining device was designed, constructed and tested. It was then compared to several other methods being investigated. This hydraulic restraining device is very effective in reducing the radial contraction. And although it also reduces the residual stresses, it does not change them from tensile to compressive as some of the other methods do. Future considerations are also disscussed.

Thesis Supervisor: Koichi Masubuchi
Title: Professor of Ocean Engineering

TABLE OF CONTENTS

Abstract 2

Table of Contents 3

List of Figures 5

List of Tables 7

Chapter 1 Introduction 8

1.1. Sources of Residual Stresses 9
1.2. Sources of Distortion 13
1.3. Objectives 14

Chapter 2 Problems Associated with Residual Stresses and Distortion 15

2.1. Stress Corrosion 15
2.2. Fatigue Failure 17
2.3. Brittle Fracture 18
2.4. Collapse Strength 19

Chapter 3 Apparatus Design 20

3.1. Criteria 22
3.2. Concept of "Restraining Shoe" 22
3.3. Design of the Hydraulic Restraining Device 23

Chapter 4 Experiment to Reduce Residual Stresses and Distortion 28

4.1. Equipment 28
4.2. Material 29
4.3. Procedure 31
4.4. Distortion Results 37
4.5. Residual Stress Results 48

Chapter 5 Discussion and Conclusions 55

5.1. Distortion Results 55
5.2. Residual Stress Results 66
5.3. Conclusions 71
5.4. Future Considerations 72

Appendix A. Equipment Details 74

Appendix B. Operating Manuals for Daytronics Converter and Vishay Strain Indicator and Printout of MINC's Fortran Program 76

Appendix C. Length of Pipe Calculations 98

Appendix D. Strain Gages 99

Appendix E. Strain/Stress Calculations 103

Appendix F. Deflection Prediction and Restraining Factor Calculations 108

References 110

LIST OF FIGURES

Figure 1-1: Schematic Representation of Changes of Temperature and Stresses During Welding 10
Figure 1-2: Radial Deflection to Relieve Residual Hoop Stress 12

Figure 3-1: Mechanical Turnbuckle 21
Figure 3-2: Hydraulic Restraining Device 24
Figure 3-3: Photograph of Hydraulic Restraining Device 26
Figure 3-4: Photograph of Hydraulic Restraining Device Positioned in the Pipe 27

Figure 4-1: VISHAY P350A Strain Indicator and SB-1 Switch and Balance Unit 30
Figure 4-2: Photograph of Hydraulic Restraining Device in Pipe, with Grid Lines, set up on Aronson Positioner 33
Figure 4-3: Photograph of Equipment Set Up 35
Figure 4-4: Longitudinal Profile of the Upper Half of the Pipe With No Restraint Comparing the Distortion of the Radius Before and After Welding 39
Figure 4-5: Longitudinal Profile of the Upper Half of the Pipe With 150 psi Restraint Comparing the Distortion of the Radius Before and After Welding 43
Figure 4-6: Longitudinal Profile of the Upper Half of the Pipe With 250 psi Restraint Comparing the Distortion of the Radius Before and After Welding 44
Figure 4-7: Comparison of Distortion at 0° 45
Figure 4-8: Comparison of Distortion at 15° 46
Figure 4-9: Comparison of Distortion at 30° 47
Figure 4-10: Comparison of Hoop Stress on Inner Surface 51
Figure 4-11: Comparison of Axial Stress on Inner Surface 52
Figure 4-12: Comparison of Hoop Stress on Outer Surface 53
Figure 4-13: Comparison of Axial Stress on Outer Surface 54

Figure 5-1: Comparison of Computed Results and Experimental Data for Distortion 56
Figure 5-2: Distortion Comparison at 0° Between This Thesis and DeBiccari 58
Figure 5-3: Distortion Comparison at 30° Between This Thesis and DeBiccari 59
Figure 5-4: Distortion Comparison at 0° Between This Thesis and DeBiccari 60

Figure 5-5: Distortion Comparison at 30° Between This Thesis and DeBiccari 61
Figure 5-6: Reduction Percentage Comparison 62
Figure 5-7: Deflection Prediction 64
Figure 5-8: Stiffness Curve 65
Figure 5-9: Inner Surface Residual Stresses 67
Figure 5-10: Residual Stresses in a Girth Welded Pipe 67
Figure 5-11: Comparison of Residual Stresses Between a Conventional Weld and a Heat Sink Weld 68

Figure D-1: Various Strain Gage Configurations 100
Figure D-2: Various Strain Gage Configurations 101

LIST OF TABLES

Table 4-1: Welding Conditions 34
Table 4-2: Distortion Measurements for Specimen without Restraint 38
Table 4-3: Distortion Measurements for Specimen with 150 psi Restraint 40
Table 4-4: Distortion Measurements for Specimen with 250 psi Restraint 41
Table 4-5: Comparison of Residual Stresses 49

Table 5-1: Comparison of Residual Stresses Between This Thesis and DeBiccari 70

Table E-1: Strain Measurements and Stress Calculations for Specimen without Restraint 105
Table E-2: Strain Measurements and Stress Calculations for Specimen with 150 psi Restraint 106
Table E-3: Strain Measurements and Stress Calculations for Specimen with 250 psi Restraint 107

Table F-1: Calculated Values for Deflection and Restraining Factor 109
Table F-2: Calculated Values for Nondimensional Deflection and Restraining Factor 109

CHAPTER 1
INTRODUCTION

Welding is a complicated process. It is preferred over other joining processes because of its high joining efficiency, water and air tightness and mechanical properties over a wide range of temperatures. However, it creates thermal strains and stresses.

These strains and stresses are due to the localized heat of the welding source and the non-uniform temperature distribution from the weld process. Accompanying stress and strain is plastic upsetting. As a result residual stresses, shrinkage, distortion, stress corrosion cracking and buckling may be produced. [1]

In circumferential butt welds of pipes, localized residual stresses and distortion are generated. The presence of these residual stresses can be detrimental to the integrity of the pipe, such as causing failure and stress corrosion cracking. [2] The biggest concern of circumferential welding is in nuclear piping and submersible vessels. This is because residual stresses and distortion can greatly affect fatigue and collapse strength. [3]

Residual stresses due to welding and thermal/mechanical loadings contribute to tensile stress. Conventional circumferential girth welding produces tensile residual stresses on the inner surface on the pipe near the weld. Therefore, it is advantageous to be able to control and reduce these tensile residual stresses. [4]

Determination of residual stresses is complex. It requires an understanding in metallurgy, heat transfer and stress analysis. [2] There have been different methods investigating residual stresses during welding. This thesis is not concerned with the metallurgy or heat transfer but with reducing residual stresses and distortion in girth welded pipe with a restraining device.

1.1. Sources of Residual Stresses

Residual stresses exist internally to the body in the absence of external forces. Therefore, the stress state is in static equilibrium within a body, i.e. internally balanced. [5] In the context of welded structures, residual stresses are confined to the neighborhood of the weld and decrease rapidly on either side of it. [6] Residual stresses also occur when a body is subjected to non-uniform temperature change, i.e. thermal stresses produced during welding.

Figure 1-1 shows the changes of temperature and stresses that occur during welding a bead on a flat plate. Section A-A is ahead of the arc; therefore, the temperature change and stresses are zero. Section B-B is at the arc so that the change in temperature is rapid and uneven. Molten metal will not support a load; therefore, the stresses are small. Near the weld, the stresses are compressive because the surrounding metal is cooler and restrains the expansion of the heated weld area. At section C-C, the area has started

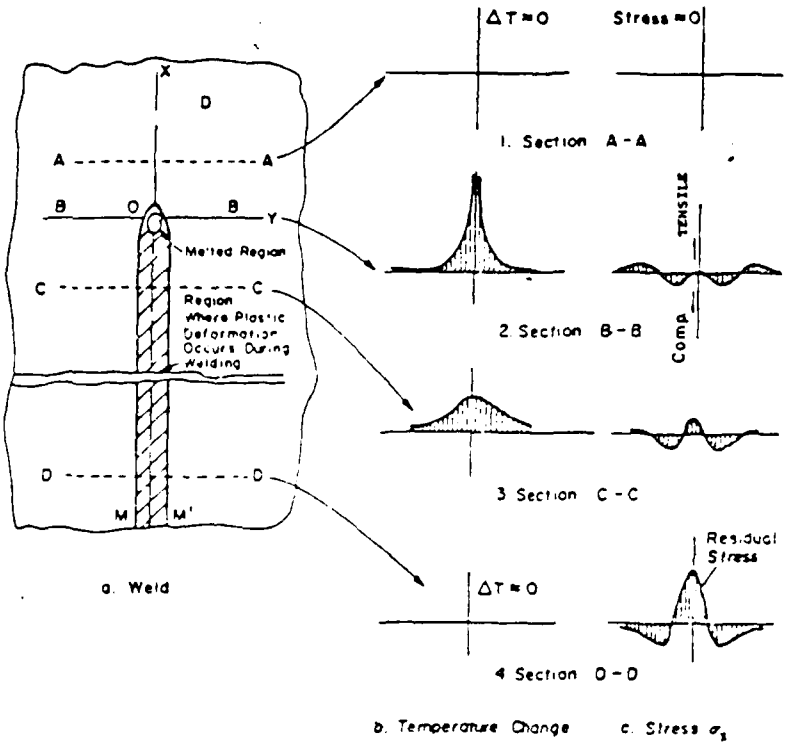

Figure 1-1: Schematic Representation of Changes of Temperature and Stresses During Welding [7]

to cool, thus contracting and causing tensile stresses. Away from the weld, the stresses become compressive to balance the tensile stresses. At section D-D, the temperature has cooled producing high tensile stresses at the weld and compressive stresses away from the weld. [7]

By analogy to a flat plate, when two cylinders are welded along their circumference, one might expect the hoop tensile stresses near the weld, lower hoop compressive stresses away from the weld and negligible axial stresses. However, radial displacements may modify the stress distributions. This mode cannot take place in a flat plate unless it is very thin and can buckle in the regions of residual compressive stresses. This radial displacement is the most critical distortion and is caused from cicumferential shrinkage (a form of longitudinal shrinkage). The displacement decreases with the distance from the weld. Figure 1-2 shows that a deflected shape will decrease both hoop tensile and compressive stresses but will introduce bending stresses in the axial direction. [3, 8]

During welding, molten metal is deposited. It is subjected to high temperatures. This hot region cools rapidly and tends to shrink. However, the cooler surrounding metal prevents it from contracting. Thus, tensile stresses are produced near the weld. As temperature goes down, the yield stress increases as does the tensile stress in the weld. The final tensile stresses can be as high as the yield stress. [9, 10]

There's a difference of opinion when it comes to the

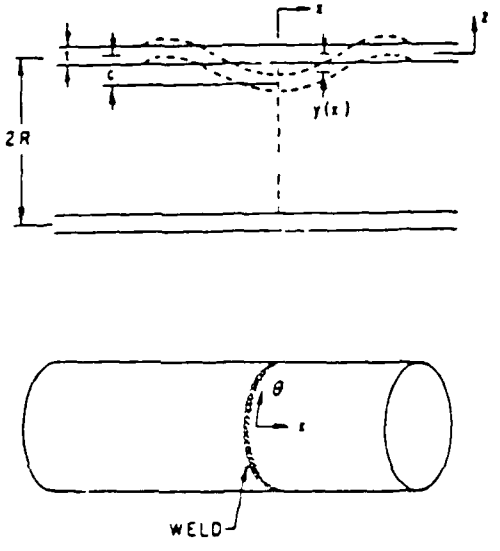

Figure 1-2: Radial Deflection to Relieve Residual Hoop Stress [8]

statement that restraint reduces residual stress. Some engineers believe residual stress increases with restraint; while others say it stays about the same. [7]

1.2. Sources of Distortion

Distortion is the change in shape or dimensions, temporary or permanent, of a welded part as a result of welding. The physical expansion and contraction are the principal causes of distortion.

During welding the metal is initially heated and subjected to large temperature gradients. Hence the metal becomes weaker and is more easily deformed. The tendency for distortion is determined by the degree of restraint present at the weld joint. Upon cooling, the metal contracts; however, the surrounding cold metal tends to resist this shrinkage But if the metal is weakened enough then this resistance is low and the metal shrinks causing distortion.[11]

It has been shown that distortion can be controlled on any given pass by lowering the heat input. However, this most likely requires more passes. The final distortion might not be reduced since it is the the sum of all the passes. Therefore, a more selective sequence might be used, i.e. a low heat input on the first pass and increasing heat inputs with each successive pass.

Along with the number of passes goes the amount of weld metal deposited. The strength of joint is determined by its design. Excess weld metal does nothing for this strength,

but it does increase the effective shrinkage force. By limited this amount, distortion can be reduced. [11, 12]

The amount of distortion depends on the wall thickness to the diameter ratio of the cylinder. As the ratio becomes smaller the distortion is greater. [13] External restraint has been shown to reduce distortion also.

1.3. Objectives

In order to reduce residual stresses and distortion, two tasks are necessary:

1. Development of a control mechanism to exert a continuous force on the inner surface to produce compressive stresses
2. Comparison of a six point hydraulic load source and a two point mechanical load source.

CHAPTER 2

PROBLEMS ASSOCIATED WITH RESIDUAL STRESSES AND DISTORTION

The purpose of this thesis is to reduce distortion and residual stresses in girth welded piping. Before one can attempt to reduce these, it is beneficial to investigate some of the problems caused by distortion and residual stresses. This chapter will discuss stress corrosion cracking (SCC), fatigue failure, brittle fracture, and collapse strength.

2.1. Stress Corrosion Cracking

Stress corrosion cracking is a form of localized failure that is more severe than other types of metal attacks. Therefore, it is a combination of stress and corrosion. SCC is the brittle fracture of a material that is otherwise ductile. [7]

Generally, it is believed that pure metals do not crack as a result of stress corrosion. Some alloys are more resistant to cracking than others, i.e. aluminum, copper, and magnesium. [14]

It has been observed to occur under low applied stress or no stresses at low. Therefore, other factors must be present. [15] Three factors that must be present for stress corrosion cracking to occur: a state of tensile stress, a corrosive environment, and a sensitized material. If one of these factors can be reduced, then cracking may be

eliminated. A corrosive environment can never be eliminated totally; sensitized material cannot always be avoided. Thus removing tensile stress is achievable. [4, 16]

No cracking has been observed when the surfaces are in compression. Tensile stresses result from the presence of internal (residual) stresses or an external (applied) load. Causes may be:

1. deformation near welds
2. unequal cooling of metal
3. phase change
4. differential thermal expansion
5. dead loading
6. pressure differentials.

The environment is the reason for corrosion. Metals react differently according to the type of environment. [14]

The biggest concern of stress corrosion cracking is its susceptibility in the heat affected zone of stainless steel weldments, in particular, pipe weldments in nuclear reactor service. These weldments directly affect the service of boiling-water and pressurized water reactors which have experienced SCC. The weldment is subjected to a complicated strain history imposed by the heating and cooling cycle. The strain history is more complex in a pipe weld than a plate weld. (In a plate stress can be relieved by bending, while circumferential restraint restricts metal movement in a pipe weld.) This strain history increases the susceptibility of SCC. [17]

2.2. Fatigue Failure

The large majority of failures that occur in service, are numerous and in fact are fatigue failures. Many of these fatigue failures involve welded structures. Fatigue is defined as the formation of a crack or cracks as a result of repeated applications or cycles of loads each of which is insufficient by itself. The danger of fatigue failure is that it is difficult to see and can grow slowly. There's no significant dimensional change in a cracked structure so a crack may propagate through the entire structure before it is discovered. [6, 15]

Materials, stress concentration, corrosion and residual stresses contribute to fatigue failure. This thesis is only concerned with the effect of residual stresses on fatigue failure. It has been debated whether or not compressive stresses on the surface increase the fatigue strength. Some believe that crack growth is retarded by compressive stresses and increased by tensile stresses. [14, 18]

Pressure vessels, their associated pipework and other various types of structures may be subjected to a low number of cycles of loads. The stress that is necessary to cause fatigue due to a small number of cycles is considerably greater than those necessary due to a high number of cycles. These stresses are usually large enough to cause considerable plastic deformation. Now the relationship between stress and strain is no longer linear but changes from cycle to cycle. [6]

It is necessary to be able to improve fatigue strength in order to reduce fatigue failure. Some possible methods are to remove or reduce the load which is causing the failures, to improve the design or to reduce the stresses. To reduce or remove the load it is first necessary to know what the load is. Sometimes this still doesn't reduce fatigue failure. A designer can choose the type and position of a weld joint or make use of some technique in order to improve fatigue strength. However, the designer may be limited. Reducing stresses is one of the purposes of this thesis.

2.3. Brittle Fracture

Brittle fracture means that separation has occurred without plastic flow. Usually brittle refers to a specimen having less than a few percent reduction in area. However, specimen that have been proved to be ductile may fail in a brittle manner. Serious brittle fractures are more likely to occur in welded structures rather than in riveted structures. Carbon steels with high tensile residual stresses have experienced catastrophic brittle fractures although the stresses may be well below the yield stress of the material. [14, 15] Thereby reducing residual stresses will decrease the chance of brittle fracture.

2.4. Collapse Strength

It is well known that initial distortion and residual stresses reduce the collapse or buckling strength of spherical and cylindrical shells subjected to external pressure. Many papers have been written on this subject. Experimental collapse pressures are frequently lower than the pressure calculated from theory. This is due to the failure of the models to meet the idealized geometry and material assumptions of the theory. Factors that decrease collapse strength are distortion, thickness, weld material properties, residual stresses, boundary effects and loadings. [7]

It is almost impossible to weld without introducing some distortion or stress. So there will be a reduction in the collapse strength. But by reducing distortion and residual stresses collapse strength increases.

CHAPTER 3
APPARATUS DESIGN

The PhD Thesis by Andrew DeBiccari, [19] showed that residual stresses and distortion were reduced when an outward force was exerted on the inner wall of the pipe while being welded. The apparatus used was a mechanical turnbuckle (see figure 3-1). The turnbuckle is adjusted by turning rods with a hexagonal nut. Once the weld has been started, the turnbuckle can not be adjusted. So when the pipe expands from the heat of the weld, there is no longer a force being exerted on the inner wall.

Also, there is no conclusive results between the circumferential positioning of the heat source and the residual stresses and distortions. One possible reason could be the fact that the "restraining shoes" attached to the turnbuckle are a two point load source. They loose their effectiveness as the distance from the rod connection increases.

Since the mechanical turnbuckle did show evidence of reducing residual stresses and distortion, then there is a possibility that an improved modification of the turnbuckle will reduce residual stresses and distortion even more. The first modification is to go from a mechanical, uncontrollable turnbuckle to a controllable hydraulic restraining device. The second modification is to determine the number of point sources feasible in the design.

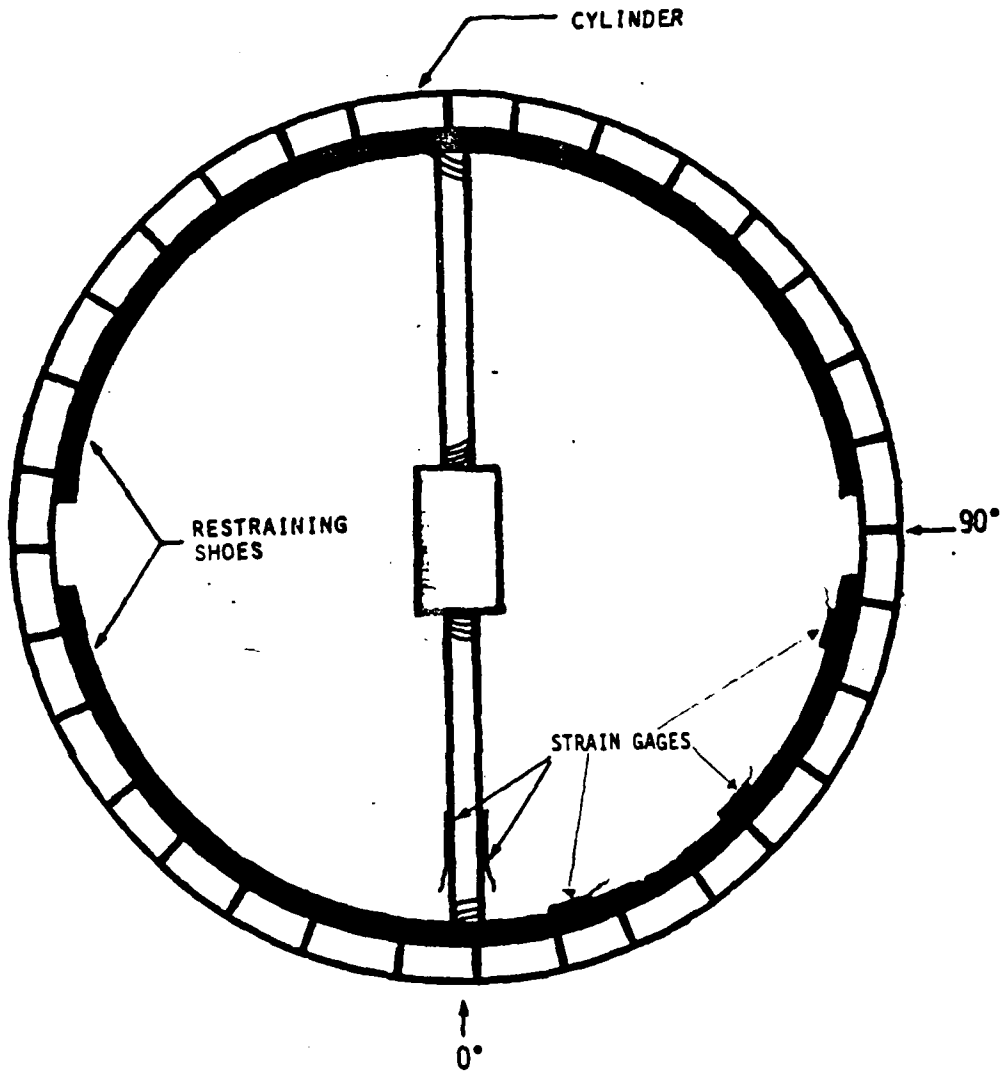

Figure 3-1: Mechanical Turnbuckle [19]

3.1. Criteria

There must be considerations in designing any apparatus. The following are the considerations for the design of the hydraulic restraining device:

a. Employing the concept of the mechanical turnbuckle "restraining shoes"

b. Ability to fit inside the pipe

c. Ability to be controlled during welding

d. Ability to expand and contract

e. Employing the maximum number of point sources feasible

3.2. Concept of "Restraining Shoe"

The mechanical turnbuckle employed the concept of "restraining shoes". These "shoes" are two (2) semicircle pieces of steel. Their dimensions are: 1/4" thick, 4" wide and have the same radius of curvature as the inner wall of the pipe. This allows the entire outer surface of the "shoe" to keep in contact with the inner surface of the pipe. Hence, a constant force is exerted on the inner wall of the pipe. Welded to the midpoint of the inner surface of each "shoe" is a nut. A 1/2" threaded steel rod screws into the nut of one "shoe" while another opposite threaded steel rod screws into the nut on the other "shoe". Both steel rods thread into a common hexagonal nut. Turning this hexagonal nut expands or collapses the mechanical turnbuckle. A gap of

1/16" between the "shoes" is allowed in order for the turnbuckle to collapse.

3.3. Design of the Hydraulic Restraining Device

The concept of the "shoes" is still easily employed. The difficult aspect is to find a hydraulic restraining device small enough to fit inside the pipe yet maximize the number of point sources.

After looking through many equipment catalogs, Gary Abel of Lincoln Controls [20] was contacted. After discussions of the idea behind the experiment, the material and the set up involved, Gary Abel suggested to mount individual hydraulic pistons in a cylindrical ring to fit inside the pipe. Then link the pistons in series with hoses to a hyraulic pump.

Upon receiving a sample of the piston, the aid of Bruce Bailey [21] was employed. Combining the criteria imposed with Gary Abel's suggestions the restraining device in figure 3-2 was designed.

The diameter of the pipe and the type of the point sources physically limit the number of point sources to six (6) for the hydraulic restraining device. Thus, there are six (6) "restraining shoes" of equal dimensions: 4" wide, 1/4" thick and arc length of 6" that has the same radius of curvature as the inner wall of the pipe. A nut is welded at the midpoint of the inner surface of the "shoe". A rod is threaded into

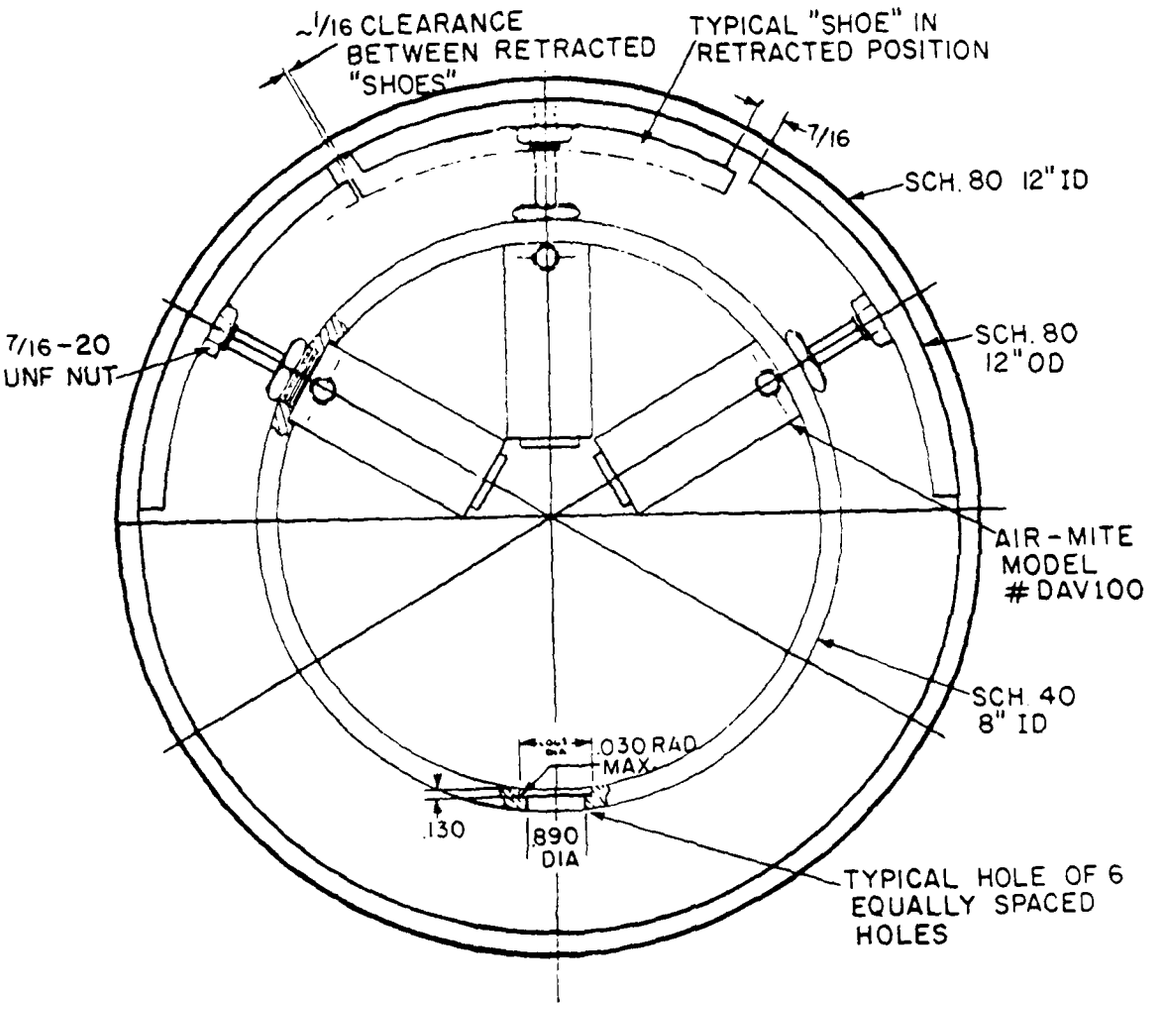

Figure 3-2: Hydraulic Restraining Device [21]

each nut and is the means for the force being exerted. Thus, the concept of the "restraining shoes" is the same whether it is for two (2) or six (6) "shoes". Figure 3-3 is an photograph of the hydraulic restraining device. One of the "shoes" is screwed off to show the nut and threaded piston rod. Figure 3-4 is an photograph showing the placement of the hydraulic restraining device inside a cylindrical pipe.

The force being exerted comes from the pistons. They are equally spaced and screwed into an 8" diameter cylindrical ring. The piston rod is that rod which is threaded into the nut. Each piston has an inlet and outlet port. The outlet port of one piston is connected to the inlet port of the next piston with copper tubing. The first inlet and last outlet ports connect directly to the hydraulic pump: a series connection.

The piston is designed for 150 psi of air. However, it can also residual stresses but for this experiment it is adequate. The intent of this thesis is to show that an outward force exerted on the inner wall will reduce distortion and residual stresses.

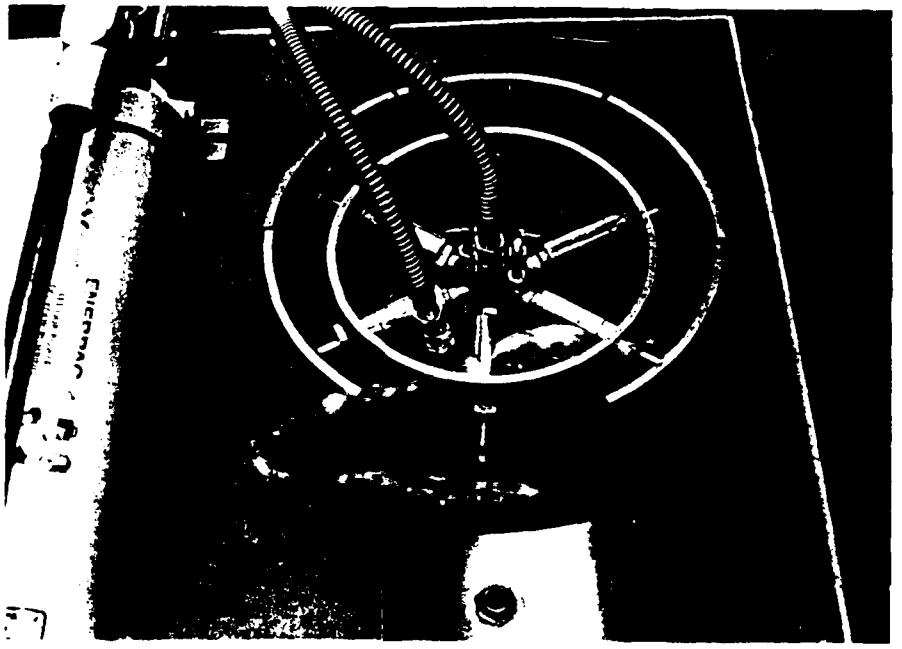

Figure 3-3: Photograph of Hydraulic Restraining Device

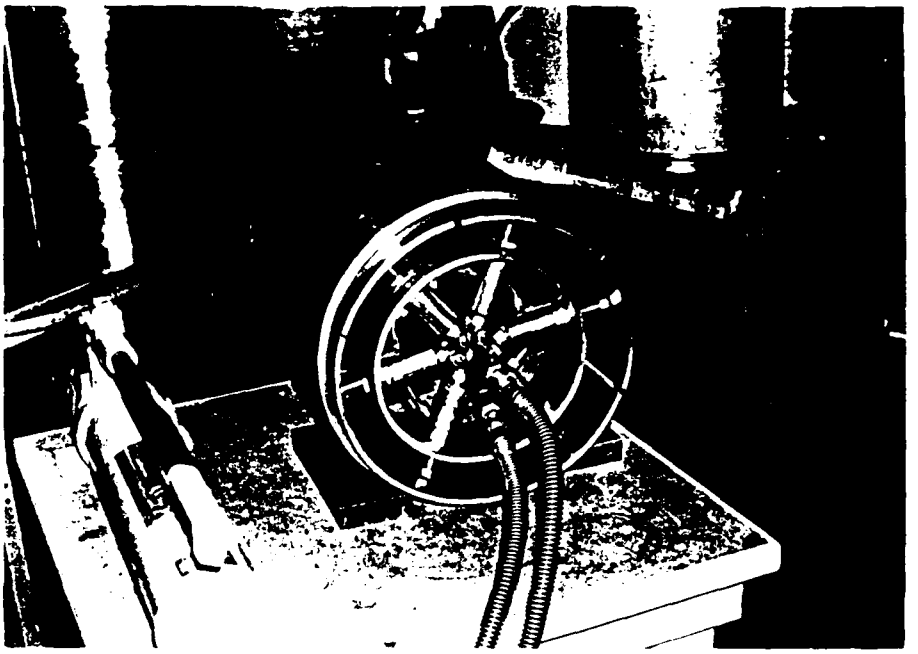

Figure 3-4: Photograph of Hydraulic Restraining Device Positioned in the Pipe

CHAPTER 4
EXPERIMENT TO REDUCE RESIDUAL STRESSES AND DISTORTION

The selection of the equipment, conditions and procedure is based on the experiment performed by Andy DeBiccari. [19] Since the hydraulic restraining device is a modification of his mechanical turnbuckle, then a comparison between the two is desired. By including a means of controlling the pressure during the welding and expanding the number of point sources for the load distribution, is is expected that the residual stresses and distortion should be less with the hydraulic restraining device than those with the mechanical turnbuckle.

4.1. Equipment

An automatic tungsten inert gas set up is the welding means for the experiment. The power supply is the MILLER Syncorwave 500, DCSP, GTA/SMA. The JETLINE Engineering Arc Length Control System, Model ALC-201, regulates the water-cooled torch, argon gas and voltage which in turn controls the arc length. The arc length control system is mounted vertically to a horizontal carriage traveler manufactured by Linde of Union Carbide. (It is stationary for the purpose of this experiment.) The filler wire feed system is a product of Airco Heliweld. Since the torch is stationary, the mechanism for rotating the pipe is an ARONSON Positioning Table with a variable speed control and tilt wheel. See

Appendix A for the details of the equipments' settings.

The Daytronic 9000 Data Acquisition System is connected to a Digital Equipment Corporation MINC-23 Laboratory Data Processing System and records the strain changes, through strain gages, exerted on the "shoe" and piston rod during welding. Also through the use of strain gages, the VISHAY P-350A Digital Strain Indicator and SB-1 Switch and Balance Unit (see figure 4-1 [22]) determine the strain (residual stress) changes in the pipe during stress relaxation. (See Appendix B for exerpts from the manuals for the Daytronics Converter and Vishay Strain Indicator and a printout of the MINC's Fortran computer program.) Agapakis [23] gives the fundamentals of the acquisition and the computer programs used in the processing of the data.

4.2. Material

Schedule 80, low carbon steel is used for the cylindrical pipe. Its inside diameter is 12" with a thickness of 5/16". The sections were cut to a length of 9 inches. (This length is chosen so the end effects of the cylinder can be ignored. See Appendix C for calculations.) There are a total of six sections, two per weld.

For the "restraining shoes", schedule 40, low carbon steel, 1/4" thickness, is used. There are six (6) "shoes" having the same radius of curvature as the inner wall of the 12" ID pipe, 4" wide with an arc length of 6".

The cylindrical ring holding the pistons is also

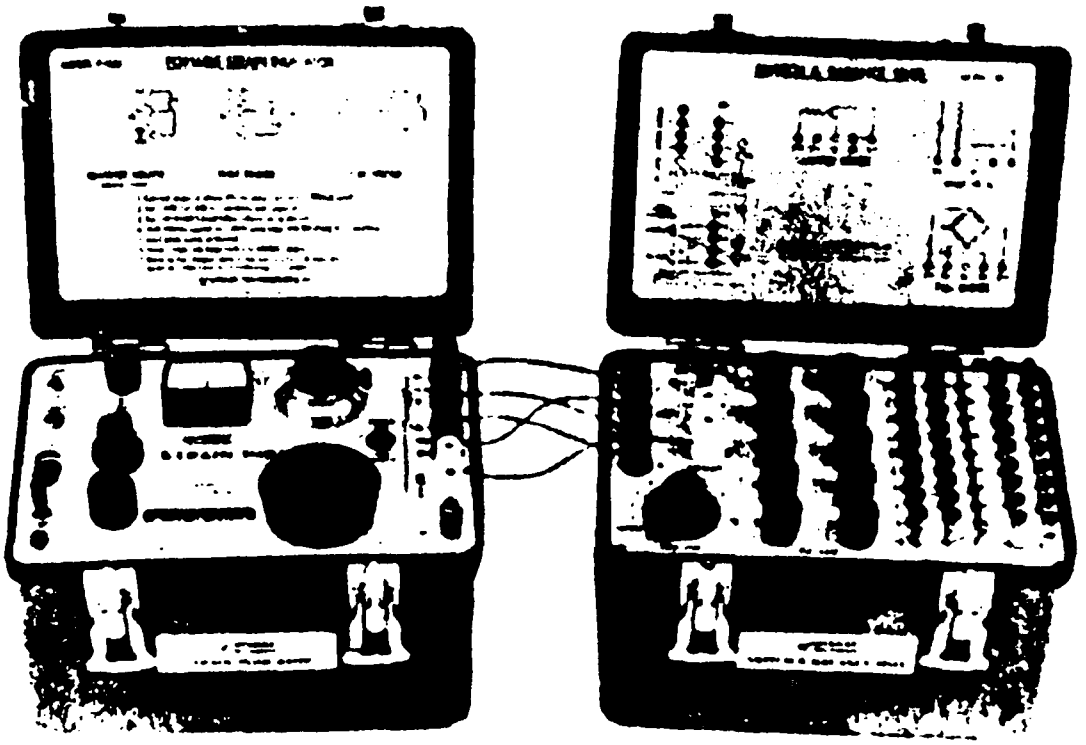

Figure 4-1: VISHAY P350A Strain Indicator and SB-1 Switch and Balance Unit [22]

schedule 40 steel with a 8" diameter.

There are a total of six (6) Air Mite pistons, Model DAV100-1, connected to a Enerpac P-84 hydraulic pump by high pressure hoses.

Three (3) types of strain gages are used. On the "shoes", SR-4 FAE-25-35 S6 EL biaxial strain gages are used during welding. (Biaxial gages measure the strains axially and circumferen- tially.) This same brand should have been used on the piston rods also, but there wasn't enough in supply so a HBM 3/350LY11 (biaxial) strain gage is used also during welding. The two are very similar but made by different companies. Triaxial rosette strain gages, SR-4 FAER-12B-35 S6 EG are used on the inner and outer wall of the pipe during stress relaxation. (Triaxial gages measure the strains in the axial, circumferential and shear direction.) See Appendix D for more details on the strain gages.

4.3. Procedure

Before performing the welding procedure, two pipe sections are tack welded at four evenly spaced locations [24] and a grid system needed is marked on the inner wall of each of the pipe specimens. Since the "shoe" covers an area in a 60° angle then only one half of the "shoe" is where the data is taken. Two reasons are behind this decision: 1) the force from the "shoe" should be symmetric on either side of the point source, i.e. the piston rod and 2) the limitation on the number of strain gages that can be hooked up to the SB-1

Switch and Balance Unit.

Figure 4-2 is an actual photograph showing the grid system marked on the inner wall by +'s. There are three (3) grid lines, one located at 0°, 15°, and 30°. Each + on the grid line is at a distance from the centerline of the weld: 0.25", 0.5", 0.75", 1.0", 1.5", 2.0", 2.5", 3.0", 4.0", 5.0" and 6.0". The diameter of each of the specimens at these locations are measured with a digital micrometer before welding.

Even though there is a pressure gage on the hydraulic pump, strain gages are placed on the piston rods and the "shoes". They are then hooked up to the Daytronic 9000 Data Acquisition System which is connected to a Digital Equipment Corporation MINC-23 Laboratory Data Processing System so that the strain change is recorded during welding.

To ensure that the set up and welding conditions are correct, a sample weld is made on a specimen that will not be used as data. In order for a comparison to be made with DeBaccari's results, the welding conditions need to be very similar. Through trial and error the welding conditions in Table 4-1 are used. They vary from DeBiccari's [19] but only slightly. Figure 4-3 is a photograph showing the set up of the equipment and pipe. The pipe is clamped onto the Aronson positioner and tilted horizontally. The wire feeder is adjusted properly and the current and voltage are set; all to ensure the feed wire is depositing into a good weld pool.

With this equipment set up and welding conditions, a single pass, gas tungsten arc process, circumferential weld

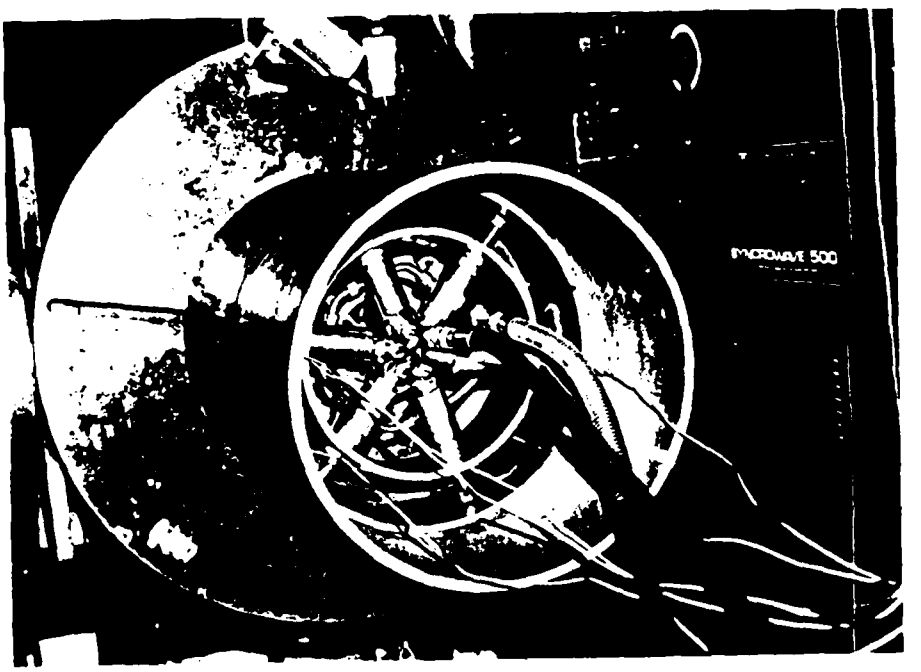

Figure 4-2: Photograph of Hydraulic Restraining Device in Pipe, with Grid Lines, set up on Aronson Positioner

Table 4-1: Welding Conditions

V = 11.0 volts

I = 250 amps

v = 3 in/min = 0.127 cm/sec

H = 2750 Watts

Feeder wire:	diameter = 0.035 in = 0.0889 cm
	feed rate = 1.45 in/sec
	= 3.68 cm/sec
Argon gas:	12 psi
Tungsten:	diameter = 3/32 in = 0.238 cm

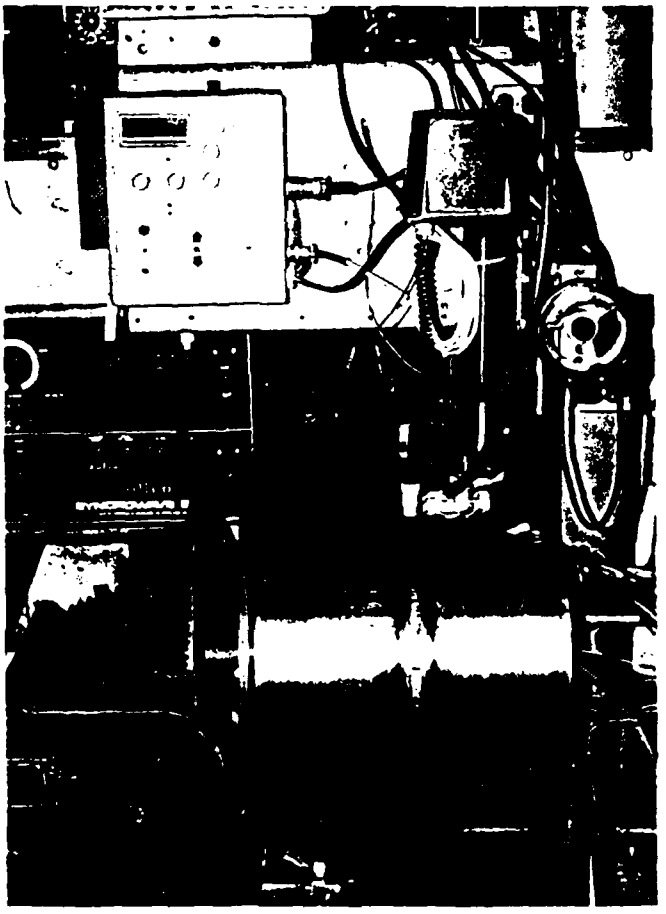

Figure 4-3: Photograph of Equipment Set Up

is made on three (3) different specimens of cylindrical pipe. One specimen does not contain the hydraulic restraining device on the inside while the other two (2) do. Pressures of 150 psi and 250 psi are set on the hydraulic pump for the two (2) specimens that contained the hydraulic restraining device. These pressures act as a force on the "shoe", hence a restraint. The strain gages are hooked up to the Daytronic 9000 and MINC-23 while welding. (It was discovered that the strain gages no longer adhered to the metal after welding. This could be due to the heat intensity being too great for the bonding. Therefore, this data is suspect.) The specimens are cooled naturally. The pressure in the hydraulic restraining device remains on the specimens while cooling.

After cooling, the diameter of each of the specimens is measured at the grid points previously described with the same digital micrometer and recorded. Then the rosette strain gages are located on the inner and outer surfaces of the pipes, 0.5" from the weld centerline at the 0°, 15°, and 30° grid lines. (Papazoglou's thesis [25] shows that the temperature distribution is the highest at a distance of 0.5" from the centerline of the weld.) They are coated with silicon for protection. Then the gages are connected to the strain indicator and switch/balance unit which measures the change in the strains.

The residual stresses are determined by the stress relaxation technique [7]. A cylindrical section containing the strain gages is removed from each of the welded specimens

by a sawing method; one cut being on the weld centerline, the second on the other side of the strain gage the same distance as that from the strain gage and the weld centerline. The sawing is performed at a slow rate and is constantly liquid cooled to avoid any unnecessary changes in the residual stresses. The strain changes are measured and recorded.

4.4. Distortion Results

The results of the distortion measurements taken on the specimen without the hydraulic restraining device are shown in Table 4-2. This table shows shrinkage as a negative value. Figure 4-4 is a longitudinal profile of half of the pipe and compares the radius before welding to the radius after welding, i.e. distortion, at the 15° angular position only. The vertical axis is adjusted for a clearer comparison.

The distortion pattern is similar for axial and angular positions. (Some discrepancies may be due to the inaccuracy of the micrometer measurements.) This is expected since the weld started and finished well enough away from the measurements and allows for an assumption of quasi stationary state condition.

The distortion measurements for the specimens with the hydraulic restraining device are shown in Tables 4-3 and 4-4. Again shrinkage is shown as a negative value. The distortion patterns are similar as in the specimen without the restraint, but the 30° angular position increases slightly

TABLE 4-2: Distortion Measurements for Specimen without Restraint

Distance (in.) from weld Centerline	Angular Position		
	0	15	30
0.25	-0.013	-0.014	0.014
0.50	-0.007	-0.013	0.019
0.75	0.006	-0.015	-0.017
1.00	-0.004	-0.011	-0.011
1.50	-0.004	-0.008	0.008
2.00	0.001	-0.008	-0.007
2.50	-0.001	-0.006	0
3.00	-0.002	-0.007	0
4.00	0	-0.005	0.003
5.00	0	-0.002	0.003
6.00	-0.001	-0.001	0.005

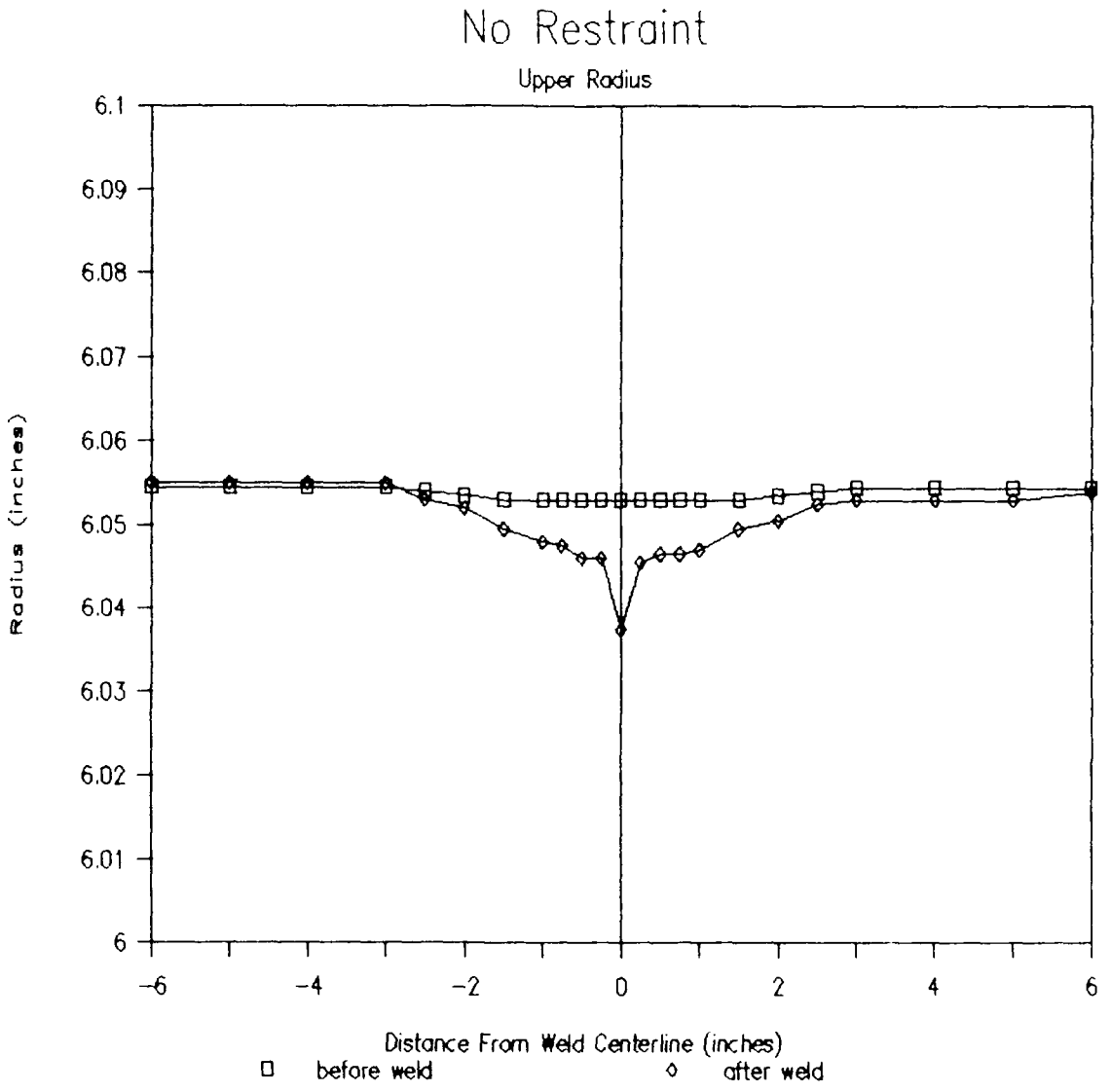

Figure 4-4: Longitudinal Profile of the Upper Half of the Pipe Comparing the Distortion of the Radius Before and After Welding

TABLE 4-5: Distortion Measurements For Specimen with 150 psi Pressure

Distance from weld Centerline	Angular Position		
	0	15	30
0.25	0.010	0.015	0.016
0.50	0.014	0.015	0.017
0.75	0.013	0.016	0.020
1.00	0.017	0.013	0.022
1.50	0.021	0.021	0.025
2.00	0.024	0.024	0.026
2.50	0.026	0.027	0.029
3.00	0.026	0.028	0.030
4.00	0.028	0.029	0.030
5.00	0.028	0.029	0.031
6.00	0.028	0.028	0.030

TABLE 4-4: Distortion Measurements for Specimen with 250 psi Restraint

Distance (in.) from weld Centerline	Angular Position 0	15	30
0.25	-0.002	-0.002	0.001
0.50	-0.002	-0.002	-0.001
0.75	-0.001	-0.001	0.004
1.00	0.001	-0.002	0.001
1.50	0.004	0.004	-0.001
2.00	0.007	-0.002	0.003
2.50	0.007	0.007	0.004
3.00	0.008	0.007	0.004
4.00	0.005	0.005	0.003
5.00	0.001	0.002	0.004
6.00	-0.003	0.002	0.003

from the 0° and 15° positions. Figures 4-5 and 4-6 are longitudinal profiles of half of the pipe and compare the radius before welding to the radius after welding, i.e. distortion, at the 15° angular position only. Again the vertical axis is adjusted for a clearer comparison. There is no explanation why the distortion measurements for the specimen with the 150 psi restraint are in expansion except that the micrometer may not have been calibrated to the correct reference value.

Figures 4-7, 4-8 and 4-9 compare the distortion of the specimen without the restraint to the specimen with the 250 psi restraint at the angular positions of 0°, 15° and 30°, respectively. For each angular position of the specimen with the 250 psi restraint, the shrinkage next to the weld centerline is considerably less, about 72% - 86%, than that of the specimen without any restraint. However, further away from the weld centerline, the 250 psi restraint specimen expands.

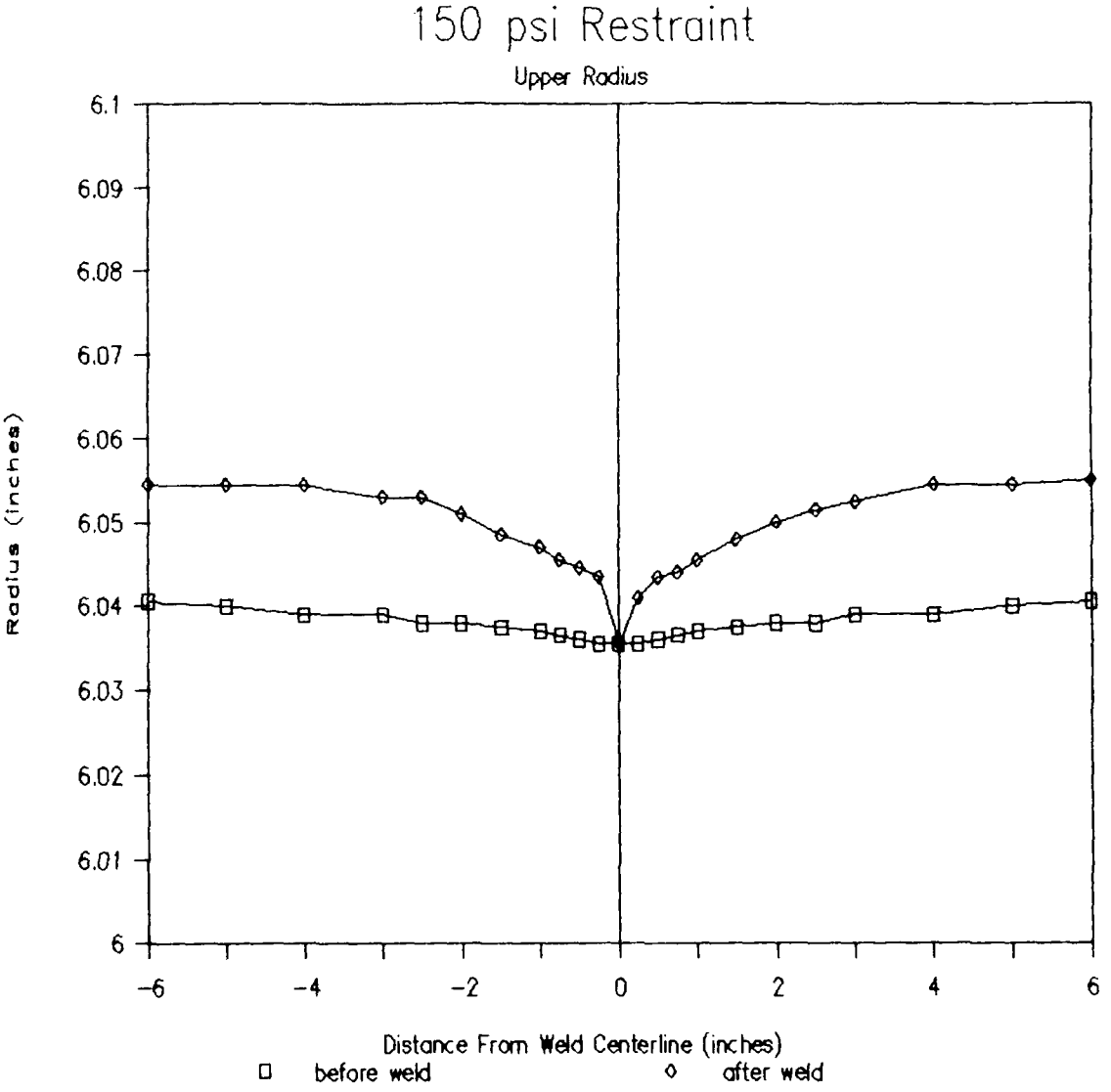

Figure 4-5: Longitudinal Profile of the Upper Half of the Pipe Comparing the Distortion of the Radius Before and After Welding

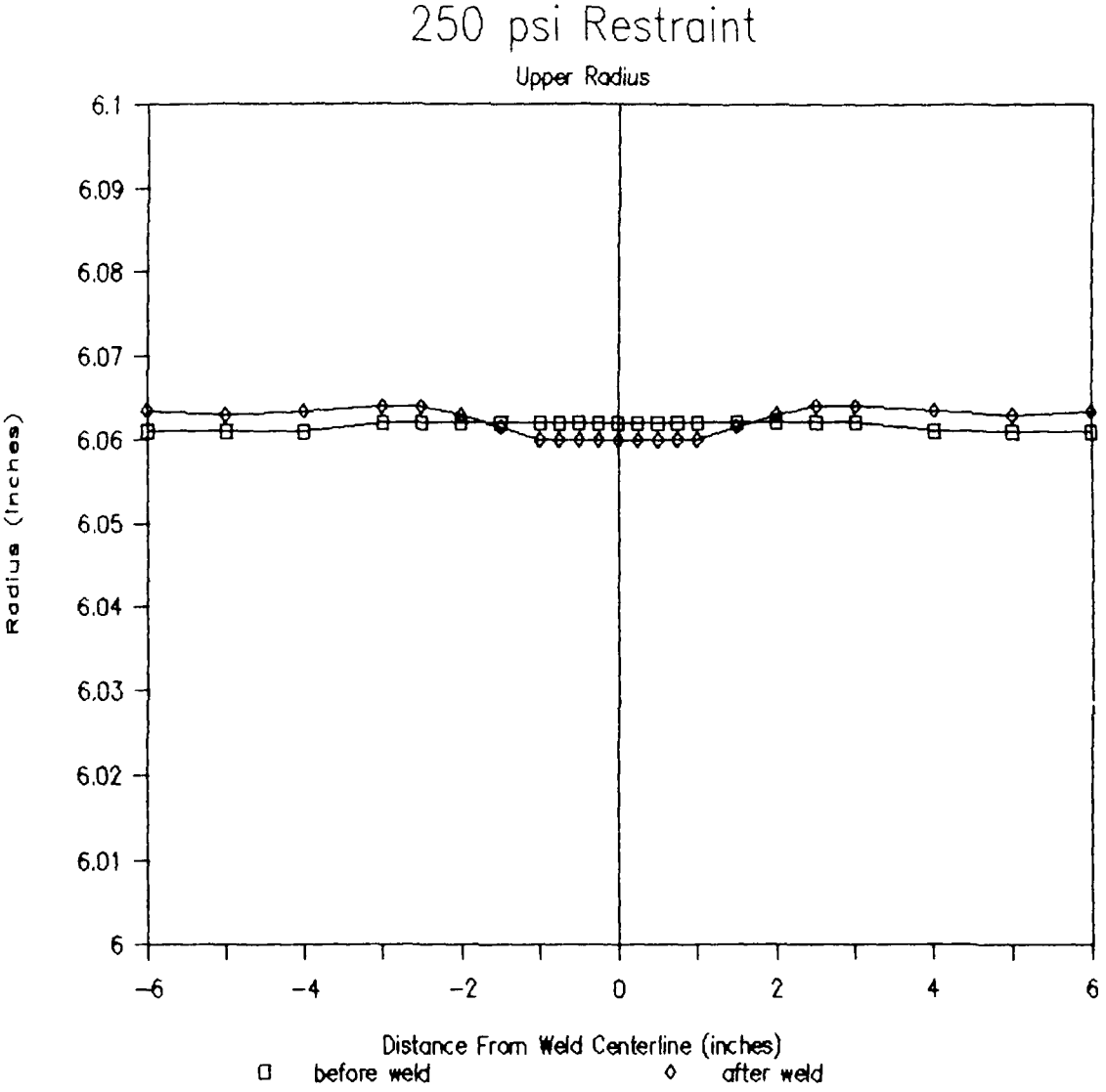

Figure 4-6: Longitudinal Profile of the Upper Half of the Pipe Comparing the Distortion of the Radius Before and After Welding

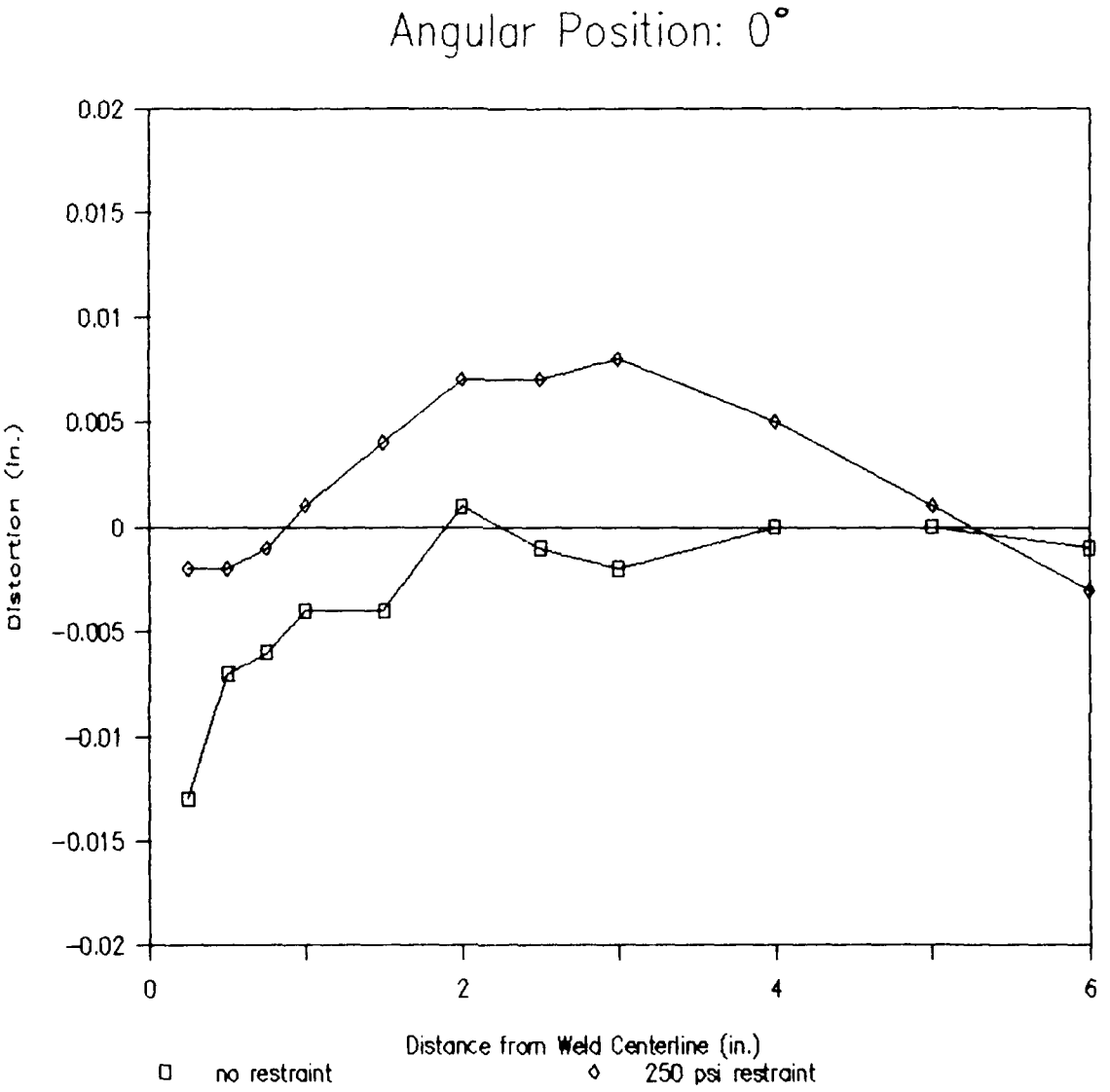

Figure 4-7: Comparison of Distortion Results between specimens with no restraint and 250 psi restraint at 0°

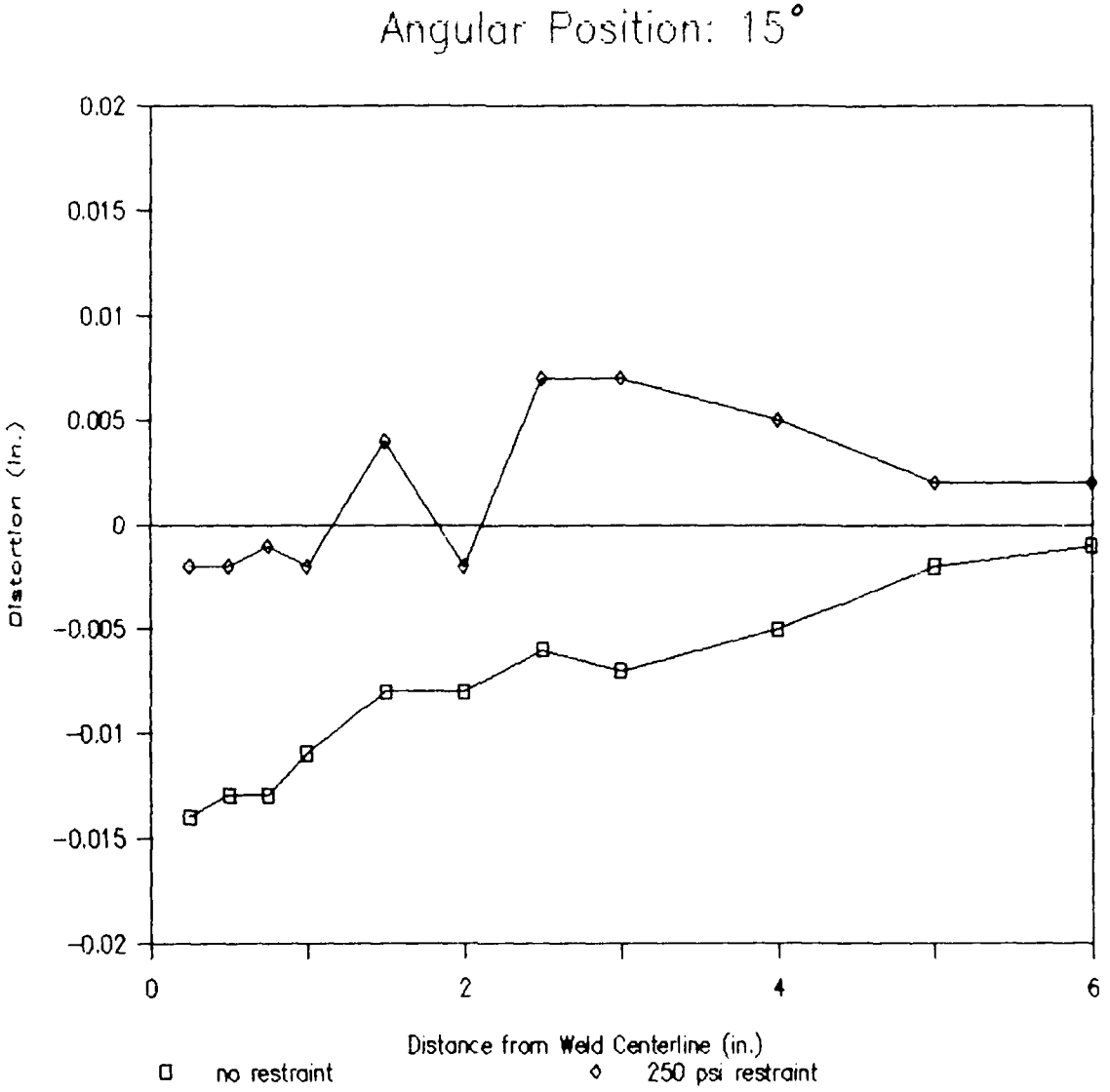

Figure 4-8: Comparison of Distortion Results between specimens with no restraint and 250 psi restraint at 15°

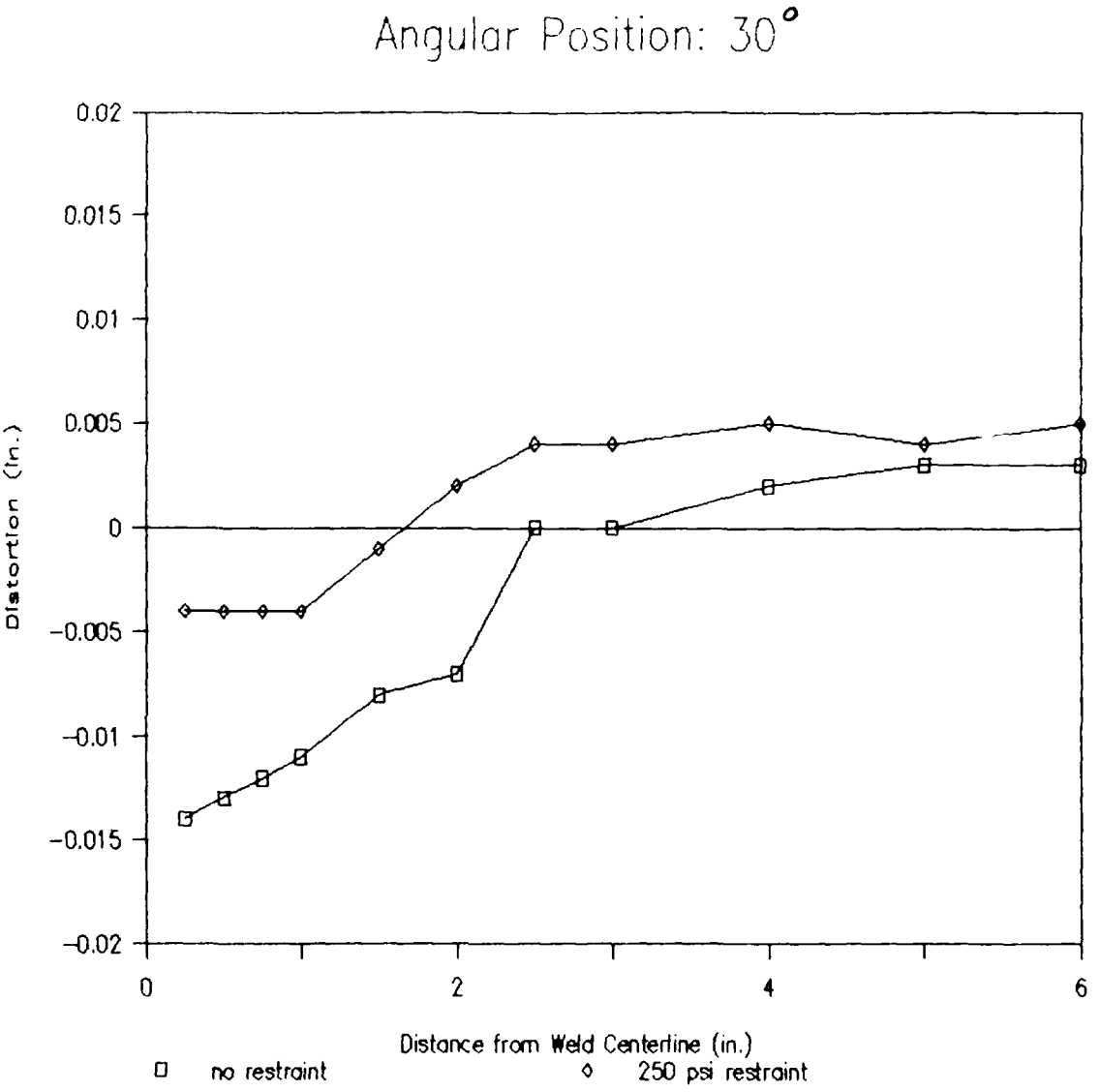

Figure 4-9: Comparison of Distortion Results between specimens with no restraint and 250 psi restraint at 30°

4.5. Residual Stress Results

The strain changes measured by the relaxation technique for each of the specimens are given in Appendix E. From the strain changes the residual stresses are calculated from [7]:

$$\sigma_x = \frac{-E}{(1-\nu^2)} (\varepsilon_x + \nu \varepsilon_\theta) \qquad (5.1)$$

$$\sigma_\theta = \frac{-E}{(1-\nu^2)} (\varepsilon_\theta + \nu \varepsilon_x) \qquad (5.2)$$

$$\gamma = \frac{-I}{G} \qquad (5.3)$$

σ_x , σ_θ and τ are the measured strains for the hoop, axial and shear directions, respectively. E is the modulus of elasticity of 30 x 10^6 psi; ν is Poisson's ratio of 0.3. G is the modulus of rigidity or shear modulus and is calculated from the following equation and the above data:

$$G = \frac{E}{2(1+\nu)} = 11.54 \times 10^6 \text{ psi} \qquad (5.4)$$

The negative signs in equations (5.1), (5.2) and (5.3) reflect that when tensile residual stresses exist, shrinkage takes place during stress relaxation. The converse is true when compressive residual stresses exist.

Table 4-5 shows a comparison of the residual stresses for the specimens. For each angular position on the inner surface from no restraint to 250 psi, there is a consistent decrease of residual stress with three exceptions. At the

Table 4-5: Comparison of Residual Stresses

Inner Surface

Position		No Restraint	150 PSI	250 PSI
0°	σ_θ	23.55	27.93	21.21
	σ_x	48.88	43.90	40.71
	$\tau_{\theta x}$	11.79	8.19	8.04
15°	σ_θ	40.31	35.88	17.25
	σ_x	63.87	49.70	43.48
	$\tau_{\theta x}$	14.10	11.10	10.00
30°	σ_θ	45.56	40.13	36.61
	σ_x	61.88	46.78	59.04
	$\tau_{\theta x}$	14.61	11.84	12.38

Outer Surface

Position		No Restraint	150 PSI	250 PSI
0°	σ_θ	9.51	1.44	-0.91
	σ_x	-31.59	-34.79	-40.44
	$\tau_{\theta x}$	0.00	-4.74	-6.76
15°	σ_θ	9.28	-3.42	-0.46
	σ_x	-35.08	-33.91	-46.64
	$\tau_{\theta x}$	-5.49	-5.91	-7.42
30°	σ_θ	2.41	-5.24	-1.28
	σ_x	-45.48	-35.77	-41.75
	$\tau_{\theta x}$	-8.75	-9.37	-7.18

different angular positions, there is a consistent, but small, increase in the stresses with the exception of three. All the stresses on the inner surface are in tension.

The stresses on the outer surface are almost all compressive with the axial stresses being very high. They become more compressive with the use of the restraint. The stresses vary very little with the angular position.

Figures 4-10 through 4-13 show a graph interpretation of this comparison for the hoop and axial stresses for both inner and outer surfaces. There are no graphs for the shear stresses because there is not a significant difference.

The next chapter discusses these results and compares them to other results.

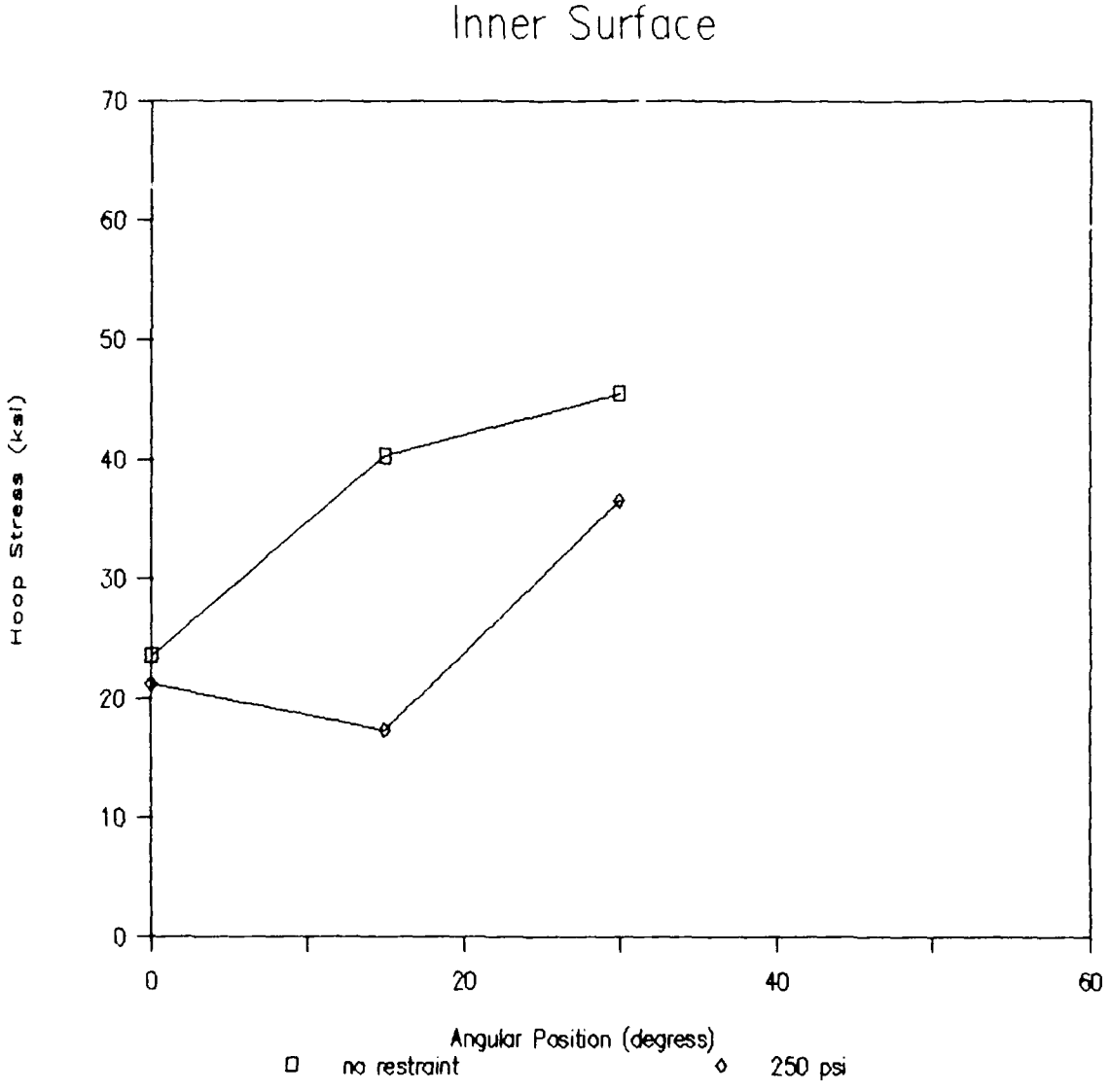

Figure 4-10: A Comparison of Hoop Stress on Inner Surface vs. Angular Position Between Specimens with No Restraint and 250 psi

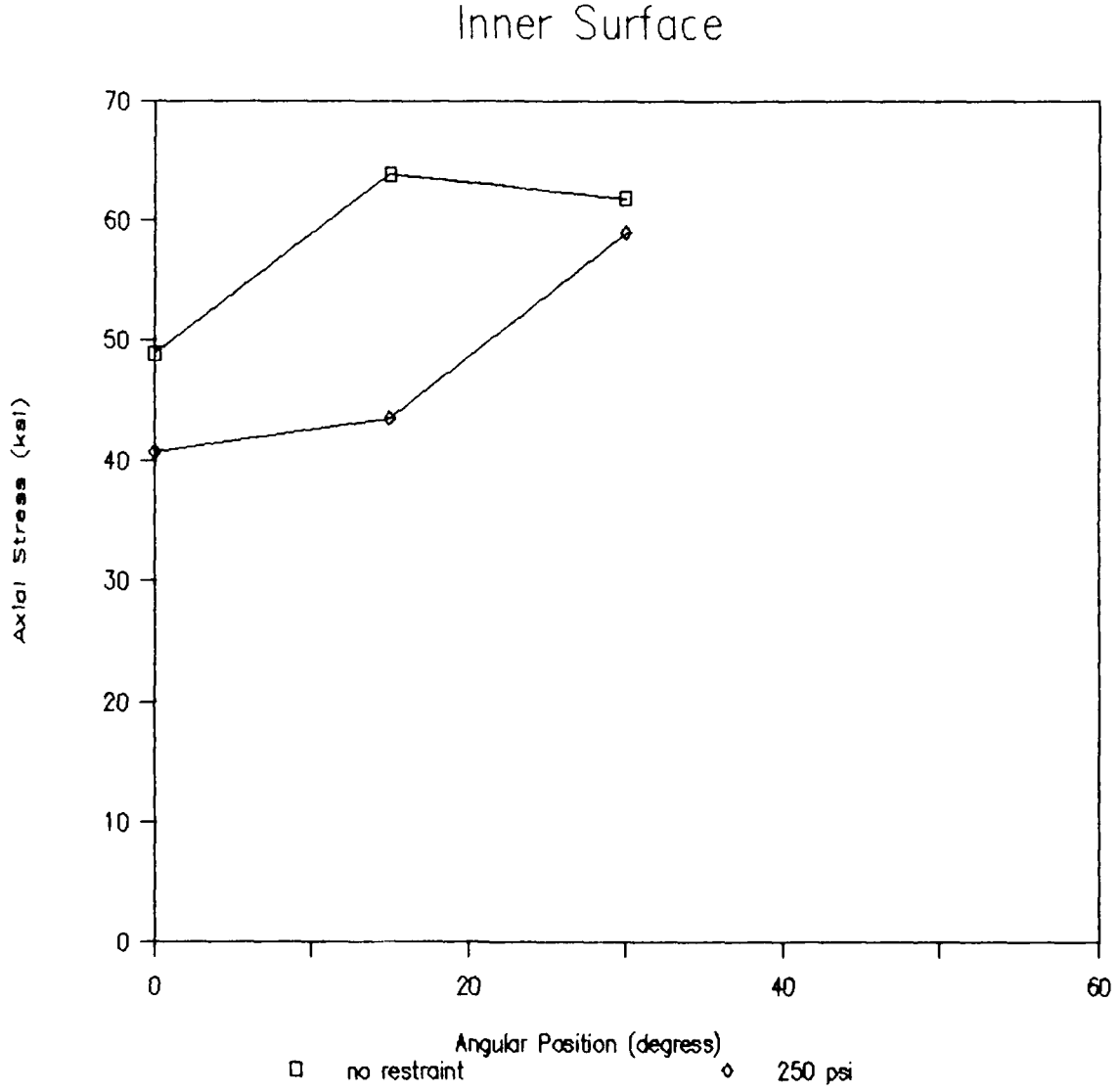

Figure 4-11: A Comparison of Axial Stress on Inner Surface vs. Angular Position Between Specimens with No Restraint and 250 psi

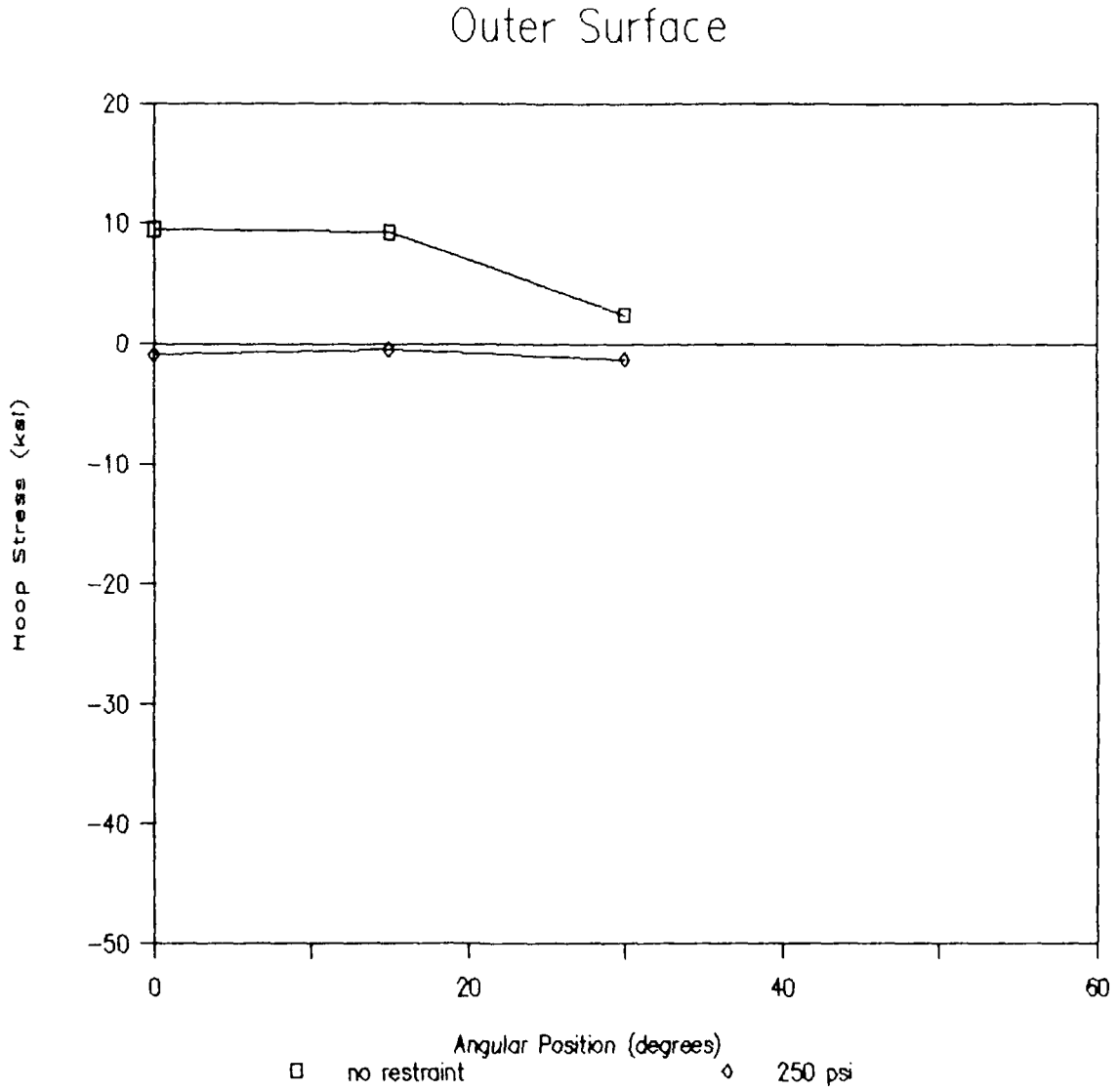

Figure 4-12: A Comparison of Hoop Stress on Outer Surface vs. Angular Position Between Specimens with No Restraint and 250 psi

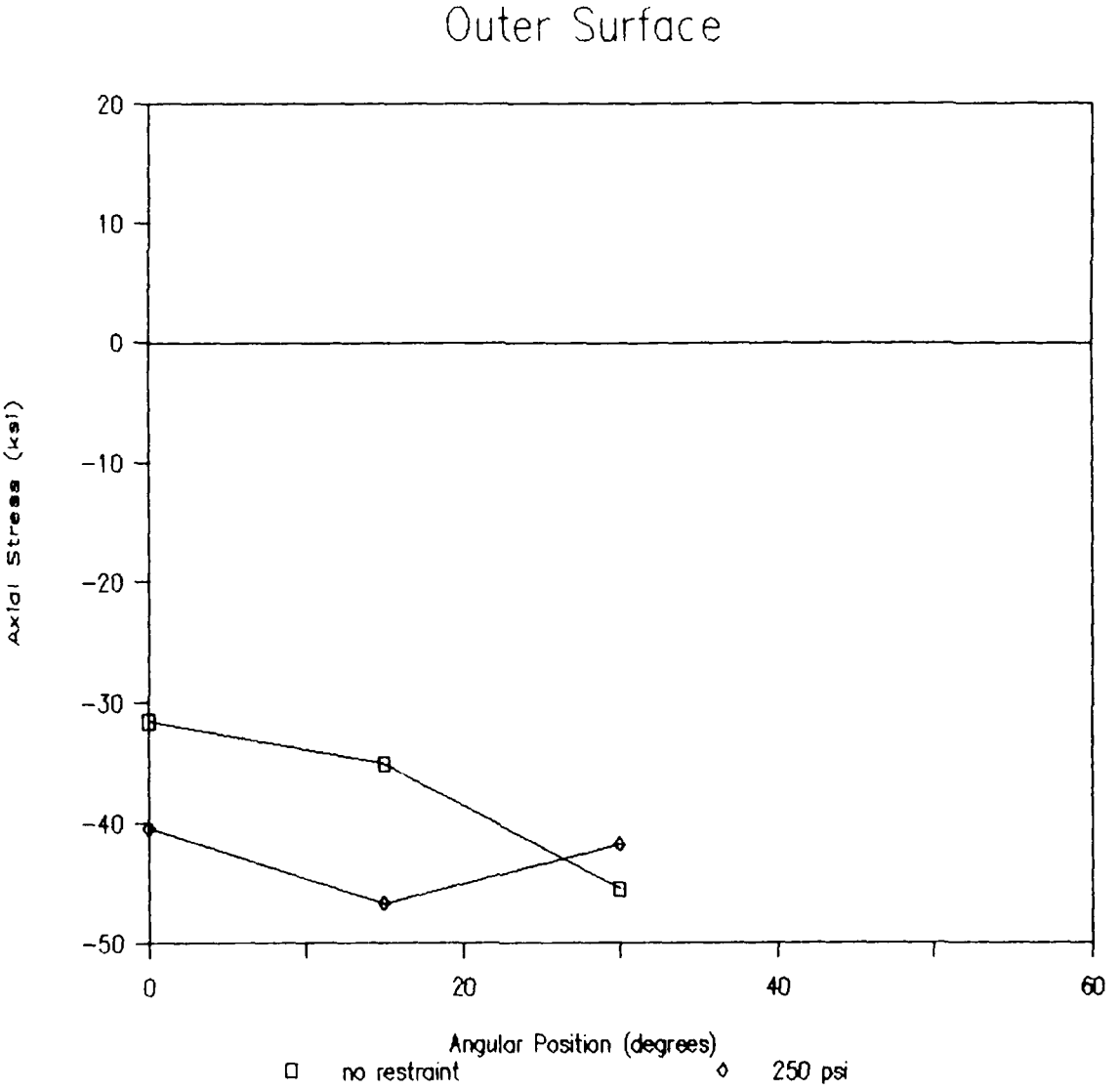

Figure 4-13: A Comparison of Axial Stress on Outer Surface vs. Angular Position Between Specimens with No Restraint and 250 psi

CHAPTER 5
DISCUSSION AND CONCLUSIONS

This chapter discusses the results of the distortion and residual stresses given in Chapter 4. These results are compared with those from other investigators. Finally, some conclusions are given.

5.1. Discussion: Distortion

Heat sink welding has cool water on the inside of the pipe while welding. This keeps the inner surface relatively cool during most of the welding. Thus there is less shrinkage than in a conventional weld. [26] No figure or numbers are given for a comparison, but the shrinkage in this thesis's experiment due to the hydraulic restraining device is also less than that in the weld without the system.

Rybicki, et. al. [27], developed a finite-element model to predict deflections in girth-butt welded pipes. Figure 5-1 [27] shows a comparison of the computed deflections and the experimental data. The band reflects the ranges of the measurements taken along axial lines at four locations, 90° apart. At 0.5", this range of deflection is more than twice that of this experiment's distortion of the specimen with no restraint.

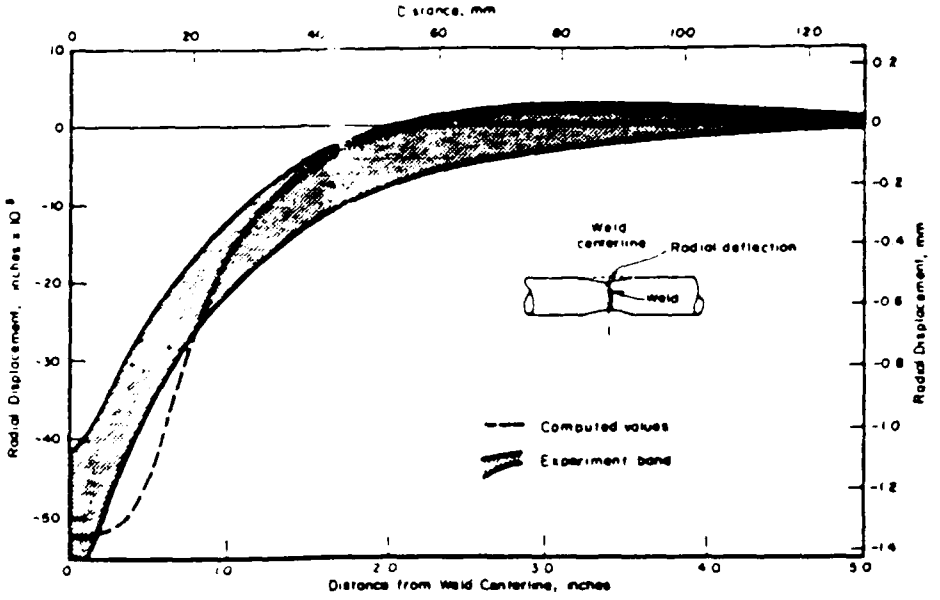

Figure 5-1: Comparison of Computed Results and Experimental Data for Distortion [27]

When comparing the distortion to DeBiccari's [19] results (see figures 5-2 through 5-5) as originally intended, the only similarity is that the distortion decreases with the distance away from the weld. This thesis's results had expected to be less than those of DeBiccari's. There's only a few data points that are. At the 0° location, both specimens has less distortion than DeBiccari's up to 1.5 inches away from the weld centerline. But at the 30° location it's greater. After the 1.5 inches distance this experiment's specimens expand instead of shrinking. One possible reason might be the fact the hydraulic restraining device provides a continuous pressure while cooling to the extent that it over compensates. Other than the pressure gage on the hydraulic pump, there's no other means to control this pressure.

Figure 5-6 shows the comparison between this thesis and DeBiccari's of the reduction percentage of distortion for the restraint to that without the restraint versus the axial position at the 0° and the 30° angular position. For this thesis, the distortion near the weld centerline, i.e. the 0° position, is reduced by 85%, whereas, in DeBiccari's it is reduced by 75%. As the angular position increases the percentage decreases, but there's still a significant reduction in both. However, DeBiccari's results have more of a reduction. Axially, away from the weld centerline, the reduction percentage increases but remember that the distortion here is less in numerical value. Therefore, the percentage changes rapidly with small numerical value

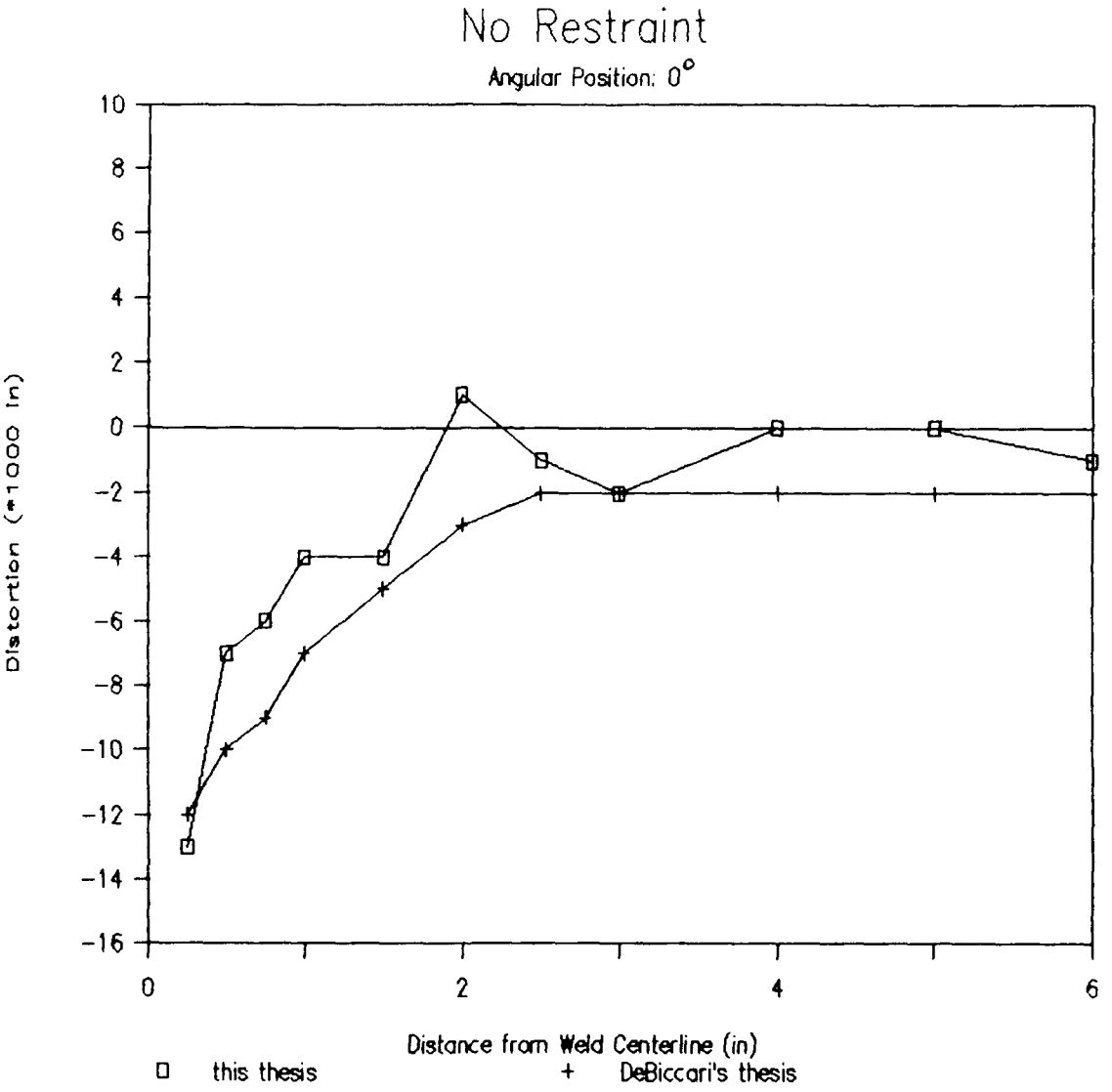

Figure 5-2: Distortion Comparison at 0° of Specimens without any restraint from This Thesis and DeBiccari's

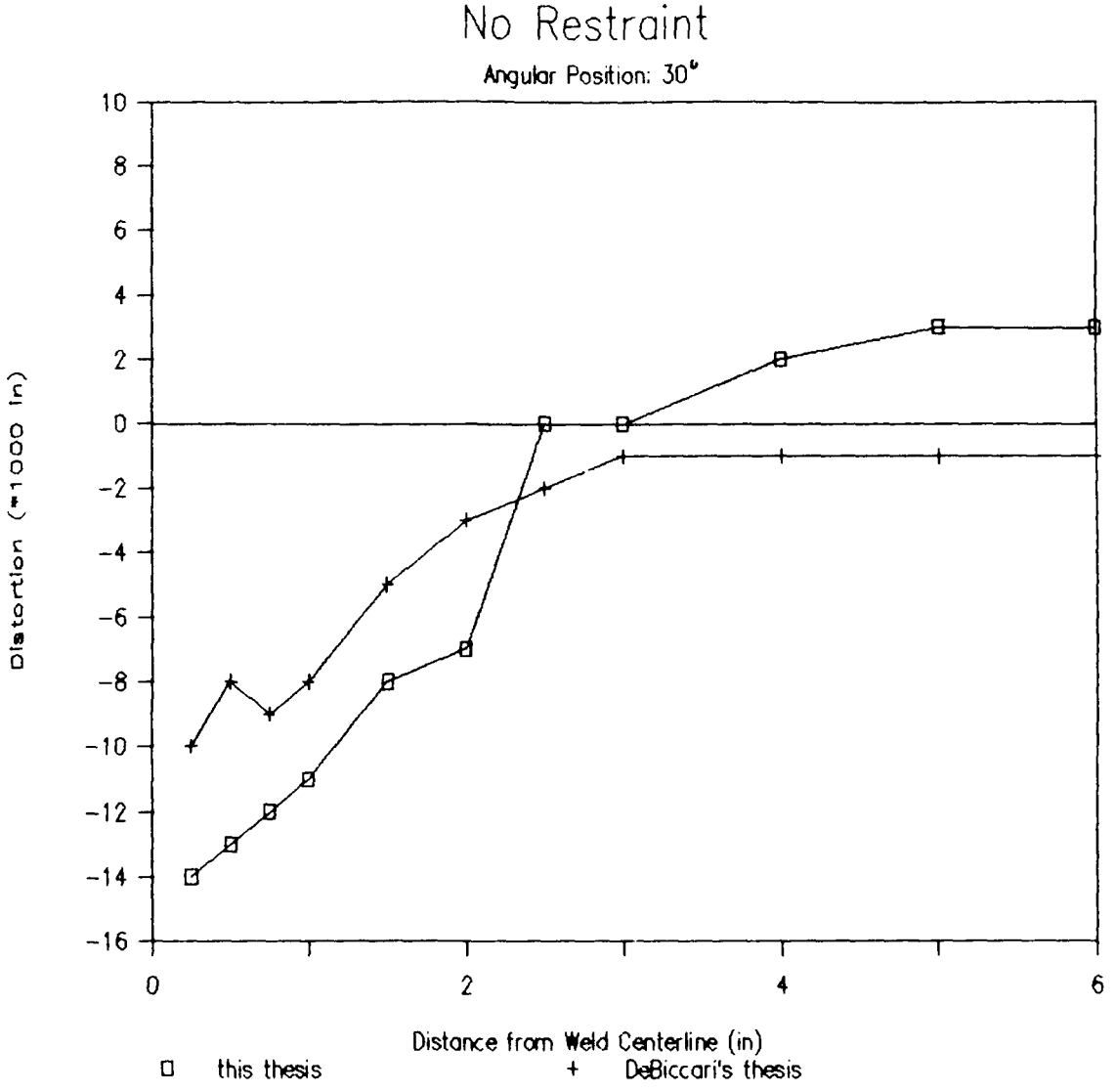

Figure 5-3: Distortion Comparison at 30° of Specimens without any restraint from This Thesis and DeBiccari's

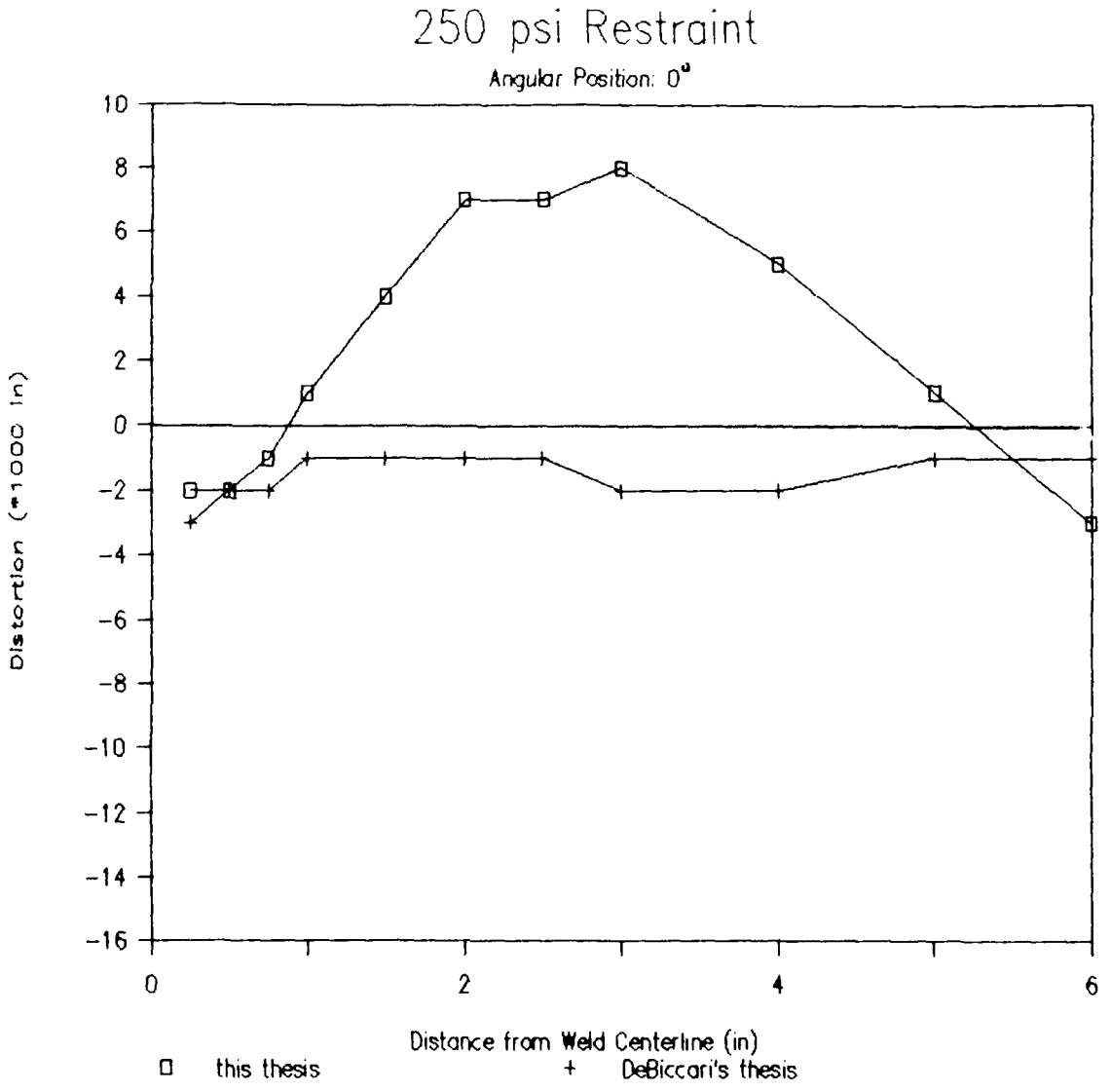

Figure 5-4: Distortion Comparison at 0° of Specimens with 250 psi restraint from This Thesis and DeBiccari's

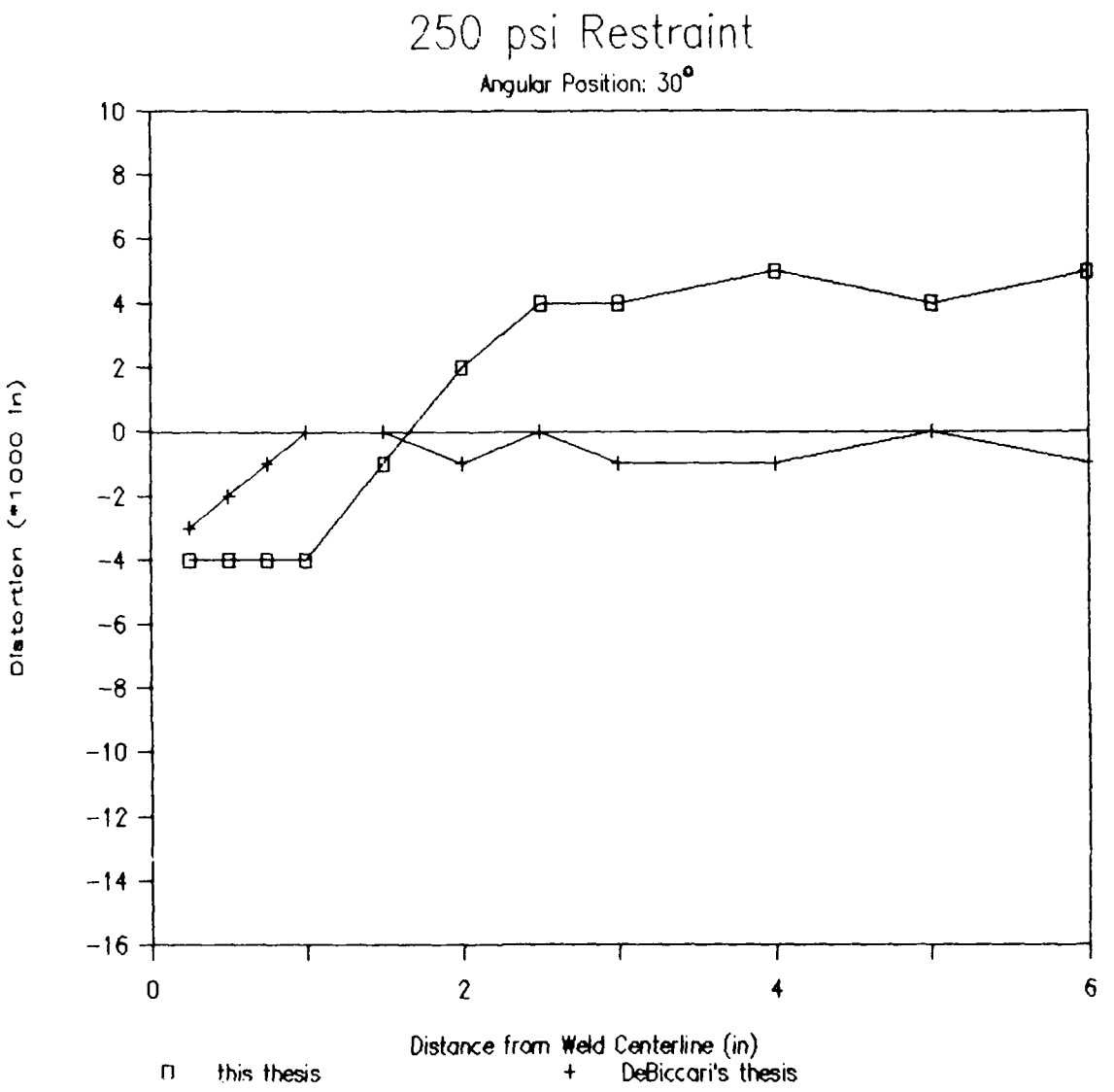

Figure 5-5: Distortion Comparison at 30° of Specimens with 250 psi restraint from This Thesis and DeBiccari's

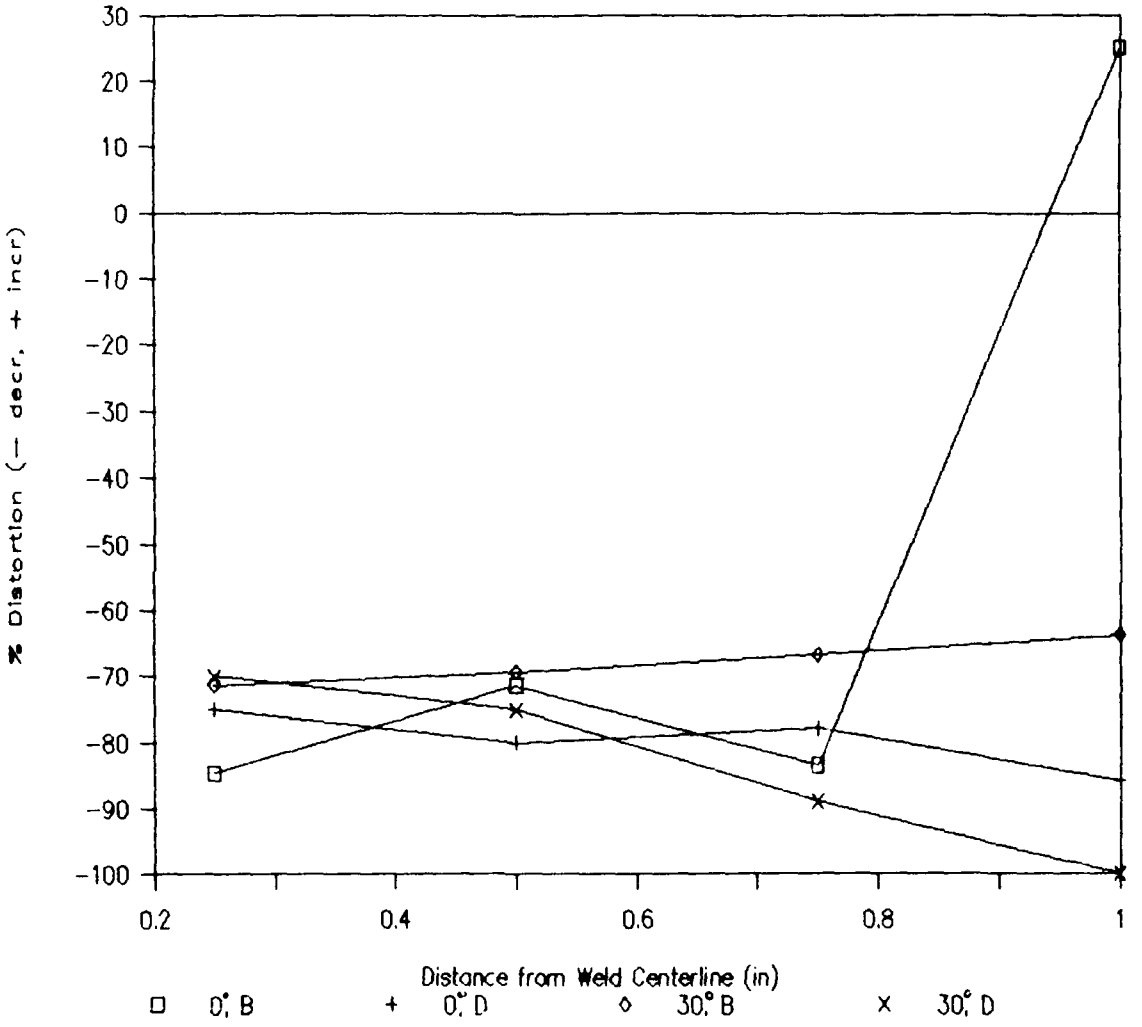

Figure 5-6: Reduction Percentage Comparison axially and circumferentially between this thesis and DeBiccari's

changes. Note that the end of the "shoe" in this thesis is at 30° and the maximum distortion is reduced by 70% while in DeBiccari's thesis it is at 90° and the reduction is only 5%. Even though figures 5-2 through 5-5 show that the hydraulic restraining device is not better at some specific locations, the percentage in reduction shows that six (6) "shoes" is more effective than two (2) semicircle "shoe", particularly at the ends.

Using the same curved beam analysis as DeBiccari [19], Castigliano's Second Theorem [28], the deflection can be predicted. (See Appendix F for calculations.) Figure 5-7 shows that uniform and varying loading are very close in deflection prediction. The measured deflection, &m, of this thesis is between the predicted values and the corrected predicted values.

Figure 5-8 compares the stiffness of the "shoe" to the nondimensionalized deflection (see Appendix F for calculations) at the angular positions 0° and 30° at 0.25 inches away from the weld centerline. The deflections of this thesis are the lines while DeBiccari's are the *. (His did not change for 0° and 30° positions.) This figure shows that DeBiccari's "shoe" applies less pressure than this thesis's "shoe". (The higher pressure is intentional.) However, it also shows that if more pressure is exerted on the inner wall then the deflection is reduced.

So for a cylinder with a given radius, the deflection can be determined and thereby setting the criteria for the stiffness at the end of the "shoe".

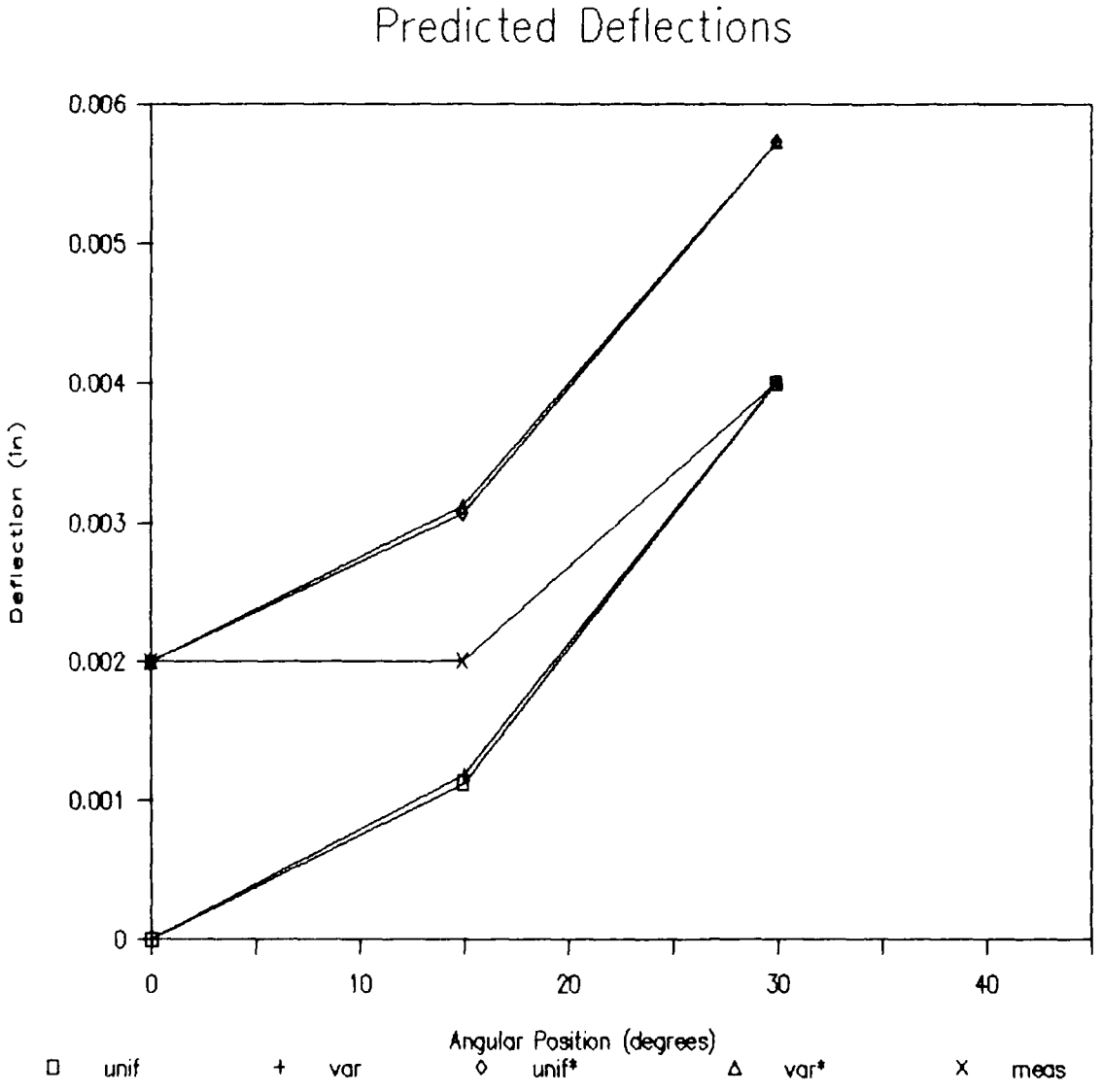

Figure 5-7: Deflection Prediction, Empirical and Corrected, for Varying and Uniform Loading

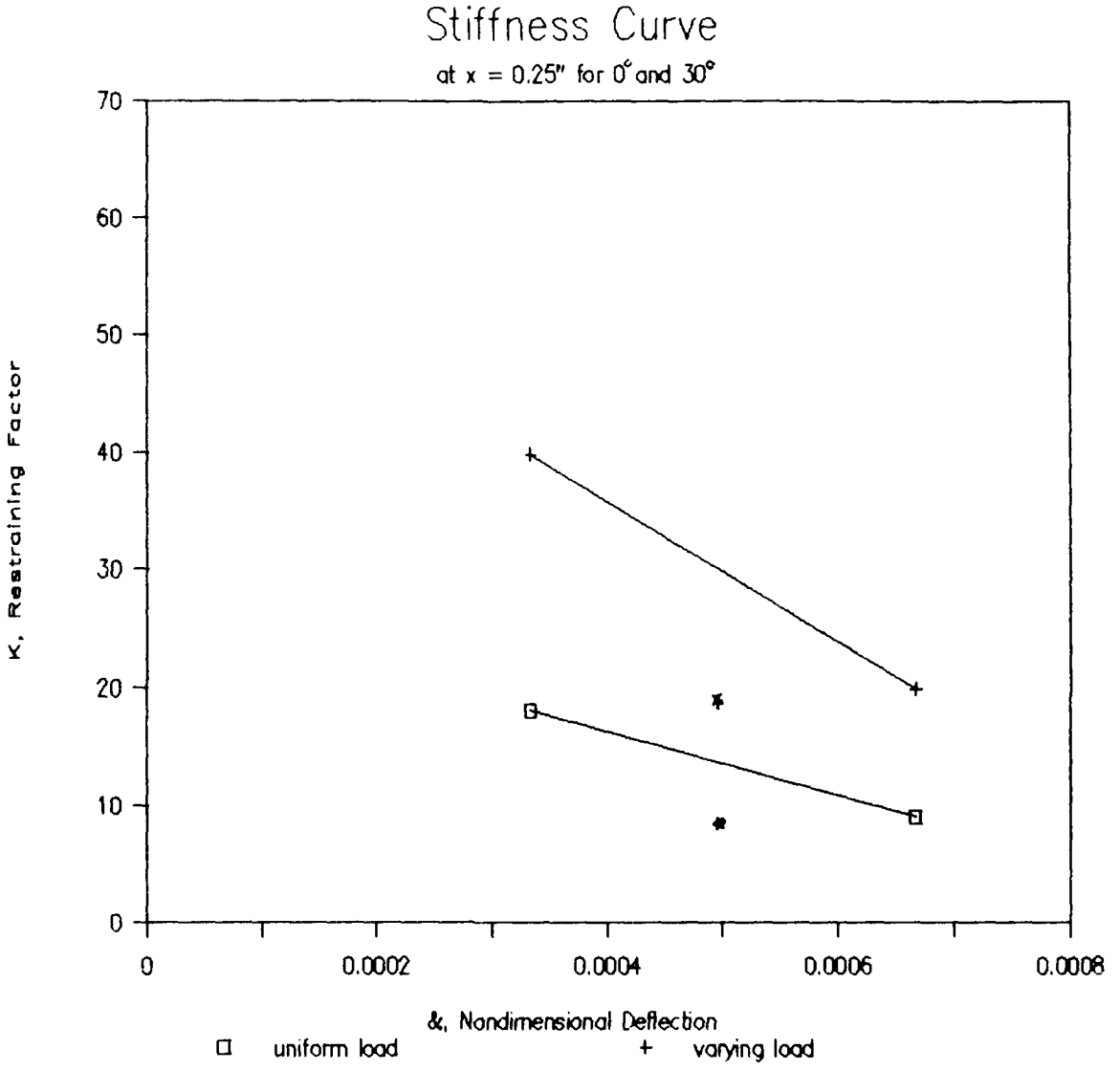

Figure 5-8: Stiffness Curve at 0.25" from weld centerline for Angular Positions of 0° and 30°

5.2. Discussion: Residual Stresses

Figure 5-9 [29] shows the axial residual stresses on the inner surface a pipe at various distances from the weld centerline. Figure 5-10 [7] shows the stresses on both the inner and outer surfaces. Close to the weld on the inner surface, the stresses are in tension and close to the yield strength. It changes very rapidly from tensile to compression within an inch. The results in [24] are similar. Because of this rapid change, this experiment only measured stresses close to the weld centerline and they are in agreement with these figures. The stresses on the outer surface are in compression and this thesis's results are in agreement with this figure.

Heat sink welding is also used to reduce axial tensile stresses or even induce compressive stresses on the inner surface of the pipe. [30] Figure 5-11 [31] compares residual stresses of a conventional weld to the heat sink weld. This experiment does not induce compressive stresses but does reduce the tensile stresses on the inner surface.

A computational model has been has been developed by Rybicki and McGuire. [4] The procedure that it is used for is Induction Heating for Stress Improvement (IHSI). IHSI process consists of placing an induction coil around a welded pipe to heat the pipe while the interior is cooled by water. In the computational model, IHSI process alters the thermal history through the pipe wall hence producing compressive stresses on the inner surface of the pipe. Rybicki states

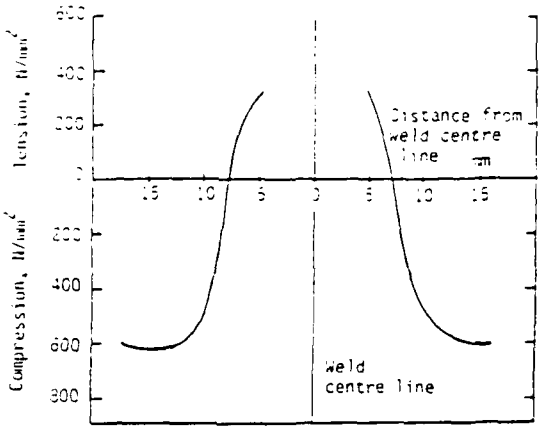

Figure 5-9: Inner Surface Residual Stresses in a Stainless Steel Pipe [29]

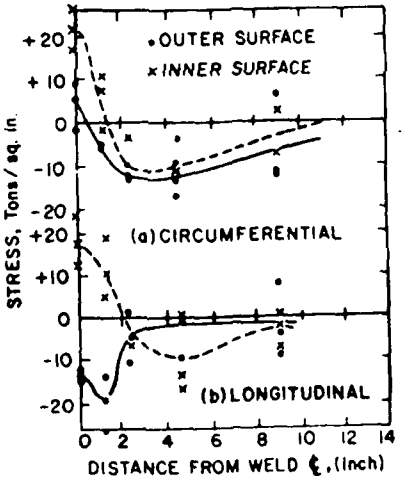

Figure 5-10: Residual Stresses in a Girth Welded, Low Carbon Steel Pipe [7]

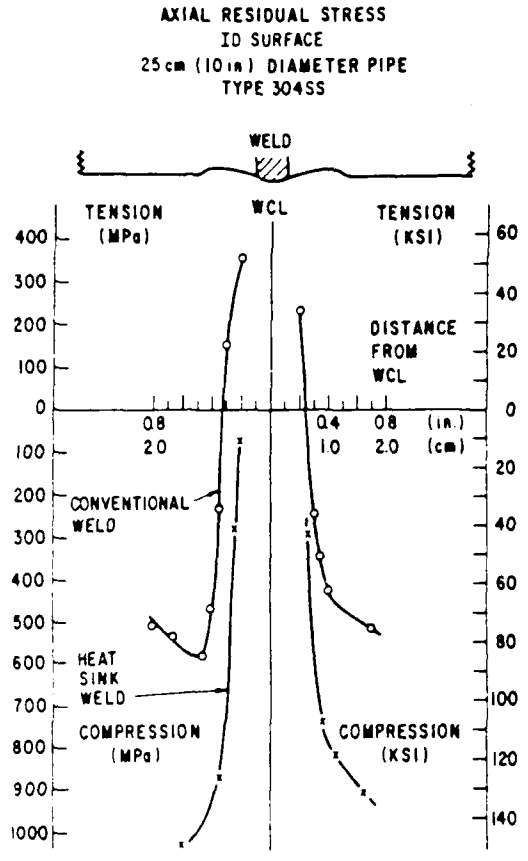

Figure 5-11: A Comparison of Residual Stresses Between a Conventional Weld and a Heat Sink Weld [31]

that these computed values of residual stress agree with experimental data.

Rybicki and Brust [16] uses a computational model to determine residual stresses for backlay welding. Backlay welding is sommelier to IHSI process but the heating is provided by a series of axial welds deposited along the outer surface of the pipe. It also changes the tensile stresses on the inner surface to compressive stresses. The computed values are in agreement with experimental data.

Table 5-1 compares the residual stresses of this thesis to DeBicarri's [19] thesis at the 0° and end of the "shoe" for no restraint and 250 psi restraint. On the inner surface, the percentage of reduction in this thesis's stresses, both axial and circumferential, is about half that of DeBiccari's. The percentage tends to increase with the angular position.

On the outer surface, the circumferential stresses for this experiment changed from tensile to compressive while DeBiccari's did not. In fact, his values increased.

One might expect that reduction percentage of the stresses would be similar to that of distortion since axial stresses are partially caused by bending stresses resulting from distortion. But that is not the case in this experiment; there's a significant difference. Thus, the reduction of stresses cannot predicted by distortion alone. This thesis does not intend to consider any of these other factors.

Table 5-1: Comparison of Residual Stresses [ksi] Between This Thesis, *, and DeBiccari's, + [19]

Inner Surface

Position	No Restraint *	No Restraint +	With "Shoe" *	With "Shoe" +
σ_θ	23.55	32.7	21.21	23.9
σ_x	48.88	38.5	40.71	16.8
σ_θ	45.56	34.7	36.61	19.9
σ_x	61.88	41.0	59.04	12.0

Reduction Percentage %	*	+
σ_θ	10	23
σ_x	17	56
σ_θ	20	43
σ_x	5	71

Outer Surface

Position	No Restraint *	No Restraint +	With "Shoe" *	With "Shoe" +
σ_θ	9.51	.6	-0.91	7.1
σ_x	-31.59	-35.1	-40.44	-15.9
σ_θ	2.41	1.7	-1.28	7.2
σ_x	-45.48	-37.7	-41.75	-17.3

Reduction Percentage %	*	+
σ_θ	109	1183 increase
σ_x	128 increase	55
σ_θ	153	423 increase
σ_x	9	54

There is a similar pattern to the stresses reduction when looking at the angular positions for a particular stress or within the same experiment. There is hardly any change in the shear stress in either way of looking.

The hydraulic restraining device does not change the inner surface's stresses from tensile to compressive but does reduce them. However, the reduction is not as much as expected. Even though the hydraulic restraining device has a pressure gage and the hydraulic pump can be controlled during welding, there's still no way to ensure that there is constant contact and uniform pressure on the inner surface. Therefore, some of the heat sink effect is lost.

There is no analysis on residual stresses with respect to the axial distance. The experiment is limited to 0.5 inches from the weld centerline because of the limitation on the strain gage indicator.

5.3. Conclusions

Distortion and residual stresses are a result of thermal strains and stress. As a result, stress corrosion cracking, fatigue failure, brittle fracture, and reduce in collapse strength may occur. Various procedures to control distortion and residual stresses have been investigated.

The purpose of this thesis is to design a hydraulic restraining device and investigate its effects on distortion and residual stresses. Employing this system, measurements have been taken of the distortion and strains (which residual

stresses are calculated from) on three specimens for a circumferential pipe weld, also known as a girth weld. The following conclusions are made:

1. Distortion is significantly reduced, a maximum of 85% when employing the hydraulic restraining device
2. By increasing the number of point sources, i.e. "restraining shoes", the end of the "shoe" is more effective
3. Distortion is reduced when pressure exerted on the inner wall increases
4. Residual stresses cannot be predicted by distortion alone
5. Residual stresses are reduced, a maximum of 20% on the inner surface and a change from tensile to compressive on the outer circumferential stress.
6. The hydraulic pistons may limit the size of the device thereby limiting the size of the pipe that it can be used in.

5.4. Future Considerations

Since stresses and distortion do not attain their final values until cooling, there is still a need to be able to sense the expansion and contraction of the specimen during welding, otherwise known as in-process control. The hydraulic restraining device design for this thesis can be controlled but it still does not guarantee that the "shoes" keep in contact with the inner surface. It does not have an

in-processing sensor. Thereby, an optimum restraining force is still unknown.

Instead of using a digital micrometer for measuring distortion, another sophisticated method should be used. There is a lot of room for human error with the setting of the micrometer. This could possibly be a reason why one of the specimens showed expansion instead of contraction.

When recording the strain changes on the pistons and "shoes" during the weld process, continue to record the changes throughout the cooling period. Also ensure the strain gages and bonding adhesive can withstand the high temperatures.

To obtain data for more of an in depth analysis, it is necessary to increase the number of strain gages that can measured simultaneously. This is a function of the equipment that is available to the laboratory.

The hydraulic restraining device, as is, cannot be used on smaller diameter pipes. A more thorough search is necessary for the design, in particular, the various sizes of the pistons. These pistons are also cumbersome for very large pipes, not to mention any pressure vessels. It would be more advantageous to find another means of exerting a continuous force.

APPENDIX A

EQUIPMENT DETAILS

1. MILLER Syncrowave 500 Power Supply Settings:

Polarity	DCSP
Contactor	Remote
Current	Panel
Hi Freq	Off
Craterfill	Out
Start Current	Off
AC Balance	Ignore
Post Flow	Adjust
Bottom Right Controls	Ignore

2. JETLINE Engineering Arc Length Control System Settings:

Voltage	11 Volts
Up/Down	Manual to position torch Auto to control arc length during weld
Touch Retract	Broken
Start Delay	Adjust accordingly
Sensitivity	Midway
Stop Retract	Adjust accordingly
Torch	Water cooled
Argon Gas	12 psi

3. LINDE J-GOV Traveler

Levers adjust sideways position

Handwheel adjusts front/back position

Toggle switch micro-adjusts torch position, stop for stationary position

4. AIRCO Heliweld Wire Feeder

Connect to stem beside torch

Range Switch on low

Feed Switch position accordingly on Reverse/Forward/Neutral

Speed Dial set on A+1.5 units (no operator's manual to convert into length per second but from timing and measuring this setting converts to 1.45 inches per second)

5. ARONSON Positioning Table

Direction Control Box for forward or reverse

Tilt Control Box for 0-90 degrees positioning

Speed Controller is a turn gage but a rpm controller is attached to convert rpm's to distance per minute

A special brace of threaded rods was made to hold the pipe onto the tilt wheel while in the horizontal position

APPENDIX B

Operating Manuals for
Daytronics Converter and
Vishay Strain Indicator

The following pages are excerpts out of manuals from references and [22] and [32] and a printout of the MINC's Fortran computer program [23].

Model 9178A
Nov. 1981

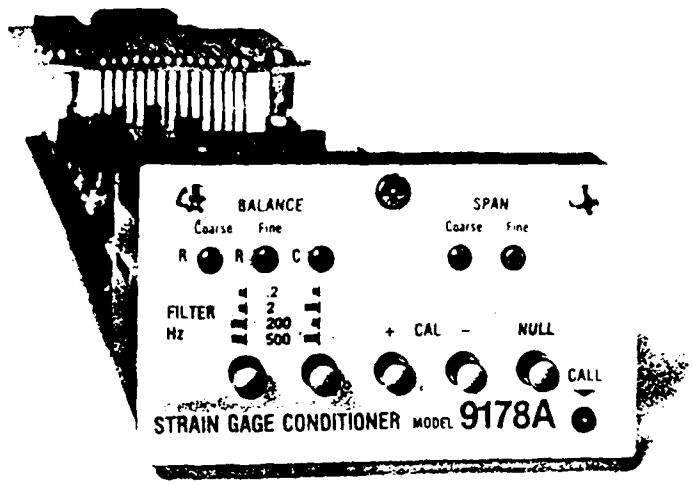

"9000" Modular
Instrument System

Model 9178A Strain Gage Conditioner Instruction Manual

The Model 9178A is a signal conditioner for use with resistance strain gage transducers requiring AC excitation. It performs all necessary balancing and calibration functions, and filters and amplifies the input signal to standard 9000 System levels.

With its phase-sensitive carrier-amplifier design, this module is intended for applications involving transformer coupling to the transducer bridge (as with rotary-transformer torque sensors) or for operations that require high sensitivity with optimum signal-to-noise characteristics.

DAYTRONIC

Manufacturer of Intelligent Instrument Systems

Daytronic Corporation • 2589 Corporate Place • Miamisburg, OH 45342 • 513/866-3300

I. Specifications and Significant I/O Connections

Table 1. Specifications, Model 9178A

Input Transducers: 4-arm bridges, 90 to 2000 ohms, nominally 1 to 5 mV/V, full scale. Internal completion of 2-arm bridges is also possible.

Cables: 4-, 6-, or 7-wire, depending on application; 5000 ft. maximum length.

Bridge Excitation: Regulated 6 V-AC at 3 kHz.

Balance Adjustment: 10-turn Coarse and Fine controls; will balance 0.8 mV/V initial unbalance.

Span Adjustment: 10-turn Coarse and Fine controls, 0.5 to 5 mV/V, full scale.

Outputs: "Prime" and "Called." Standard Five-Volt Data Signal (see "Appendix," *9000 Catalog*).

Frequency Response: Selectable low-pass cutoff frequencies of 0.2, 2, 200, and 500 Hz; down 60 dB per decade above cutoff. Full-scale slew time is 1.4/f seconds, where f is cutoff frequency.

Common-Mode Rejection: Greater than 120 dB.

Output Ripple and Noise: 0.15% of full scale (rms), maximum.

Accuracy*: 0.1% of full scale.

Dimensions: Standard single-width module.

Operating Temperature Range: +40° F to +130° F (+4.4° C to +54.4° C).

Power Requirements: Obtains power from Mainframe Supply.

* Referenced to the Five-Volt Output, and including the combined effects of nonlinearity, line-voltage variations between 105 and 130 V, ambient temperature variations of ±30 F degrees about starting value, and six-months drift of zero and span. Rated accuracy assumes operation with the Model 9530A Digital Indicator (or equivalent), using System Reference Voltage in a ratiometric technique. Possible errors contributed by transducer or cable are not included.

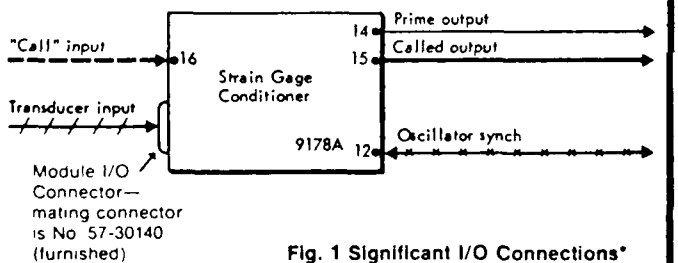

Fig. 1 Significant I/O Connections*

* For graphic symbols used in this figure, see "Introduction to Input Signal Conditioners," *9000 Catalog*. For standard signal interface specifications, bus functions, and pin assignments, see "Appendix," *9000 Catalog*.

Module I/O Connector: Provides connection for external transducer.

Call Input: Logic signal that places "Called Output" on the *Called Signal Bus* (see "Glossary," *9000 Catalog*).

Called Output: Analog output placed on the *Called Signal Bus* when and only when the 9178A is in receipt of a "Call Input" signal.

Prime Output: Continuously available analog output brought to system Patch-Wire Facility for interconnection with other system elements or peripheral devices.

Oscillator Synchronization: Allows all system 3-kHz excitation signals to be synchronized from a single "Master" source, to prevent development of beat frequencies (see Step 2, below).

II. Installation and Cabling

1. Carefully read the "Initial Instructions" section (IV) of your *9000 System Manual*.

2. OSCILLATOR SYNCHRONIZATION: Remove the module from its slot and make sure the Master/Slave Switch ("S1" of Fig. 8) has been properly set. If your system contains *only one 9178A* and *no 9130 or 9132 modules*, set the 9178A at "MASTER"; if you have *more than one 9178A* or *a 9178A and one or more 9130 or 9132 modules*, set ONE of these modules (either a 9178A, 9130, or 9132) at "MASTER," and the remaining modules at "SLAVE." Refer to your *Model 9130* or *9132 Instruction Manual* for switch location.

3. TRANSDUCER I/O CONNECTION: When connecting a *non-Daytronic* transducer to the *Module I/O Connector* at the rear of the 9178A module, use the appropriate cabling as given in Fig. 2. When a Daytronic transducer is used, the necessary cable is normally supplied with the system. Fig. 3 gives the cable for connecting a Lebow 1600 Series Rotary Torque Transducer (only).

   NOTE: In all but the shortest four- and six-wire cables, extraneous voltage drops can produce significant errors when a "Shunt Calibration" procedure (described in Section III) is attempted. The *seven-wire* configuration, however, provides a separate path for "Calibration Current," thus allowing valid transfer of transducer calibration data, irrespective of cable length. For optimum accuracy, we therefore recommend seven-wire cabling whenever you intend to perform a "Shunt Calibration."

III. Calibration

DEADWEIGHT CALIBRATION: You can achieve the most accurate results through an overall "Deadweight Calibration," which necessarily takes into account all fixed resistance characteristics of the transducer/cable system.

1A. Turn mainframe power ON. Allow 5 minutes for warm-up.

2A. Check to make certain that the mainframe FAULT indicator is out. If this light is ON, see Part 4 of "Initial Instructions" and also the respective *Mainframe Instruction Manual*.

3A. Set the front-panel Coarse and Fine SPAN controls fully clockwise (see Fig. 4).

4A. ZERO ADJUSTMENT: Establish a zero input by removing all load from the strain gage transducer. Push the front-panel NULL button and alternately adjust the R and C BALANCE controls to produce a minimum output value for the 9178A (minimum = least positive or most negative). This output may be displayed via a Model 9515A, 9530A, 9590, or 9635.

Release the NULL button and bring the output reading to zero by means of the Coarse and Fine R BALANCE controls.

5A. SPAN ADJUSTMENT: Apply an *accurately known* value of input loading to the transducer — a value (positive or negative) from 80% to 100% of the transducer's nominal rating. Using the Coarse and Fine SPAN controls, adjust the 9178A output to equal this value.

6A. SYMMETRY ADJUSTMENT: See Step 5B, below.

SHUNT CALIBRATION—an easier though less accurate technique — may be employed when overall "deadweighting" is impossible or inconvenient, and is good for a general accuracy of 1% to 3%.*

* Greater accuracy is possible, if the transducer manufacturer specifies a precisely known "Equivalent Input."

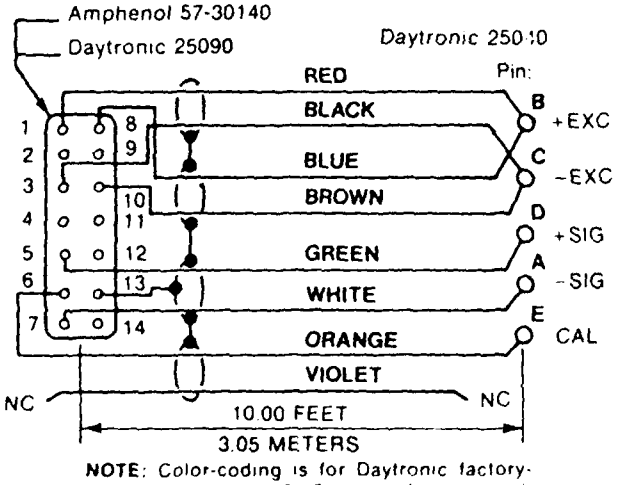

NOTE: Color-coding is for Daytronic factory-wired cable Model 85-S, using four twisted, shielded pairs of AWG #24 wire

Fig. 3 Cabling for Lebow 1600 Series

Fig. 2 Transducer Cabling

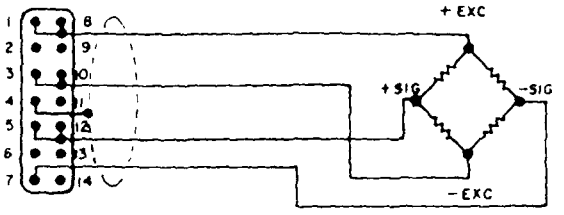

4-WIRE CONFIGURATION

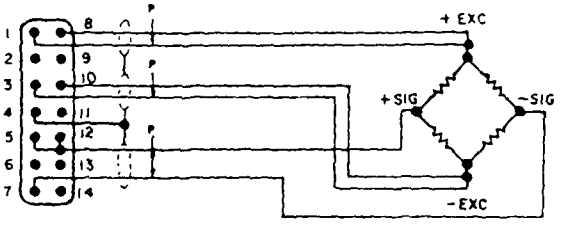

6-WIRE CONFIGURATION

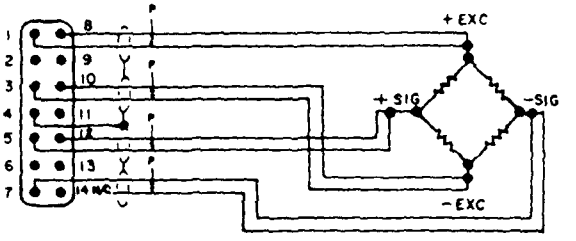

7 - WIRE CONFIGURATION

If a fixed resistor is shunted across one arm of a strain gage bridge, it produces an unbalance equivalent to that of a particular value of mechanical input.** If this "Equivalent Input" value is accurately known, you can use it as a reference point for calibrating the system.

1B. First determine the "EQUIVALENT INPUT" VALUE for your particular combination of *Shunt Calibration Resistance* (R_c, in ohms)** and transducer.

a. If the transducer manufacturer *does not* specify an "Equivalent Input" (X), you may easily calculate this value, which depends on the transducer's *Bridge Resistance* (R_b, in ohms) and *Full-Scale Sensitivity* (K, in mV/V full scale) — two variables almost always given by the manufacturer. Use this equation to find X as a *percentage of full-scale output*:

$$X = \frac{25000\ (\text{mV/V})\ R_b}{K\ R_c}\ \%\ ,$$

where R_c = 59000 ohms, unless a replacement resistor has been installed (see below).

** The Model 9178A is normally shipped with a precision 59 kilohm calibration resistor installed for this purpose (labelled "R86" in Fig. 8)

For example, suppose you have a load cell with a full-scale rating of 1000 lb. The manufacturer specifies a 350-ohm bridge and a full-scale sensitivity of 2 mV/V. Using the 9178A's internal shunt resistor, an "Equivalent Input" would be produced equal to

$$X = \frac{25000\ (\text{mV/V}) \times 350\ \text{ohms}}{2\ \text{mV/V} \times 59000\ \text{ohms}}\% = 74.15\%\ \text{of a full-scale reading.}$$

Because only nominal values have been used, this is an approximation, but good for general calibration accuracy of 1% to 3%.

To determine the *actual input simulated by the shunt*, simply multiply X by the rated full-scale capacity of the transducer. In the above example, this would yield 741.5 lb.

b. If the transducer manufacturer *specifies* an "Equivalent Input" for some R_c *other than 59 kilohms*, you can either (1) *replace* the 59 K shunt in the 9178A with a resistor of the value specified by the manufacturer, and then proceed to use the given "Equivalent Input"; or (2) you can calculate an "Equivalent Input" usable with the installed 59 K calibration resistor:

$$X_s = X_m \frac{R_c}{59000},$$

where X_s is the "Equivalent Input" simulated by the shunt; X_m is the "Equivalent Input" specified by the manufacturer; and R_c is the calibration resistance specified by the manufacturer.

For example, if the manufacturer has calibrated a 1000-lb. load cell using a 39-kilohm shunt resistor, and specifies an "Equivalent Input" of 637 lb., then the input simulated by the 9178A's 59-kilohm resistor will be

$$X_s = 637\ \text{lb.} \frac{39000\ \text{ohms}}{59000\ \text{ohms}} = 421\ \text{lb.}$$

2B. Follow Steps 2A through 4A of the DEADWEIGHT CALIBRATION procedure, above.

3B. SPAN ADJUSTMENT: Push the +CAL button. Using the Coarse and Fine SPAN controls, adjust the 9178A output to equal the "Equivalent Input" simulated by the shunt (i.e., the value determined in Step 1B).

4B. NEGATIVE CALIBRATION: If a *negative* "Equivalent Input" is also provided, press the -CAL button, and confirm that the same settings of the Coarse and Fine SPAN controls (from Step 3B) also produce this negative output reading. If not, see Step 5B.

5B. SYMMETRY ADJUSTMENT: If, after Step 5A or 4B, you find that the transducer does not behave symmetrically in both positive and negative directions, first remove the front panel (two screws in upper corners) to access the Symmetry Adjustment at the extreme right. Do not remove the module from its slot. (This adjustment has been factory-set for assumed symmetrical transducer characteristics.)

Repeat the procedure for *positive* calibration. Then press the -CAL button and adjust the symmetry control to get a reading equal to the negative input applied ("deadweighted") or simulated (by shunt).

Fig. 4 Model 9178A Front Panel

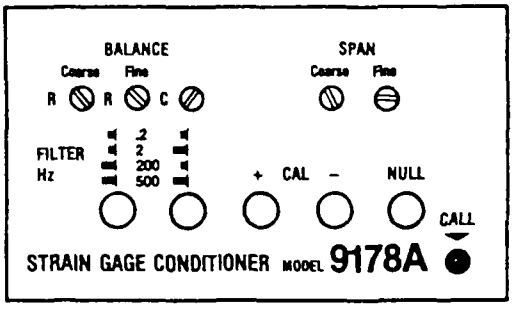

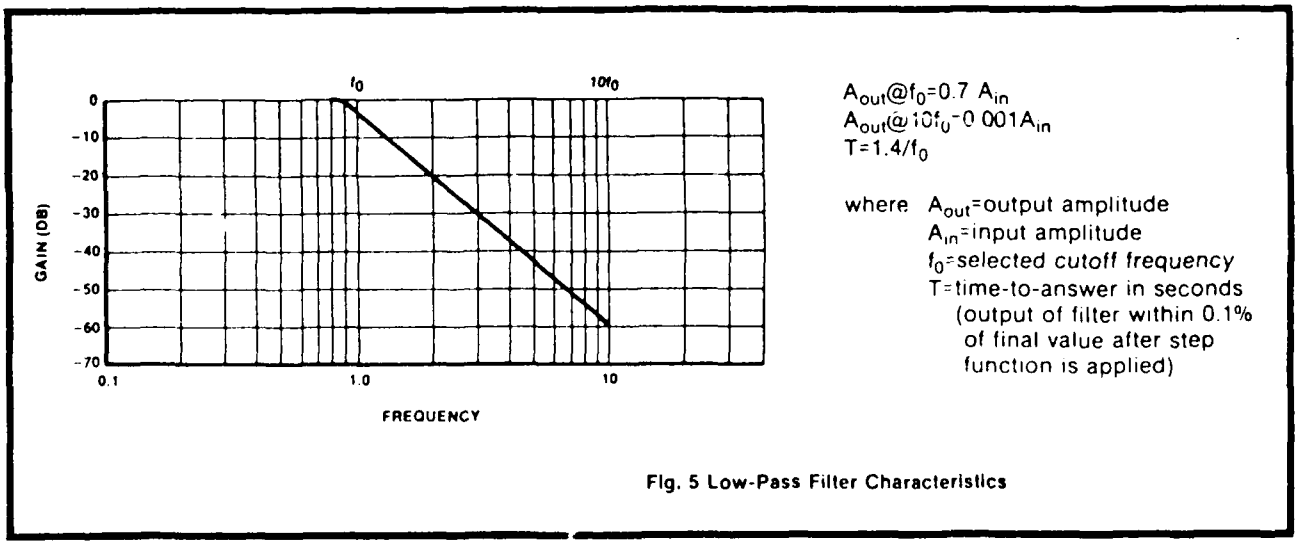

Fig. 5 Low-Pass Filter Characteristics

IV. Operation

The only required procedure is low-pass FILTER SELECTION, by means of the two graphically coded push buttons on the front panel (see Fig. 4 and the following table).

Switch 1	Switch 2	Cutoff Frequency
IN	IN	0.2 Hz
IN	OUT	2 Hz
OUT	IN	200 Hz
OUT	OUT	500 Hz

Lowering the cutoff frequency means more effective noise elimination — but also an increased time-to-answer ("*slew time*"). The equations in Fig. 5 give the fundamental relationships.

The front-panel CALL indicator lights when a "Call Input" command is present.

V. *Verification of Normal Operation*

In the event of a system malfunction, the following procedures should help you determine whether or not the Model 9178A is a possible source of failure. For general troubleshooting strategy, see the section entitled "Malfunction—Diagnosis and Repair" in the "Initial Instructions" section (IV) of your *9000 System Manual*.

1. To verify 9178A operation, first arrange to view the module output directly on the system Digital Indicator (or equivalent). Remove from the mainframe any other modules that might unduly load the observed output signal.

2. To check ZERO and SPAN operation,

   a. Establish a zero input by removing all load from the strain gage transducer. Attempt to *zero* the 9178A output via the front-panel BALANCE controls, as in Step 4A of Section III. Then push the +CAL button and attempt to adjust the output via the SPAN controls, so that it equals the value of the "Equivalent Input" simulated by the shunt resistor (as in Step 3B of Section III). You may also confirm up-scale spanning of the 9178A by means of the **Model 9413 Strain Gage Simulator**, which connects to the 9178A Module I/O Connector (in place of the transducer) and has a push button for transmission of a step-function input of approximately 12 mV (i.e., 2 mV per V of excitation).

   b. If conditions appear normal, and the 9178A output is stable (*free of drift*) and quiet (free of excessive *noise*), then skip to Step 5.

3. If you are *unable to ZERO and SPAN correctly*, you should ascertain whether the fault lies in the module or in the transducer/cable system. To do so, you may

   a. Substitute a transducer/cable known to be in good condition, and repeat Step 2; or

   b. Connect to the 9178A I/O Connector a *star-bridge* circuit in an exact condition of balance and repeat Step 2.

      The *Model 9413* constitutes such a *star bridge*. Also, you may easily construct the necessary circuit yourself, following the diagram in Fig. 6. (Use 180-ohm, 10%-carbon resistors for a 350-ohm bridge, and 56-ohm resistors for a 120-ohm bridge. Solder pairs of resistors separately, and then connect the two junctions by a separate jumper wire. Use a short 4-wire cable, as shown.)

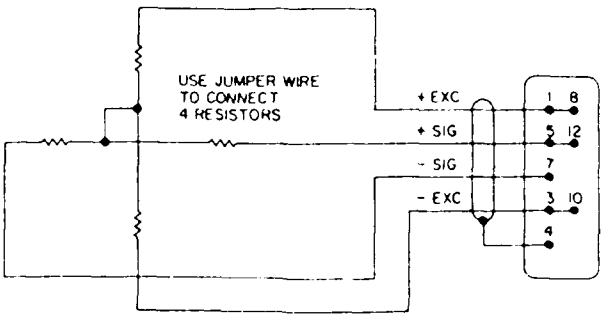

Fig. 6 Star Bridge Diagram

   c. If the abnormal conditions observed in Step 2 have now disappeared, your original transducer and cable are suspect. However, if you are still unable to ZERO and SPAN correctly, the 9178A module is probably faulty.

4. In the event of excessive *output noise*, you can easily check low-pass *filter operation*. Arrange to view the module output directly on a *DC-coupled oscilloscope*. For proper terminals, consult the System Block Diagram and Mainframe Patch-Wire Connections Drawing included in Section III of your *9000 System Manual*.

   a. Select the *500-Hz* cutoff frequency (both buttons OUT). Press the +CAL button, and observe the square-wave response of the output.*

   b. Then select the *0.2-Hz* cutoff (both buttons IN). Again press the +CAL button.* The response should now be very *slow*, requiring about seven seconds to reach final value.

   c. If the FILTER buttons have no effect on the square-wave response, the module is probably faulty. If, however, you see the response described in Step b, then the noise probably originates from pickup in the test leads or from common-mode effects of ground loops or other sources.

5. *Output nonlinearity* can result from a damaged transducer, an excessive signal level, or a faulty conditioner. If you suspect a nonlinear output,

   a. Establish a zero input by removing all load from the transducer, and adjust the BALANCE controls for zero output, as in Step 4A of Section III. (You may also use the *Model 9413* or a similar *star-bridge* circuit to simulate a transducer in an exact condition of balance—see Step 3,b). Push the +CAL button and note the displayed output-signal value (y_1).

   b. Remove the module and replace the installed *calibration resistor* (r_1, labelled "R86" in Fig. 8) with

* You may also use the *Model 9413 Strain Gage Simulator* to provide this up-scale step-function input

another (r_2) of approximately 50% *greater* value. The 9178A is normally shipped with an r_1 of 59 kilohms (indicating an r_2 of about 88.5 K). Do not use an r_2 lower than r_1; this might produce an off-scale output outside the module's linear range.

c. Reinsert the module, push the +CAL button again, and note the new output-signal value (y_2).

d. The observed output values should bear an *inverse* relation to the corresponding resistances: $y_1/y_2 = r_2/r_1$, so that an r_2 value about 50% greater than r_1 should yield a y_2 value about 66.6% of y_1. This check will confirm the essential linearity of the module.

VI. Circuitry and Parts

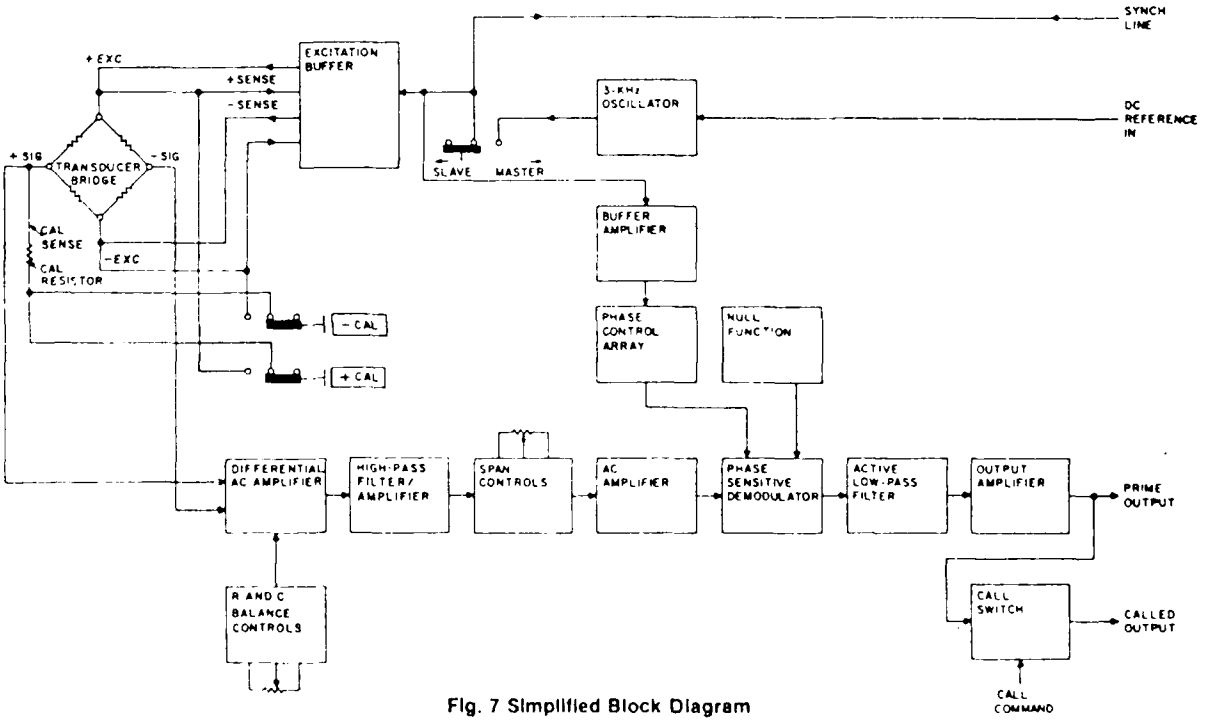

Fig. 7 Simplified Block Diagram

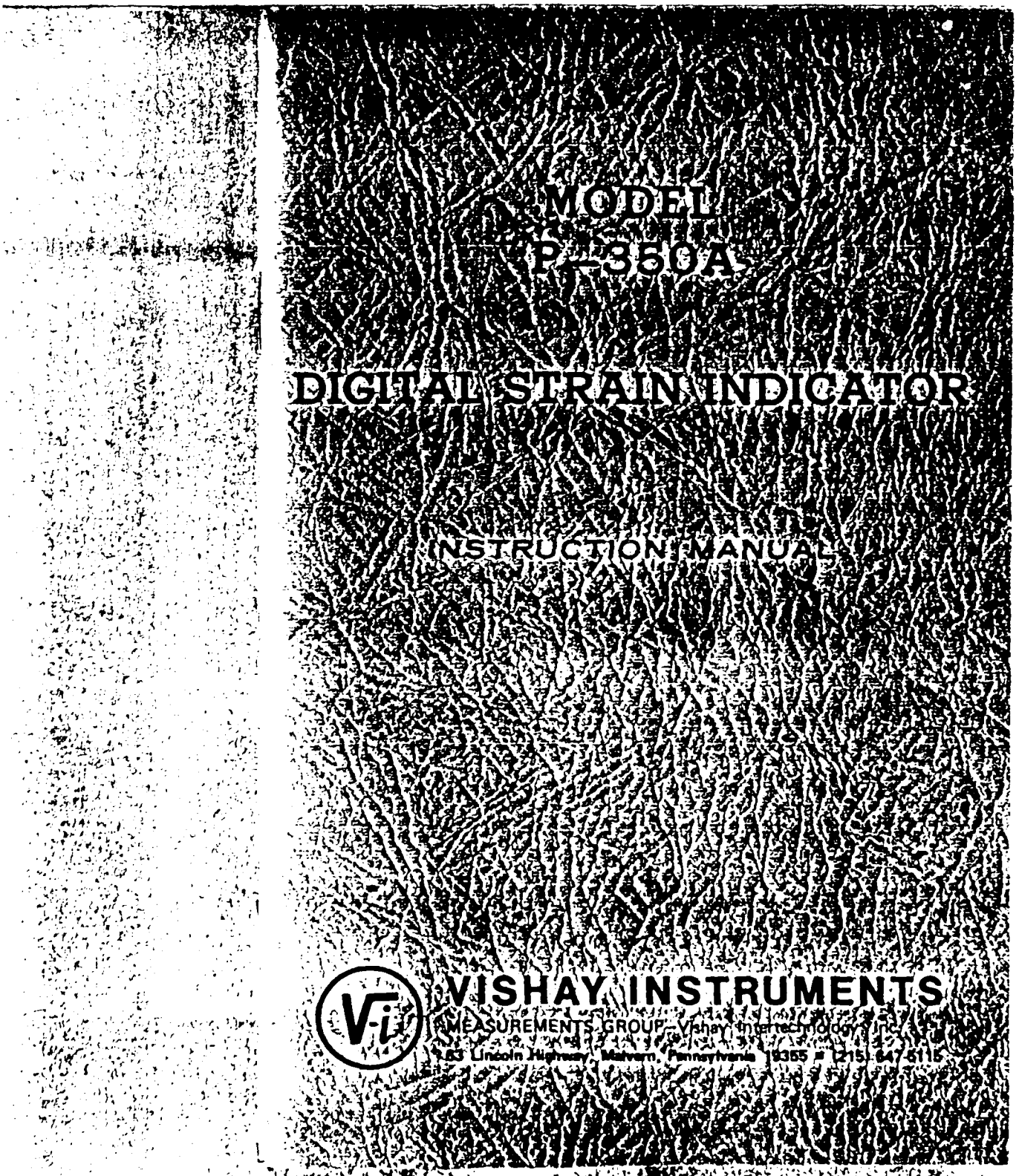
MODEL
P-350A
DIGITAL STRAIN INDICATOR
INSTRUCTION MANUAL
VISHAY INSTRUMENTS
MEASUREMENTS GROUP, Vishay Intertechnology, Inc.
63 Lincoln Highway, Malvern, Pennsylvania 19355 • (215) 647-5115

3.0 DESCRIPTION OF CONTROLS

3.1	CALIB Switch	Shunts both the 120Ω and 350Ω internal dummies to read 5000με at GF=2. Thus can be used either to verify instrument accuracy or to compensate for lead-wire desensitization on quarter bridge operation.
3.2	OUTPUT Jack	Two DC outputs available; requires 3-circuit plug (provided). "Shank" connection used as ground return for both. Disconnects Null Meter when used.
		Scope output ("ring" connection): Provides filtered DC for observing dynamic signals with high-impedance scope or recorder (source impedance 7,000Ω). Linear range 0±250 millivolts with sensitivity variable (using SENSITIVITY Control) from approx. 0.2 to 20 mv/με. Noise and ripple approx. 3με + 1mv. Flat ±5% DC to 60 Hz.
		Galvo output ("tip" connection): Provides unfiltered DC current to an external null meter or oscillograph galvanometer. (Meter must highly reject 1kHz carrier components.) Suggested external meter: ±1/2 ma, 100Ω resistance. SENSITIVITY control adjusts sensitivity from approx. 0.08 to 8με/ua.

3.3	115 VAC Receptacle	Receives the female end of the detachable 3-wire line cord. (Not used on BAT operation.)
3.4	POWER Switch	The only On-Off switch on the instrument. Pushed to the left, the instrument will operate on the internal battery. Pushed to the right, it will operate on the AC power supply. On battery operation, the unit is automatically shut off when the lid is closed.
3.5	BAT TEST Pushbutton	With the POWER switch on BAT, depressing this pushbutton will deflect the Null Meter to indicate battery condition. Although a weak battery does not directly affect accuracy, the Null Meter may become somewhat insensitive.
3.6	SENSITIVITY Control	A gain control for the amplifier driving the Null Meter. The control can vary the sensitivity of the meter by a factor of approx. 100:1. Normally this control is turned fully clockwise to yield a Null Meter sensitivity of approximately 40 microstrain full-scale in either direction. At lower settings of the control the Null Meter itself can be used for direct strain readout of static or dynamic signals up to 1 Hz. The SENSITIVITY Control is also used in conjunction with the OUTPUT jack for true dynamic measurements.
3.7	BALANCE Switch	Used to disconnect the initial BALANCE circuit if desired. Usually kept in ON position.
3.8	BALANCE Control	Used to compensate for the initial unbalance in a gage circuit (up to 2000με) to read 0000 at no load. Subsequent readings then are direct-reading "Indicated Strain". The control should be locked after adjusting on a given strain gage installation.
3.9	RANGE EXTENDER	Used to change sign (for tension or compression readings) and to extend the range of the STRAIN counter in increments of 10,000με.
3.10	Null Meter	A zero-center galvanometer used to determine instrument balance in adjusting the BALANCE and Rebalance knobs. Normally all readings are taken with the pointer on "0", although other applications exist (see paragraph 3.6). It is also used to check the condition of the internal battery.

3.11	Rebalance Knob & STRAIN Counter	Used to bring the Null Meter to "0" in making a strain measurement - the Counter then displays the strain in micro-inches per inch (microstrain or με). The knob mechanism has a range of 10,000 micro-strain. The basic calibration assumes a single active strain gage.
3.12	GAGE FACTOR Dial	A 10-turn locking control used to set the appropriate Gage Factor. This control can be varied from nominally 0.10 to 10.00.
3.13	BRIDGE Selector	Used to switch the internal dummy half bridge into the circuit for quarter and half bridge applications.
3.14	Binding Posts	For attachment of lead-wires to the strain gage(s) or transducer. The hook-up for a single gage is marked on the panel. Other typical arrangements are shown on a brief instruction plate attached to the inside of the instrument cover.

98

4.0 OPERATING PROCEDURE

4.1 Static Measurements ("Null Balance"):

4.1.1 Connect the gage(s) as shown on the plate inside the lid.

4.1.2 Select the proper position of the BRIDGE selector, FULL OR HALF/QUARTER.

4.1.3 Set the GAGE FACTOR dial as desired for the particular gage and/or application and lock. (On quarter bridge operation, the CALIB switch use is described in Section 4.4.)

4.1.4 Turn the SENSITIVITY knob fully clockwise (for maximum meter sensitivity).

4.1.5 Turn the large rebalance knob counterclockwise to a STRAIN counter reading of "0000".

4.1.6 Turn the RANGE EXTENDER knob to "+" (without digit).

4.1.7 Push the POWER switch to BAT or AC. The latter will require installation of the 115 VAC line cord.

4.1.8 Turn toggle switch above the BALANCE Control to ON.

4.1.9 With a No-Load condition on the test specimen turn the BALANCE knob to null (zero) the Null Meter (clockwise to move the pointer to the right). Lock the knob.

If it is impossible to null the Meter using the BALANCE control, lock the control in any position and use the large Rebalance knob to obtain the null in accordance with paragraph 4.1.11. Record the STRAIN Counter sign and reading of this NO-LOAD condition. Resume instructions with paragraph 4.1.10.

4.1.10 Load the test specimen as desired.

For the procedures that follow it is assumed that the Null Meter has been nulled with the strain counter at +0000 prior to the application of a load.

4.1.11 Meter deflects left: Rotate the large Rebalance

knob clockwise until the Meter comes to null. Read the STRAIN counter and sign.

If the Meter remains to the left at full counter reading, rotate the RANGE EXTENDER knob clockwise until the Meter pointer moves to the right, then rotate the large Rebalance knob counterclockwise to null.

Meter deflect right: turn the RANGE EXTENDER switch counterclockwise until the Meter pointer moves to the left. Then rotate the large Rebalance knob clockwise to obtain a Meter null. Read the STRAIN counter and sign.

4.1.12 The STRAIN Counter reading (meter nulled) is the "Indicated Strain." A "+" quantity indicates tension in the "Active" gages, a "-" quantity indicates compression.

For those No-Load cases where the Null Meter could be nulled only by use of the large Rebalance knob, a pretest STRAIN counter sign and reading were obtained for zero load. The test load should now be applied and the Meter nulling procedures repeated using the Rebalance knob. Under these conditions, the "Indicated Strain" is determined from the following with due regard to signs:

Indicated Strain = (Final Reading) - (No-Load Reading).

4.2 Low-Frequency Measurements (Static to 1 Hz)

Occasionally there are situations in which a strain level is fluctuating at a slow rate, but too rapidly for an operator to maintain null on the Null Meter. In these cases a simple technique is available to obtain data without additional equipment. (Accuracy better than 5 percent.)

4.2.1 Under static conditions (by use of a separate gage installation, if static output of active gage cannot be achieved), turn the SENSITIVITY Control to approximately 10 o'clock position.

4.2.2 Bring the Null Meter to exact null with the initial BALANCE and/or large Rebalance knobs. Note the STRAIN reading and sign.

4.2.3 Rotate the Rebalance knob (in either direction) that number of microstrain from the noted reading which you desire to represent full scale on the Meter (usually a round number, such as 500).

4.2.4 Adjust the SENSITIVITY Control so that the Meter deflects precisely to the full scale mark.

4.2.5 Return to the original STRAIN Counter setting and re-zero using the BALANCE Control, if necessary.

4.2.6 If readjustment was necessary in 4.2.5, return to the full scale setting and refine the SENSITIVITY Control to give an exact full scale indication.

4.2.7 The Null Meter is now calibrated so that strain readings can be taken directly from the Null Meter (in the example, each meter division now represents 50 microstrain). The strain level representing zero meter deflection (needle pointing at "0") can be adjusted with the Rebalance knob.

This system is limited to frequencies of less than 1 Hz because of meter damping and visual limitations.

4.3 Dynamic Measurements (Static to 60 Hz)

For higher frequency dynamic measurements the Portable Strain Indicator is used in conjunction with an oscilloscope or high-input-impedance oscillograph.

The approximate frequency response of the scope OUTPUT is shown on the following page. Note that the indicated output is about one-half the true strain at about 150 Hz; the general usefulness of this output for frequencies above 100 Hz will depend on the nature of the test.

Since the source impedance of the scope OUTPUT is approximately 7,000 ohms, it is recommended that the oscilloscope or oscillograph input impedance be above 100K, preferably 1 megohm.

Connections: Using the standard 3-circuit plug provided, connect the scope ground to the "shank" connection and the signal input to the "tip" connection.

While the maximum output of the scope OUTPUT is approximately ±500 millivolts, it preferably should be used to only ±250 millivolts to maintain good linearity (approx. ±2%).

Depending on the setting of the SENSITIVITY control, the scale factor for the scope OUTPUT can be varied from approximately 0.2 to 20 microstrain per millivolt. This range provides adequate flexibility for measuring low or high amplitude dynamic strains.

The output can be used for measuring small dynamic strains superimposed on large static strains. In this case the static level is balanced out with the Indicator using the large Rebalance knob and RANGE EXTENDER until the dynamic trace of the strain is displayed symmetrically about the zero DC output level of the Scope OUTPUT.

Calibration of the scope OUTPUT can be achieved with either shunt calibration across the active strain gage(s) or by use of the large Rebalance knob on the Indicator. Shunt calibration is somewhat more accurate but not as convenient.

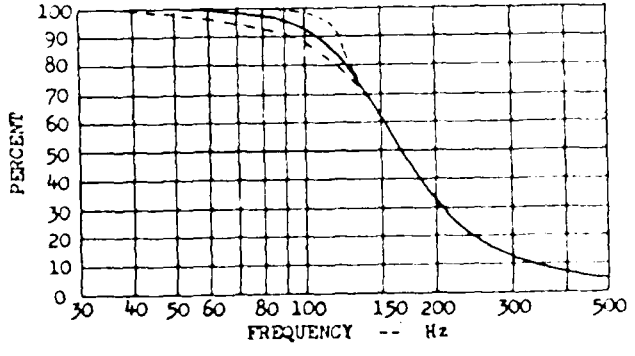

P-350A Oscilloscope Output Frequency Response

4.4 CALIB Circuit

The internal calibration circuit only functions when using the internal dummy on 120Ω or 350Ω on quarter bridge operation.

It can be used to (1) verify instrument calibration, (2) accurately set the GAGE FACTOR Control over a range of 0.2 to 10.0, and (3) compensate for lead-wire desensitization on quarter bridge operation, even when the lead resistance is not known.

4.4.1 Instrument Calibration

a. Connect any accurate (±0.1% or better) non-inductive 120Ω or 350Ω strain gage or resistor in standard quarter-bridge manner. Lead resistance must be negligible (less than 0.05Ω, 0.02Ω preferable).

b. Set GAGE FACTOR at exactly 2.000.

c. With STRAIN counter at +0000, adjust initial BALANCE Control as usual.

d. Turn CALIB Switch On.

e. Turn large Rebalance Knob to obtain null. Reading should be +5000 ±5 at 75°F.

Note: With a perfect external circuit, the tolerance of internal components should yield a reading of +5με. However, the span of the P-350A is adjusted to "bracket" errors as best as possible over the range of the instrument. Conceivably it could have been set to read +5με at 5000με because other readings tended to be negative up to 0.1%. Thus a relatively large error at +5000με does not necessarily mean that the instrument is not properly calibrated.

4.4.2 To accurately set GAGE FACTOR.

Due to inherent linearity limitations on the GAGE FACTOR Control, settings other than 2.000 cannot be

guaranteed very precisely; this is especially true below 1.500. The following procedure is independent of potentiometer linearity.

a. Connect any accurate (±0.1% or better) non-inductive 120Ω or 350Ω strain gage or resistor in standard quarter bridge manner. Lead resistance must be neglibible (unless the circuit is the one to be tested - in which case this procedure eliminates the effect of this lead resistance).

b. Set GAGE FACTOR at approximately the desired value.

c. With the STRAIN counter at +0000, adjust initial BALANCE Control as usual.

d. Turn CALIB Switch On.

e. Set STRAIN counter at calculated value:

$$\text{STRAIN} = \frac{10,000}{GF} \qquad (4\text{-}1)$$

f. If Null Meter is not at "0", adjust GAGE FACTOR Control slightly to get "0". Lock GAGE FACTOR.

g. Turn CALIB Switch OFF.

4.4.3 To compensate for lead wire resistance:

As discussed in paragraph 6.2.1, even modestly long lead wires can affect the accuracy of strain measurements. The traditional solution is, knowing the lead-wire resistance, to calculate a special "Gage Factor" for the instrument. The unique CALIB circuit in the P-350A provides a variant of this procedure for which the lead-wire resistance need not be known: it is only applicable on quarter bridge circuits using the internal dummies provided.

a. Connect the gage to the P-350A as usual (3-lead circuit).

b. With the STRAIN counter at +0000, adjust initial BALANCE as usual.

c. Turn CALIB Switch On.

d. Set STRAIN counter at exactly +5000με.

e. Adjust GAGE FACTOR CONTROL to center the Null Meter.

f. Read GAGE FACTOR Control and calculate deviation from 2.000.

g. Apply this calculated deviation to the Gage Factor on the strain gage package; set this new value into the GAGE FACTOR control and perform the desired tests.

Example: In (f) above, reading was 1.965, or a deviation of -0.035.
Suppose GF from package was 2.080;
Set GAGE FACTOR at:
2.080 - 0.035 = 2.045

4.5 Detachable Cover

The instrument as supplied is equipped with hinges which will allow removal of the cover. To effect removal, bend the open-sided portion of the cover hinge upwards far enough to clear the center section of the body hinge. If you prefer a permanently attached cover, please disregard these instructions.

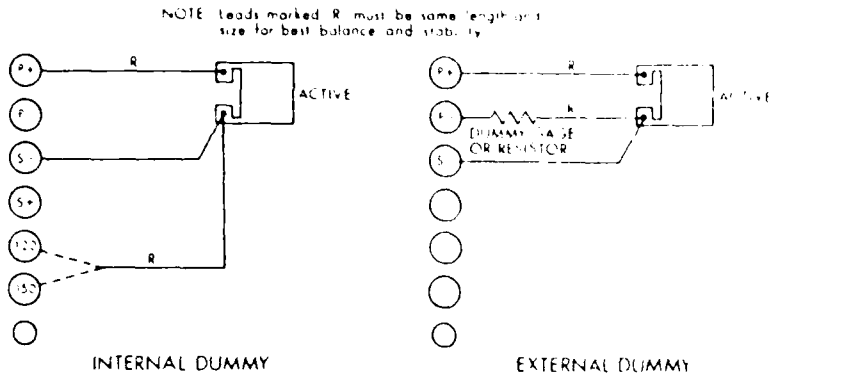

QUARTER BRIDGE

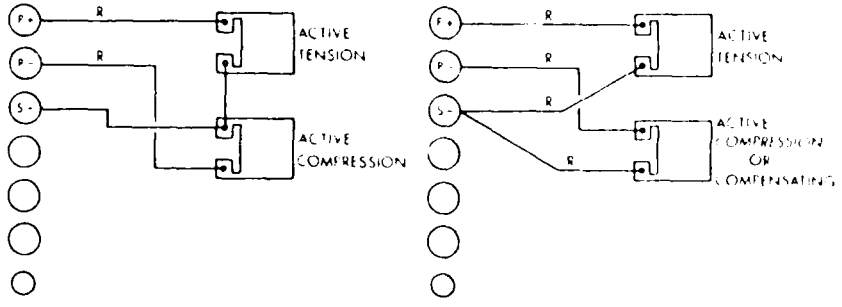

HALF BRIDGE

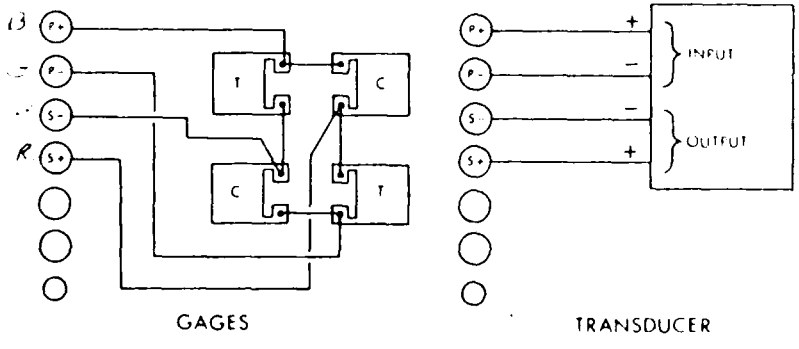

FULL BRIDGE

FIGURE 1 INPUT CONNECTIONS

5.0 INPUT CONNECTIONS

5.1 The P-350A readily adapts to various bridge circuits, but it is important to note that a basic condition for proper operation requires that the instrument must always have a four-arm bridge (internal or external) at the input and this bridge must have certain symmetry. Some forms of this bridge are theoretically linear but most are non-linear, although the non-linearity can usually be neglected.

The most common forms of bridge hook-up for strain measurements are shown in Figure 1.

5.2 In quarter bridge (single gage) operation good strain gage practice dictates the use of the three-wire circuit. However, the P-350A can be used with two-wire circuits: Short together terminals *S-* and *D* at the Indicator.

Due to the high temperature coefficient of resistance of copper wire, ambient temperature changes on the lead wires can give a large false indication of strain when only two lead wires are used. (Using 10 feet [3 meters] of twisted-pair AWG #30 [0.25 mm dia.] wire to a 120Ω gage, the apparent zero could shift almost 200 microstrain for a 10°F [5.6°C] change. Even using AWG #20 [0.81 mm dia.] wire in this situation, the shift would be about 18με.) The recommended three-wire system puts half of the temperature-induced lead wire resistance change in series with the dummy gage while the other half remains in series with the active gage. Equal changes in lead resistances in these adjacent arms then do not effect the strain measurement.

The best approach is to get in the habit of ALWAYS using three leads -- don't guess it doesn't matter in a particular test and then get erratic data.

5.3 For quarter bridge operation it is suggested that the Strain Indicator be at approximately the same ambient temperature as the active gage and test structure. This is because the "dummy" gage in the Indicator is also a standard strain gage and produces the normal apparent strain (due to non-ideal temperature compensation.) For "room temperature" testing between 60° and 100°F [15° and 40°C], the residual apparent strain caused by a temperature difference between the "active" and "dummy" gages can generally be neglected, but where either gage is below 60°F [15°C], best zero stability will be achieved by either (1) being certain that both the active gage and Indicator are close to the same temperature or, (2) use of a true unstrained "compensating" gage in the environment of the active gage.

```
      C*************************************************************
      C
      C     PROGRAM    PARALL.FOR
      C
      C     PROGRAM TO TRANSFER ASCII DATA PARALLELLY BETWEEN
      C
      C     MINC-23 AND DAYTRONIC 9635 COMPUTER INTERFACE MODULE
      C
      C     THROUGH THE IEEE-488 INSTRUMENT INTERFACE BUS
      C
      C         NOW SET TO SAMPLE ONLY 10 CHANNELS :
      C         #01 TO 04 FOR STRAIN GAGES
      C         #20 TO 24 FOR T/C's
      C
      C     CHANGE IX VALUES ACCORDING TO WHAT YOU SAMPLE
      C
      C*************************************************************
      C
      C     AUTHOR: J.A.
      C
      C     LAST MODIFICATION 20-MAY-83 (J.A.)
      C
      C     MODIFIED BY H.M.
      C
      C                          11-APR-86
      C
      C*************************************************************
      C
      C
0001        LOGICAL*1 FNAME(16),BUF(20)
0002        LOGICAL*1 BUF1(4),BUF2(6),BUF3(4),BUF4(7)
      C
      C     If a different number of channels (NCHAN not 10) are sampled
      C     change the DIMENSIONS of the followins arrays accordingly
      C     IX(2,NCHAN),BOUT(9*NCHAN),BOT(9,NCHAN),VAL(9,NCHAN)
      C
0003        LOGICAL*1 IX(2,10),BOUT(90)
0004        LOGICAL*1 BOT(9,10),VAL(9,10)
0005        LOGICAL*1 YN,YNST,YNFL
0006        DIMENSION T(3000)
0007        EQUIVALENCE (BOUT(1),VAL(1,1))
0008        INTEGER*4 ITM1,ITM0
      C
      C     ASCII commands to be send to the 9635
      C
0009        DATA BUF1/'L','O','C',"15/
0010        DATA BUF2/'C','H','N','I','X',"15/
0011        DATA BUF3/'U','N','L',"15/
0012        DATA BUF4/'D','L','Y',' ','0','0',"15/
      C
      C     Array IX contains the numbers of the channels to be sampled
      C     If different channels are sampled it should be changed accordingl
      C
0013        DATA IX/'0','1','0','2','0','3','0','4','2','0',
FORTRAN IV V02.5 Fri 11-Apr-86 09:40:32 PAGE 002
     1    2'2','1','2','2','2','3','2','4','2','5'/
      C     2'1','0','1','1','1','2','1','3','1','4'/
      C
      C     NCHAN should be set to the number of channels that you sample
      C
0014        NCHAN=4
```

channels =

these are thermocouples channels ⇒ ignore

```
0015 .        NCHR1=4
0016          NCHR2=6
0017          NCHR3=4
0018          NCHR4=7
0019          INSTR=1
0020          NCHR=20
      C
      C       Output file initialization
      C
0021          TYPE *, ' WHAT IS THE NAME OF THE OUTPUT FILE ?'
-- 0022       ACCEPT 701,(FNAME(I),I=1,14)
0023  701     FORMAT(14A1)
0024          FNAME(15)=0
0025          OPEN(UNIT=15,NAME=FNAME,TYPE='NEW',ACCESS='SEQUENTIAL',
             1FORM='FORMATTED')
0026          TYPE *,' DO YOU WANT AN INFORMATION FILE TO BE CREATED (Y/N) ?'
0027          ACCEPT 70,YN
0028  70      FORMAT (A1)
0029          IF (YN.NE.'Y') GO TO 100
0031          CALL INFO
      C
      C
0032          TYPE *,'     HOW MANY CHANNELS DO YOU WANT TO SAMPLE ?'
0033          ACCEPT *,NCHAN
      C
      C
      C       Time steps definition
      C
0034  100     TYPE *,'     ENTER TIME LIMITS FOR EVERY INTERVAL'
0035          TYPE *,'        ( ENTER T1,T2,T3 IN 1/10 SECONDS )'
0036          ACCEPT *,T1,T2,T3
0037          TYPE *,'   ENTER TIME STEP SIZE FOR EVERY INTERVAL '
0038          TYPE *,'          (TI1,TI2,TI3 IN 1/10 SECONDS)'
0039          TYPE *,' NOTE THAT THE TIME STEPS MUST BE '
0040          TYPE *,' GREATER THAN OR EQUAL TO 0.1 SEC ! '
0041          TYPE *,' (FOR 5 STRAIN GAGES AND 5 THERMOCOUPLES)    '
0042          ACCEPT *,TI1,TI2,TI3
0043          N=1
0044          TI=TI1
0045          T(1)=0.0
0046   40     IF(T(N).GE.T1) TI=TI2
0048          IF(T(N).GE.T2) TI=TI3
0050          IF(T(N).GE.T3) GO TO 41
0052          T(N+1)=T(N)+TI
0053          N=N+1
0054          GO TO 40
0055  41      CONTINUE
FORTRAN IV      V02.5       Fri 11-Apr-86 09:40:32                PAGE 003

0056          TYPE 702 ,(T(IJK),IJK=1,N)
0057  702     FORMAT(1H ,15(/1X,8F10.2))
0058          TYPE *,'**** ARE TIME STEPS OK ?? (Y/N) ****'
0059          ACCEPT 70,YNST
0060          IF (YNST.EQ.'N') GO TO 100
      C
      C       Set the 9635 response time to 0 (Default is 384 msecs)
      C
0062          CALL IBSEND (BUF4,NCHR4,INSTR)
0063          CALL IBTERM()
      C
      C       Sampling phase
      C
0064          PAUSE ' TYPE A CARRIAGE RETURN TO START SAMPLING !!'
0065          TYPE *,'TYPE A SECOND CARRIAGE RETURN TO STOP !!'
```

```
      C
0066          CALL GTIM(ITM0)
0067          CALL CVTTIM(ITM0,IH0,IM0,IS0,IT0)
      C
      C       Loop for all time steps
      C
0068          DO 121 JJ=1,N
0069    1     CALL GTIM(ITM1)
0070          CALL CVTTIM(ITM1,IH1,IM1,IS1,IT1)
0071          TIM=(IH1-IH0)*36000.+(IM1-IM0)*600.+(IS1-IS0)*10.+(IT1-IT0)/6.
0072          IF(TIM.LT.T(JJ)) GO TO 1
0074          CALL GTIM(ITM1)
0075          CALL CVTTIM(ITM1,IH1,IM1,IS1,IT1)
0076          TIM=(IH1-IH0)*36000.+(IM1-IM0)*600.+(IS1-IS0)*10.+(IT1-IT0)/6.
      C
      C       Send  "LOC"  (9635 memory freeze)  command
      C
0077  901     CALL IBSEND (BUF1,NCHR1,INSTR)
0078          JJ1=JJ-1
0079          QQQ=TIM/10.
0080          TYPE 718,JJ1,QQQ
0081  718     FORMAT(3X,I5,F10.3)
      C
      C       Loop for all channels
      C
0082          DO 103 JL=1,NCHAN
0083          DO 104 J=1,20
0084  104     BUF(J)=' '
0085          BUF2(4)=IX(1,JL)
0086          BUF2(5)=IX(2,JL)
      C
      C       Send  "CHN X"  (channel sampling) command
      C
0087  902     CALL IBSEND (BUF2,NCHR2,INSTR)
      C
      C       Input parallel data from the 9635
      C
FORTRAN IV      V02.5      Fri 11-Apr-86 09:40:32                PAGE 004

0088  900     CALL IBRECV (BUF,NCHR,INSTR)
      C
      C       Get rid of LF,CR or unreadable characters
      C
0089          DO 111 I=4,12
0090          JLI=(JL-1)*9+I-3
0091          IF (BUF(I).NE.'15) GO TO 112
0093          BUF(I)=' '
0094  112     IF (BUF(I).NE.'0) GO TO 11
0096          BUF(I)=' '
0097  11      IF (BUF(I).NE.'12) GO TO 111
0099          BUF(I)=' '
0100  111     BOUT(JLI)=BUF(I)
0101  103     CONTINUE
      C
      C       Send "UNL" (9635 memory unfreeze) command
      C
0102  903     CALL IBSEND (BUF3,NCHR3,INSTR)
      C
      C       Set data to proper format
      C
0103          DO 93 I=1,NCHAN
0104          J9=9
0105          DO 92 IL=1,9
0106          IL1=9-IL+1
0107          IF(HAL(IL1,I).EQ.' ') GO TO 92
```

```
0110            J9=J9-1
0111    92      CONTINUE
0112            DO 94 J1=1,J9
0113    94      BOT(J1,I)=' '
0114    93      CONTINUE
        C
        C       Write the data to the disc and display some on the terminal
        C       If NCHAN is changed, FORMAT 703 must be changed accordingly
        C
0115            WRITE (15,703)QQQ,((BOT(IL,I),IL=1,9),I=1,NCHAN)
0116    703     FORMAT(1X,F10.3,4X,4(1X,9A1))
        C       TYPE 704,((BOT(IL,I),IL=1,9),I=1,3),((BOT(ML,M),ML=1,9),M=6,8)
0117    704     FORMAT (15X,6(1X,9A1))
        C
        C       Check if a carriage return has been typed to stop sampling
        C
0118            IY=ITTINR()
0119            IF(IY.GE.0) GO TO 122
0121    120     CONTINUE
0122    121     CONTINUE
        C
        C       End of time steps loop
        C
0123            GO TO 125
0124    122     TYPE *,'DO YOU WANT TO CONTINUE SAMPLING IN THE SAME FILE (Y/N
0125            ACCEPT 70,YNFL
0126            IF (YNFL.NE.'N') GO TO 120
FORTRAN IV      V02.5       Fri 11-Apr-86 09:40:32                  PAGE 005

        C
        C       Store sampling information on the disk and close output file
        C
0128    125     WRITE(15,710) T1,T2,T3,TI1,TI2,TI3,N
0129    710     FORMAT(/5X,'TIME LIMITS FOR EACH INTERVAL      :',3F10.3/
               15X,'TIME STEP SIZES FOR EACH INTERVAL :',3F10.3/
               25X,'TOTAL NUMBER OF TIME STEPS        :',I5)
0130            CLOSE (UNIT=15)
0131            STOP
0132            END
FORTRAN IV      Storage Map for Program Unit .MAIN.

Local Variables, .PSECT $DATA, Size = 030136 ( 6191. words)

Name    Type  Offset     Name    Type  Offset     Name    Type  Offset
I       I*2   030010     IH0     I*2   030052     IH1     I*2   030064
IJK     I*2   030050     IL      I*2   030116     IL1     I*2   030120
IM0     I*2   030054     IM1     I*2   030066     INSTR   I*2   030004
IS0     I*2   030056     IS1     I*2   030070     ITM0    I*4   027766
ITM1    I*4   027762     IT0     I*2   030060     IT1     I*2   030072
IY      I*2   030124     J       I*2   030110     JJ      I*2   030062
JJ1     I*2   030100     JL      I*2   030106     JLI     I*2   030112
J1      I*2   030122     J9      I*2   030114     N       I*2   030042
NCHAN   I*2   027772     NCHR    I*2   030006     NCHR1   I*2   027774
NCHR2   I*2   027776     NCHR3   I*2   030000     NCHR4   I*2   030002
QQQ     R*4   030102     TI      R*4   030044     TIM     R*4   030074
TI1     R*4   030026     TI2     R*4   030032     TI3     R*4   030036
T1      R*4   030012     T2      R*4   030016     T3      R*4   030022
YN      L*1   027756     YNFL    L*1   027760     YNST    L*1   027757

Local and COMMON Arrays:

Name      Type    Section Offset  ------Size-----  Dimensions
BOT       L*1 Vec $DATA   000250  000132 (   45.)  (9,10)
BOUT      L*1     $DATA   000116  000132 (   45.)  (90)
```

Change to match # of channels

AD-A187 720 REDUCTION OF RESIDUAL STRESSES AND DISTORTION IN BIRTH WELDED PIPES(U) MASSACHUSETTS INST OF TECH CAMBRIDGE DEPT OF OCEAN ENGINEERING P K BARNES JUN 87 2/2

UNCLASSIFIED N00228-85-G-3262 F/G 11/6.2 NL

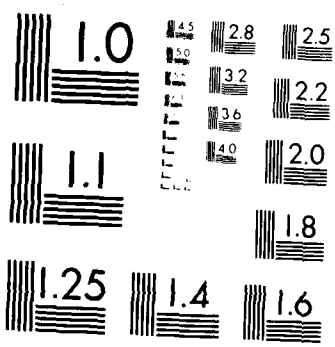

```
BUF2    L*1        $DATA    000050  000006 (     3.) (6)
BUF3    L*1        $DATA    000056  000004 (     2.) (4)
BUF4    L*1        $DATA    000062  000007 (     4.) (7)
FNAME   L*1        $DATA    000000  000020 (     8.) (16)
IX      L*1        $DATA    000071  000024 (    10.) (2,10)
T       R*4        $DATA    000402  027340 ( 6000.) (3000)
VAL     L*1 Vec    $DATA    000116  000132 (    45.) (9,10)
```

Subroutines, Functions, Statement and Processor-Defined Functions:

Name	Type	Name	Type	Name	Type	Name	Type	Name	Type
CVTTIM	R*4	GTIM	R*4	IBRECV	I*2	IBSEND	I*2	IBTERM	I*2
INFO	I*2	ITTINR	I*2						

BOOT UP MINC

Step 1 : Insert SYSTEM DISK in the left drive (SY:).

Step 2 : Insert PROGRAM DISK in the riget drive (DK:).

Step 3 : Turn on the power switch.

Step 4 : Enter date and time
ex. 12-Jan-87 (return)
14:00 (return)

LOAD IB (2)

EDIT FILE

Step 1 : Type R KED (return) (From SYSTEM DISK)

Step 2 : * appears on the screen, then type FILE NAME which you want edit.

Step 3 : Edit file using cursole key.

Step 4 : When you finish editting, hit (gold key) (command key) EXIT (enter key). Then * appears on the screen, please hit ctrl- C.

COMPILE AND LINK SOURCE FILE

MINC has only FORTRAN COMPILER.

Step 1 : Make SOURCE FILE following the above steps. SOURCE FILE NAME MUST HAVE .FOR discription.
ex. TEST.FOR

Step 2 : Type FORT FILE NAME (return).
ex. FOR TEST

Step 3 : Type LINK FILE NAME ,SY:~~PLTSVK~~ IBLIB
ex. LINK TEST,SY:~~PLTSVK~~
note: SY:PLTSVK is object file of plot sobroutines

RUN YOUR SOFTWARE (From PROGRAM DISK)

Step 1 : Type RUN FILE NAME (return).
ex. RUN TEST

FORMAT
INIT

APPENDIX C

PIPE LENGTH CALCULATIONS

In order for the end effects of the cylinder to be ignored, then the length of the pipe needs to be determined so that the cylinder will behave as one of infinite length. This happens when [33]:

$$l > \frac{2\,PI}{b} = 6.86 \text{ inches} \qquad (C.1)$$

where l is the half length of the cylinder

and

$$b^4 = \frac{3(1-v^2)}{(rt)^2} = 0.915 \text{ inches}^4 \qquad (C.2)$$

$$PI = 3.14159$$

where v = 0.3, Poisson's ratio
r = 6.3125", outer radius of pipe
t = 0.3125", wall thickness

As long as the half length of the cylinder is greater than 6.86 inches then the cylinder will behave as that of infinite length and end effects can be ignored. The half length of 9 inches ensures the infinite length assumption.

APPENDIX D

STRAIN GAGES

The electrical conductivity of metals is explained from the concepts of quantum mechanics. The theory indicates that a perfectly periodic metallic crystal lattice has perfect conductivity, zero electrical resistance. Resistance to the passage of electrons arises from irregular spacing of the metal ions. Thermal vibrating creates this irregularity. Hence, electrical resistance increases on heating. Residual stresses are a result of heating during, thus contributing to this electrical resistance. [34]

Residual stresses are measured by the elastic strains existing in the body. Strain gages measure these strains by measuring the electrical resistance. A strain gage consists of a thin metallic foil, bonded within insulating backing called a carrier matrix or grid material. Figures D-1 [23] and D-2 [35] show a variety of strain gage configurations. The electrical resistance of this grid material varies linearly with strain. When the specimen is loaded or stress relieved, the strain on its surface is transmitted to the grid material by the adhesive and carrier matrix. The strain of the specimen is determined by measuring the change in the electrical resistance of the grid material. [36]

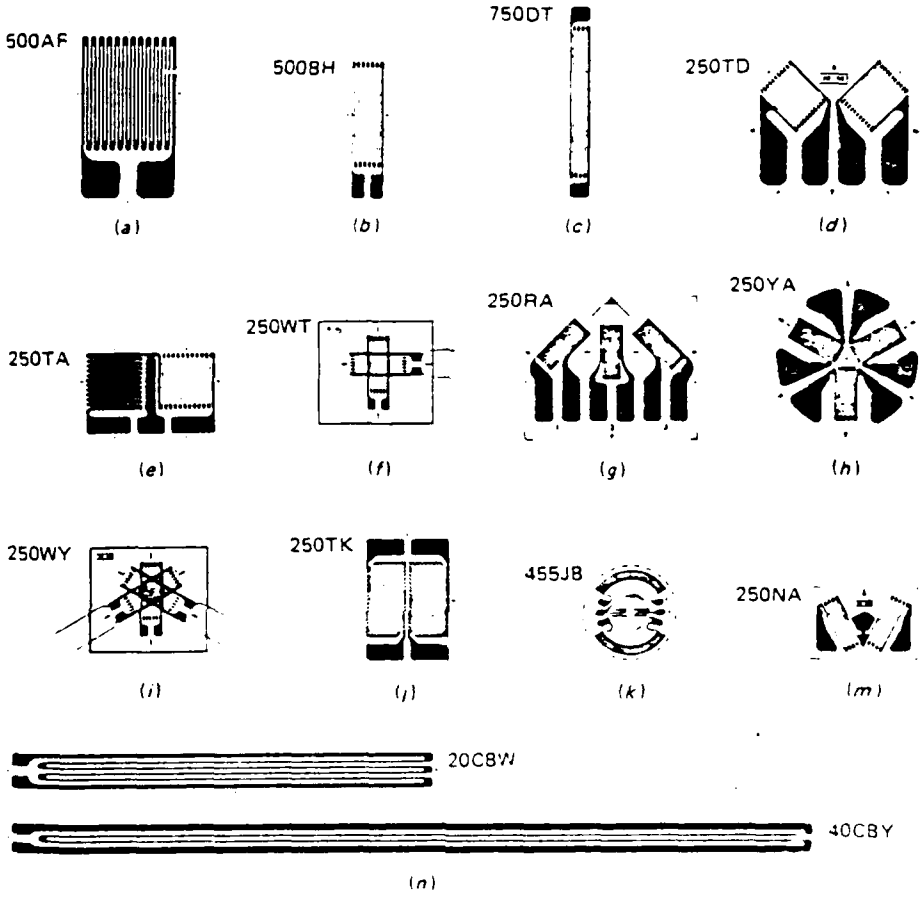

Figure D-1: Various Strain Gage Configurations [?3]

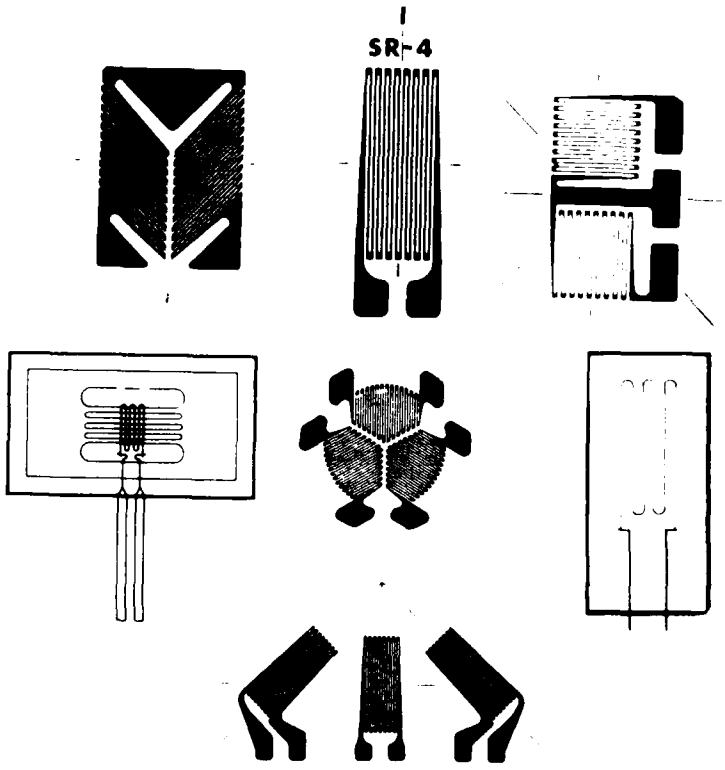

Figure D-2: Various Strain Gage Configurations [35]

Application of Strain Gages

To apply the strain gages to the surface of the specimen, the surface is roughened with 240 grit sandpaper and cleaned with isopropyl alcohol. When no more contaminants are visual after cleaning with isopropyl alcohol, then the strain gage is be bonded to the surface.

Do not touch the gage with hands, use tape or tweezers. To ensure the gage is in the correct position, tape it to the surface with transparent tape. Lift the gage leaving some of the tape adhered, like a hinge, and apply the catalyst to the back of the gage. Then apply the adhesive to the surface where the gage will adhere. Replace the gage on the surface, cover with a teflon film to protect skin from catalyst and adhesive, and press down firmly for approximately one minute. Inspect the gage for full adhesion. If not, repeat the steps with a new gage. If it is fully adhered, then remove the tape and solder leads to the terminal strip. [35]

APPENDIX E

STRAIN/STRESS CALCULATIONS

Stress is related to strain by the following equations [7]:

$$E\,\varepsilon_x = \sigma_x - \nu(\sigma_\theta + \sigma_z) \tag{E.1}$$

$$E\,\varepsilon_\theta = \sigma_\theta - \nu(\sigma_z + \sigma_x) \tag{E.2}$$

$$E\,\varepsilon_z = \sigma_z - \nu(\sigma_x + \sigma_\theta) \tag{E.3}$$

$$\tau = G\,\gamma \tag{E.4}$$

Rearranging these equations give:

$$\sigma_x = E\,\varepsilon_x + \nu(\sigma_\theta + \sigma_z) \tag{E.1a}$$

$$\sigma_\theta = E\,\varepsilon_\theta + \nu(\sigma_z + \sigma_x) \tag{E.2a}$$

$$\sigma_z = E\,\varepsilon_z + \nu(\sigma_x + \sigma_\theta) \tag{E.3a}$$

$$\gamma = \frac{-I}{G} \tag{E.4a}$$

Substituting above equations into equation (E-1a) gives:

$$\begin{aligned}\sigma_x &= E\,\varepsilon_x + \nu\,(E\,\varepsilon_\theta + \nu\,(\sigma_z + \sigma_x) + \sigma_z) \\ &= E\,\varepsilon_x + \nu\,E\,\varepsilon_\theta + \nu^2\,\sigma_z + \nu^2\,\sigma_x + \nu\,\sigma_z\end{aligned} \tag{E.1b}$$

Grouping the alike terms leave:

$$(1-\nu^2)\,\sigma_x = E\,(\varepsilon_x + \nu\,\varepsilon_\theta) + (\nu^2 + \nu)\,\sigma_z \tag{E.1c}$$

For this experiment stress in z direction is zero. Therefore:

$$\sigma_x = \frac{E}{(1-\nu^2)}\,(\varepsilon_x + \nu\,\varepsilon_\theta) \tag{E.1d}$$

By the same analogy:

$$\sigma_\theta = \frac{E}{(1-\nu^2)}\,(\varepsilon_\theta + \nu\,\varepsilon_x) \tag{E.2b}$$

Using equations (E.1d), (E.2b) and (E.4a) the stresses are calculated from the strain change measured from the VISHAY strain indicator while the specimens were cut. Tables E-1, E-2 and E-3 show the strain change measurements and stress calculations for each specimen.

Table E-1: Strain Measurements and Stress Calculations for Specimen without Restraint

Strain/ Stress	Angular Position		
	Inner Surface		
	0	15	30
$\varepsilon_\theta * 10^6$	-296	-705	-900
$\varepsilon_x * 10^6$	-1394	-1726	-1607
$\gamma_{\theta x} * 10^6$	-1022	-1222	-1266
σ_θ [ksi]	23.55	40.31	45.56
σ_x [ksi]	48.88	63.87	61.88
$\tau_{\theta x}$ [ksi]	11.79	14.10	14.61
	Outer Surface		
	0	15	30
$\varepsilon_\theta * 10^6$	-633	-660	-535
$\varepsilon_x * 10^6$	1148	1262	1540
$\gamma_{\theta x} * 10^6$	0	476	758
σ_θ [ksi]	9.51	9.28	2.41
σ_x [ksi]	-31.59	-35.08	-45.48
$\tau_{\theta x}$ [ksi]	0.00	-5.49	-8.75

Table E-2: Strain Measurements and Stress Calculations for Specimen with 150 psi Restraint

Strain/ Stress	Angular Position		
	Inner Surface		
	0	15	30
$\varepsilon_\theta * 10^6$	-492	-699	-870
$\varepsilon_x * 10^6$	-1184	-1298	-1158
$\gamma_{\theta x} * 10^6$	-710	-962	-1026
σ_θ [ksi]	27.93	35.88	40.13
σ_x [ksi]	43.90	49.70	46.78
$\tau_{\theta x}$ [ksi]	8.19	11.10	11.84
	Outer Surface		
	0	15	30
$\varepsilon_\theta * 10^6$	-396	-225	-183
$\varepsilon_x * 10^6$	1174	1096	1140
$\gamma_{\theta x} * 10^6$	411	512	812
σ_θ [ksi]	1.44	-3.42	-5.24
σ_x [ksi]	-34.79	-33.91	-35.77
$\tau_{\theta x}$ [ksi]	-4.74	-5.91	-9.37

Table E-3: Strain Measurements and Stress Calculations for Specimen with 250 psi Restraint

Strain/ Stress	Angular Position		
	Inner Surface		
	0	15	30
$\varepsilon_\theta * 10^6$	-300	-140	-630
$\varepsilon_x * 10^6$	-1145	-1277	-1602
$\gamma_{\theta x} * 10^6$	-697	-876	-1073
σ_θ [ksi]	21.21	17.25	36.61
σ_x [ksi]	40.71	43.48	59.04
$\tau_{\theta x}$ [ksi]	8.04	10.11	12.38
	Outer Surface		
	0	15	30
$\varepsilon_\theta * 10^6$	-374	-451	-375
$\varepsilon_x * 10^6$	1339	1550	1379
$\gamma_{\theta x} * 10^6$	586	643	622
σ_θ [ksi]	-0.91	-0.46	-1.28
σ_x [ksi]	-40.44	-46.64	-41.75
$\tau_{\theta x}$ [ksi]	-6.76	-7.42	-7.18

APPENDIX F

DEFLECTION PREDICTION AND RESTRAINING FACTOR CALCULATIONS

Castigliano's Second Theorem [28] gives calculations for deflections and restraining factor of a curved beam:

```
&u= pR^4{1-[(theta/2)-1]cos(theta)-0.5sin(theta)}/EI
&v= wR^4{[3theta-PI]sin(theta)+[PItheta-theta^2]cos(theta)
Ku= pR^4/(&uEI)
Kv= wR^4/(&vEI)
```

Using this thesis's data at 30° at x = 0.25":

$$\&u = \&v = 0.004"$$

$$p = 0.036 * EI/R^4$$
$$w = 0.079 * EI/R^4$$

Using DeBiccari's data for same:

$$\&u = \&v = 0.003"$$
$$p = 0.027 * EI/R^4$$
$$w = 0.059 * EI/R^4$$

Then:

```
&u = 0.036133 *{1-[(theta/2)-1]cos(theta)-0.5sin(theta)}
&v = 0.009956 *{[3theta-PI]sin(theta)+[PItheta-theta^2]cos
Ku = 0.036133 /&m
Kv = 0.079655 /&m
```

where &m is the measured distortion. However, &u and &v are for zero distortion at 0° and in these theses there is distortion at 0°. So there must be a correction factor in the equations:

$$\&*u = \&u + 0.002\cos(\text{theta})$$
$$\&*v = \&v + 0.002\cos(\text{theta})$$

The following table, Table F-1, gives the results of the above equations.

Table F-1: Calculation Values for Deflections and Restraining Factor

Theta radians	Theta degrees	&u	&v	&*u	&*v	&m
0.0000	0	0.00000	0.00000	0.00200	0.00200	0.002
0.2618	15	0.00112	0.00118	0.00306	0.00311	0.002
0.5236	30	0.00400	0.00400	0.00573	0.00573	0.004
0.7854	45	0.00784	0.00750	0.00926	0.00891	
1.0472	60	0.01188	0.01092	0.01288	0.01192	
1.3090	75	0.01545	0.01374	0.01597	0.01425	
1.5708	90	0.01807	0.01564	0.01807	0.01564	

For figure 5-8, a nondimensional distortion, &e: the ratio of the measured distortion to the radius, is plotted against the restraining factor, K. The data are at 0.25" away from the weld centerling and for 0° and 30°. The following table, Table F-2, show the calculated values.

Table F-2: Calculated Values for Nondimensional Deflections and Restraining Factor

This Thesis				DeBiccari's Thesis			
&m	&e	Ku	Kv	&m	&e	Ku	Kv
0.002	3.33E-04	18.06	39.83	0.003	5.00E-04	9.03	19.91
0.004	6.67E-04	9.033	19.91	0.003	5.00E-04	9.03	19.91

REFERENCES

[1] Masubuchi, K., "Thermal Stresses and Metal Movement During Welded Structural Materials Especially High Strength Steels", International Conference on Residual Stresses in Welded Construction and Their Effects, London, England, 15-17 November 1977, pp. 1-13.

[2] Chandra, U., "Determination of Residual Stresses due to Girth-Butt Welds in Pipes", Journal of Pressure Vessel Technology, Volume 107, Number 2, May 1985, pp. 178-184.

[3] Fujita, Y., Nomoto, T., Yasuzawa, Y., Yamada, S., Matsumura, H., Hasegawa, H., Ino, I., and Takasugi, N., "A research on Welding Deformation of Spherical Shell Structures", Naval Architecture and Ocean Engineering, Volume 20, 1982.

[4] Rybicki, E. F., and McGuire, P. A., "A Computational Model for Improving Weld Residual Stresses in Small Diameter Pipes by Induction Heating", Journal of Pressure Vessel Technology, Transactions of the ASME, Vol. 103, August 1981, pp. 294-299.

[5] Treuting, R. G., Lynch, J. J., Wishart, H. B., and Richards, D. G., Residual Stress Measurements, American Society for Metals, Cleveland, Ohio, Copyright 1952.

[6] Gurney, T. R., Fatigue of Welded Structures, Cambridge University Press, New York, 1968.

[7] Masubuchi, K., Analysis of Welded Structures, Pergamon Press Inc., New York, 1980.

[8] Vaidyanathan, S., Todaro, A. F., and Finnie, I., "Residual Stresses Due to Circumferential Welds", Journal of Engineering Materials and Technology, Transactions of the ASME, October 1973, pp. 233-237.

[9] Narayanan, R., "The Influence of Residual Shrinkage Stresses on the Ultimate Strengths of Stiffened Steel Flanges", International Conference on Residual Stresses in Welded Construction and Their Effects, London, England, 15-17 November 1977, pp. 165-172.

[10] Macherauch, E., "Different Sources of Residual Stresses as a Result of Welding", International Conference on Residual Stresses in Welded Construction and Their Effects, London, England, 15-17 November 1977, pp. 267-282.

[11] Phillips, A. L., Editor, Welding Handbook: Section One, American Welding Society, 1968.

[12] Vaidyanathan, S., Weiss, H., and Finnie, I., "A Further Study of Residual Stresses in Circumferential Welds", Journal of Engineering Materials and Technology, Transactions of the ASME, October 1973, pp. 238-242.

[13] Ohsawa, M., Nakajima, H., Nagai, A., and Minehisa, S., "Distortion of Thick Cylinder Welds by Narrow Groove MIG Welding", Technical Report X-1035-83, International Institute of Welding, 1983.

[14] Masubuchi, K., 13.15 Class Notes, 1985.

[15] Papazoglou, V. J., Masubuchi, K., Goncalves, E., and Imakita, A., "Residual Stresses Due to Welding and Computer-Aided Analysis of Formation and Consequences", SNAME Transactions, Volume 90, 1982, pp. 365-390.

[16] Rybicki, E. F., and Brust, F. W., "A Computational Model of Backlay Welding for Controlling Residual Stresses in Welded Pipes", Journal of Pressure Vessel Technology, Transactions of the ASME, Vol. 103, August 1981, pp. 226-232.

[17] Atteridge, D. G., Bruemmer, S. M., Charlot, L. A. and Page, R. E., "Evaluation and Acceptance of Welded and Repair-Welded Stainless Steel for LWR Service", NUREG/CR-3613-3, PNL-4941, September 1985.

[18] Ray, Samarjit, "Study of Residual Stresses in Welding", Indian Welding Journal, April 1984, pp. 45-52.

[19] DeBaccari, Andrew, "Control of Distortion and Residual Stresses in Girth Weld Pipes", MIT PhD Thesis, 1986.

[20] Abel, G., Lincoln Controls, Woburn, MA., personal conversation.

[21] Bailey, B, Mechanical Engineer, Laboratory of Nuclear Science, MIT, Cambridge, Ma., personal conversation.

[22] Vishay Intertechnology, Inc., Model P-350A Digital Strain Indicator Instruction Manual, Vishay Instruments, Malvern, PA.

[23] Agapakis, John E., "Fundamentals of Computer-Aided Experimentation for Welding", Report No. 83-16, Department of Ocean Engineering, MIT, Cambridge, MA.

[24] Rampaul, H., Pipe Welding Procedures, Industrial Press Inc., NY, NY. 1973.

[25] Papazoglou, V. J., "Analytical Techniques for Determining Temperatures, Thermal Strains and Residual Stresses During Welding", MIT PhD Thesis, 1981.

[26] Chrenko, R. M., "Residual Stress Studies of Austenitic and Ferritic Steels", International Conference on Residual Stresses in Welded Construction and Their Effects, London, England, 15-17 November 1977, pp. 79-88.

[27] Rybicki, E. F., Schmueser, D. W., Stonesifer, R. W., Groom, J. J., and Mishler, H. W., "A Finite-Element Model for Residual Stresses and Deflections in Girth-Butt Welded Pipes", Journal of Pressure Vessel Technology, Transactions of the ASME, Vol. 100, Number 3, August 1978, pp. 256-262.

[28] Timoshenko, S., Strength of Materials, Part II, Robert E. Krieger Publishing Co., Inc., New York, 1955.

[29] Chrenko, R. M., "Thermal Modifications of Welding Residual Stresses", Residual Stress and Stress Relaxation, Kula and Weiss, Editors, Plenum Press, New York, 1982, pp. 61-70.

[30] Sagawa, W., Shimizu, T., Enomoto, K., and Sakata, S., "Residual Stresses in Girth Butt Welded Pipes and Treatment to Modify These", The International Journal of Pressure Vessels and Piping, Volume 16, Number 4, 1984, pp. 299-319.

[31] Leggatt, R. H., "Residual Stresses at Girth Welds in Pipes", Welding in Energy-Related Projects, Pergamon Press Inc., NY, 1984, pp. 429-440.

[32] Daytronic Corporation, "Model 9178A Strain Gage Conditioner Instruction Manual", "9000" Modular Instrument System, Miamisburg, OH, Nov 1981.

[33] Ugural, A. C., Stresses in Plates and Shells, McGraw-Hill Book Company, 1981.

[34] Treuting, R. G., Lynch, J. J., Wishart, H. B., and Richards, D. G., Residual Stress Measuremnts, American Society for Metals, Cleveland, Ohio, Copyright 1952.

[35] BLH Electronics, "SR-4 Strain Gage Catalog", Waltham, MA, 1980.

[36] Omega Engineering Inc., "Omega Quick Selection Guide Y Series Foil Strain Gages", copyright 1984 by Omega Engineering Inc., USA.

END

FILMED

FEB. 1988

DTIC